universität wien

MASTERARBEIT

Titel der Masterarbeit

„Entwicklung neuer Prodrug-Strategien für die Krebstherapie“

verfasst von

Björn Bielec, BSc.

angestrebter akademischer Grad

Master of Science (MSc)

Wien, 2015

Studienkennzahl lt. Studienblatt:	A 066 862
Studienrichtung lt. Studienblatt:	Masterstudium Chemie
Betreut von:	O. Univ. Prof. Dr. Dr. Bernhard K. Keppler

universität wien

MASTER THESIS

„Development of novel anti-cancer prodrug strategies“

Björn Bielec, BSc.

Submitted in part fulfillment of the requirements for the degree

Master of Science (MSc)

Vienna, 2015

To my beloved family and my aunt Christel. We miss you.

“Function follows vision, vision follows reality”
Friedrich Kieslers

Acknowledgements

First, I would like to thank O. Univ. Prof. Dr. Dr. Bernhard K. Keppler for giving me the opportunity to work on this interesting and innovative topic at the Institute of Inorganic Chemistry of the University of Vienna.

My supervisor Dr. Christian Kowol for his great supervision throughout this work and for countless interesting and inspiring discussions all over the field of chemistry. Thank you for everything!

Dr. Petra Heffeter for the supervision at the Institute of Cancer Research, for always having an open mind for my biological questions and for the advisory at fluorescence spectroscopy measurements.

A.o.Prof Dr. Markus Galanski and the NMR service team, especially Nadine Sommerfeld and Josef Mayer, for measuring a countless number of NMR spectra.

My lab colleague Alessio for the nice and interesting working atmosphere, many interesting talks about football and the world (of chemistry).

The Kowol group Josef, Claudia, Britta, Karla and Sebastian for the nice working atmosphere and many many many funny talks! It was a great part of my life!

Dr. Wolfgang Kandioller for the interesting talks and discussions on the balcony!

Karla, Christian and Matthias from the analytic team for measuring mass spectra samples and a friendly ear for any questions and requests.

Mag. Elfriede Limberger for managing all the administrative affairs.

Günther Plasser, Sylwia Kur, Sebastian Ludyga and Norbert Kandler for their support with chemicals and solvents and other kinds of administrative problems.

The whole working group for assistance whenever it was needed and especially Claudia, Karla, Sonja, Ewelina, Britta, Josef, Iker, Felix, Paul, Christian, Matthias and Masha for the funny, encouraging and challenging discussions and talks.

My lovely girlfriend Sarah for the all-time support while writing this thesis and learning to love my german dialect. I'm also getting used to cats!

My parents, who gave me the opportunity to fulfill my dream to study and supports me in every aspect of my life. I don't know how I can just ever give a part of all this in return.

My brother Kevin for being there all the time although physically departed by distance.

Last but not least, all my friends offside university, especially Thomas, Martin, Karin, Katrin, Ralu, Aaron, Stefan and my whole football team for taking my mind off work and making me laugh when I did not felt like doing it.

For financial support: Initiative Krebsforschung

Abstract

Despite the great progress in cancer treatment over the last decades, most patients still suffer from severe side effects during cancer therapy. These side effects often dramatically reduce the patient's quality of life and, even, can prevent further treatment. One approach to decrease these side effects is the design of so-called tumor activatable prodrugs. Thus, a deactivated drug species is applied and specifically activated inside the tumor tissue. This type of prodrugs usually consists of three different moieties: a trigger unit which enables the selective release of the drug, a linker unit and the anti-cancer drug. Though, some prodrugs like capecitabine (Xeloda®) are already applied in clinical anti-cancer therapy, there is great demand for the development of novel highly specific prodrug systems.

This master thesis focused on two topics. The first topic is the development of a novel trigger system specific for cathepsin activation. Cathepsins are proteolytic enzymes which are known to be overexpressed in various types of cancer and therefore highly promising for tumor specific prodrug activation. Interestingly, despite the high number of different cathepsins, prodrug systems are currently only known for cathepsin B. The new concept comprises the use of highly specific fragments of cathepsin inhibitors as triggers which are connected to the drug via a self-immolative linker unit. This concept was developed in this master thesis for cathepsin K, a protease which is known to be expressed in bone metastases of breast and colon cancers. To this end, the modified inhibitor moiety was synthesized and connected to a para-aminobenzyl alcohol linker and a fluorophore in 11 steps. The final product was characterized by NMR spectroscopy and mass spectrometry and cleavage was studied by fluorescence spectroscopy.

The second topic of this master thesis was the development of a prodrug strategy for the anablastic lymphoma kinase (ALK) inhibitor crizotinib. Crizotinib is approved for non-small cell lung cancer treatment, however, its application is limited by severe side effects like hepatic and gastrointestinal toxicity. Hence, a trigger system was attached to a position which is crucial for the drug-target interaction. The final release of the drug was investigated by HPLC measurements.

Summarizing, a new trigger system for cathepsin-specific activation of prodrugs was developed and a strategy to synthesize prodrugs of the approved kinase inhibitor crizotinib.

Zusammenfassung

Trotz großer Fortschritte in der Entwicklung von Krebstherapeutika in den letzten Jahrzehnten, leiden viele Patienten nach wie vor unter drastischen Nebenwirkungen. Diese können die Lebensqualität der Patienten massiv reduzieren und sogar bis zum Therapieabbruch führen. Eine Möglichkeit die Nebenwirkungen eines Wirkstoffs zu mindern, bietet das sogenannte Prodrug-Konzept. Dabei wird ein Therapeutikum chemisch deaktiviert und erst selektiv im Tumorgewebe wieder aktiviert. Eine solche Prodrug besteht normalerweise aus drei Einheiten: dem Trigger, der die spezifische Aktivierung des Wirkstoffs ermöglicht, einem Linker und dem Wirkstoff selbst. Obwohl bereits einige dieser Systeme wie Catecitabine (Xeloda®) klinisch angewendet werden, besteht ein großer Bedarf nach neuen, hochspezifischen Prodrug-Systemen.

Diese Masterarbeit beschäftigt sich mit zwei Themen. Ersteres ist die Entwicklung eines neuen Konzepts für cathepsin-selektive Triggereinheiten. Cathepsine sind proteolytische Enzyme, welche in diversen Tumorarten überexprimiert werden. Trotz der großen Vielfalt von Cathepsinen existieren derzeit allerdings nur Triggereinheiten für Cathepsin B. Das neue Konzept umfasst den Einbau hochspezifischer Inhibitorfragmente in die Triggereinheiten, welche dann über selbstzerstörende Linker an einen Wirkstoff gebunden werden. Dieses Konzept wurde in dieser Masterarbeit für Cathepsin K umgesetzt, ein Enzym, das in Metastasen von Brust- und Darmkrebspatieten exprimiert wird. Dazu wurde in 11 Stufen eine modifizierte Inhibitoreinheit über einen selbstzerstörenden *para*-Aminobenzylalkohol-Linker an einen Fluorophor gebunden. Die synthetisierte Prodrug wurde mittels NMR-Spektroskopie und Massenspektrometrie charakterisiert und die Freisetzung des Fluorophors mittels Fluoreszenzspektroskopie untersucht.

Das zweite Thema dieser Masterarbeit beschäftigt sich mit der Entwicklung einer Prodrug des *anablastic lymphoma kinase* (ALK)-Inhibitors Crizotinib. Diese Verbindung ist bereits klinisch zur Behandlung von nichtkleinzelligen Bronchialkarzinomen zugelassen, zeigt jedoch stark leberschädigende und gastrointestinale Nebenwirkungen. Daher wurde an der entscheidenden Stelle für die Bindung zwischen Wirkstoff und Enzym eine Trigger-Einheit implementiert. Die Freisetzung des Wirkstoffs aus der synthetisierten Prodrug wurde mittels HPLC-Messungen untersucht.

Zusammenfassend wurde erfolgreich ein neues Triggersystem für die cathepsin-selektive Aktivierung entwickelt und ein Prodrug-Konzept für den Tyrosinkinase-Inhibitor Crizotinib etabliert.

Table of Contents

I. INTRODUCTION

Cancer is defined as malignant tissue neoformation, which is characterized by unregulated cell growth and destructive invasion of surrounding tissue. Next to cardiovascular diseases, cancer is the second leading death cause in Europe. With a world population amount of 11%, the European countries carry 25% of cancer incidences worldwide, which can be attributed to the high life expectancy. The total amount of cancer related deaths in Europe in 2012 was 1.75 million people.[1] In Austria about 38 000 people are diagnosed with cancer each year, with men being slightly higher affected than women.[2] While prostate cancer shows the highest incidence rate for men, the highest mortality rate belongs to lung cancer (Figure 2). A similar deviation between incidence and mortality is visible for ovary cancer in women displaying the highest incidence rate of 30%. Ovary cancer, however, is not found in the top 5 mortality cancer deaths (Figure 2).

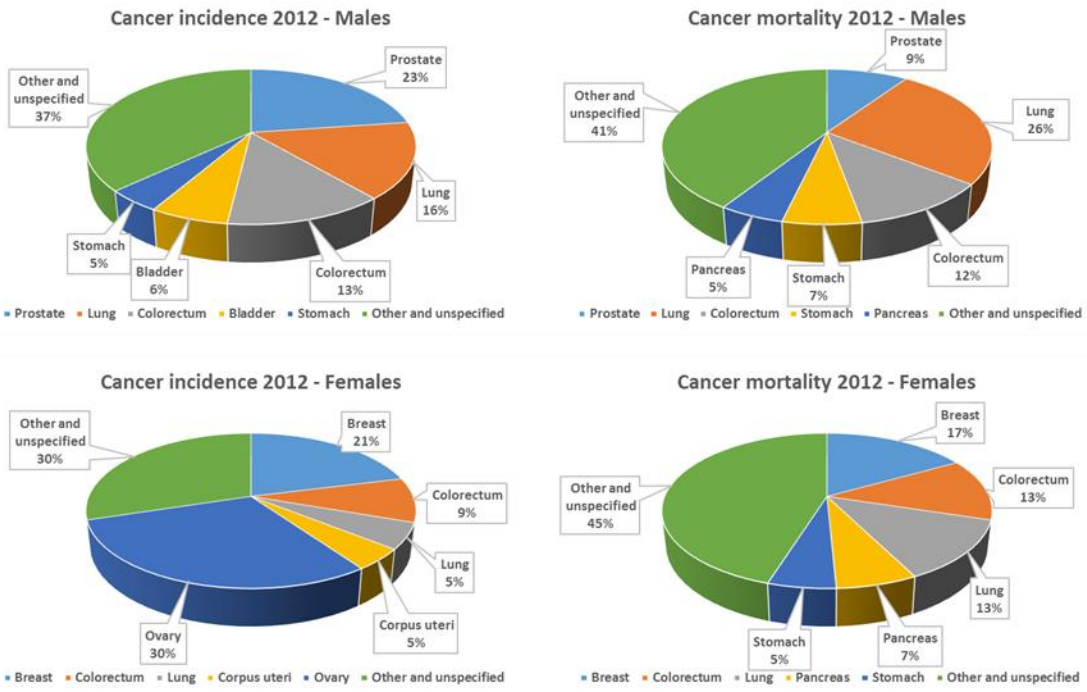

Figure 1 - Estimated cancer incidence and mortality rates for men and women in 2012 in Europe[1]

a. Cancerogenesis

The development of solid cancer is closely related to the abnormal formation of neoplastic tissue known as tumorigenesis. Tumorigenesis is characterized by the loss of regulative control of proliferation and apoptosis in somatic cells.[3] This loss may be caused by changes in the genome (mutation) or epigenetic factors (aberration in gene expression). Former describes mutations of the genome like point mutation, frame shift mutations, deletions or translocations which alter the genetic sequence. These changes mostly result in apoptosis. If a genetic mutation does not lead to apoptosis, this mutation is called stable and inherited to following generations. By this, stable changes in the genome can raise the probability of cancer incidences for succeeding generations as known for colon cancer[4]. The second process included in cancerogenesis is epigenetic modification. Epigenetic changes do not lead to modifications in the genomic sequence but to differentiation in gene expression. The molecular backgrounds of this process are DNA methylation (gene hyper- and hypomethylation) or chromatin condensation. In case of cancer, epigenetic gene aberration can provide the activation of oncogenes or the silencing of tumor-suppressor genes.[5] In difference to genetic changes, epigenetic changes are just passed down via mitosis and partially deleted at fertilization. Combining both processes, the epigenetic progenitor model of cancer, shown in Figure 2, describes the evolution of a cancer cell from so called progenitor cells. Progenitor cells are intermediate stage cells which can act like stem cells but are already more specified.[6] According to this model, the genetic pool of progenitor cells is altered by genetic and epigenetic changes in tumor promotor genes, oncogenes or tumor suppressor genes. Uncontrolled proliferation and, by this, the development of benign tumors (cell clusters without the ability to invade into surrounding tissue) is strongly related to so called gate-keeper mutations (GKM). Gate-keeper genes encode proteins which stabilize cell growth and proliferation. Further changes concerning oncogenes and tumor suppressor genes lead to the development of primary cancer cells which gained the ability to invade surrounding tissue. Increased aberrations may also lead to increased genetic and epigenetic plasticity. By this, cancer cells gain abilities like increased invasion potential (e.g. into bone), metastasis or drug resistance. The previously described changes in tumor suppressor genes and oncogenes vary for every specific cancer type. Despite

its enormous diversity, Hanahan and Weinberg proposed six different hallmarks of cancer which cells must acquire to transform into cancerous cells. The six hallmarks of cancer include sustaining proliferation signaling, evading growth suppressor genes, resisting cell death, enabling of replication immortality, inducing angiogenesis and the activation of invasion and metastasis.[7]

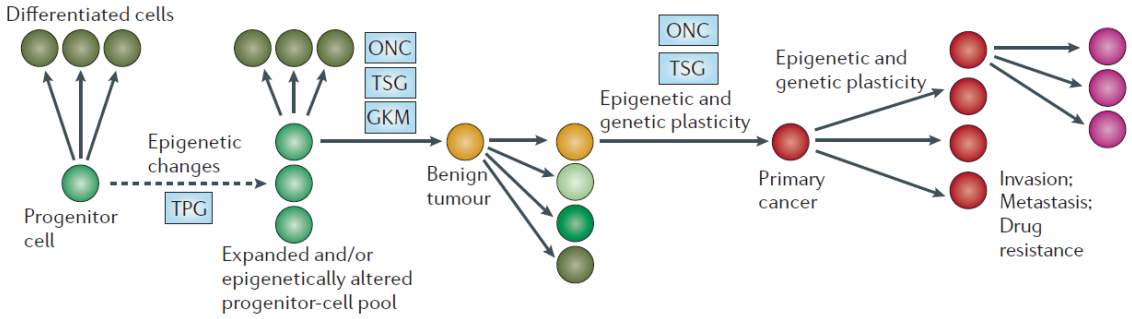

Figure 2 - The epigenetic progenitor model of cancer (ONC – oncogene, TSG – tumor suppressor gene, TPG – tumor promotor gene, GKM – gatekeeper mutation)[8]

b. Cancer Therapy

The commonly used clinical treatment strategies against cancer are surgery, radio- and chemotherapy. Surgery is usually the first treatment used to remove primary tumors, but limited by tumor size and location. Radiotherapy is a local therapy and mostly used in adjuvant therapy to reduce the size of a tumor before surgical removal. Chemotherapy is a systemic treatment with antiproliferative or cytotoxic substances to remove metastases as well as solid tumors and non-solid tumors. Several different classes of chemotherapeutic drugs are known and introduced in the following pages.

Alkylating agents

In the 1940s, Goodman and Gilman used nitrogen mustard in a systemic approach to tread advanced non-Hodgkin lymphoma.[9] This became commonly known as the birthmark of modern chemotherapy. Following studies showed that nitrogen mustards form DNA crosslinks and, by this, induce apoptosis. This observation lead to the development of different nitrogen mustards which are still applied in common antitumor regimens like mechlorethamin (Morbus Hodgkin) or chlorambucil (chronic lymphatic leukemia).

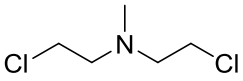

Mechlorethamin

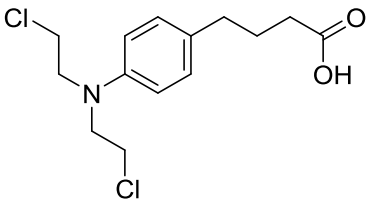

Chlorambucil

Antifolates

A further approach for anticancer therapy was developed by Sidney Farber in the late 1940s. Administering the vitamin folic acid to children with megaloblastic anemia seemed to stimulate proliferation of the acute lymphoblastic leukemia (ALL). Hence, the administration of folate analogues was thought to block folate-requiring enzymes. One representative of those antifolates is methotrexate which showed brief but significant remissions in children with ALL.[10] Eight years after the discovery of its antiproliferative effect, methotrexate was the first single component cancer therapy agent curing a patient[11]. Another sixteen years later, methotrexate was used in combined therapy with leucovorin (another antifolate) after surgical removal of the primary tumor as first adjuvant therapy.[12] The activity of antifolates remains on the active transport into the cell via the reduced folate transporter 1 (RTF1) and the inhibition of

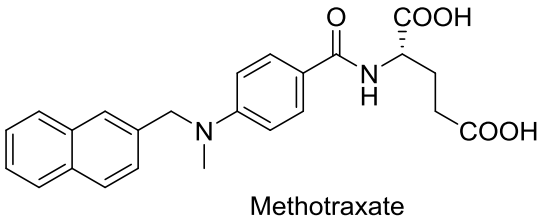

Methotraxate

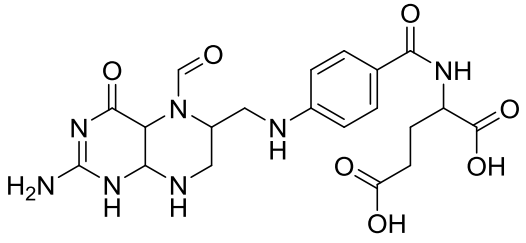

Leucovorin

the enzyme dihydrofolate reductase (DHFR) responsible for the synthesis of thymidylate and purines. Mutations in this pathway lead to drug resistance against antifolates, which was the beginning of a deeper understanding of drug resistance mechanisms as well as tumor biology[13].

Antimetabolites

Antimetabolites are derivatives of cell metabolites which are important for DNA and RNA synthesis. First reported in the 1950s, Hitchings and Elion studied purine derivatives such as 6-mercaptopurine which are incorporated into DNA instead of normal purine leading to cell growth inhibition.[14] It was shown, that already small differences in the structure of cell metabolites can lead to inhibition of proliferation and growth of a cell. In cancer treatment, antimetabolites are typically part of adjuvant therapies. For example, 5-fluorouracil is included in the therapy of colon cancer, resulting in remarkably extended life spans, for patients with metastases in the lymph nodes after surgical removal of the primary tumor.[15] In addition, antimetabolites in combination with other therapeutics can circumvent drug resistance development, which was first shown in 1965 using the POMP regimen [methotrexate (antifolate), vincristine (a Vinca alkaloid), 6-mercaptopurine (antimetabolite) and prednisone (immunomodulator)].[16]

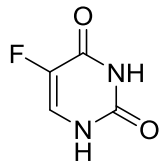

5-Fluorouracil

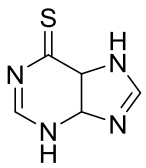

6-Mercaptopurine

Natural products

In 1955 the National Cancer Chemotherapy Service Center (NCCSC) was founded at the National Cancer Institute (NCI) to focus research on drug discovery and screening programs. One outcome of the NCCSC was the screening of natural products out of plant and microbial metabolites. Based on this screening program new substance classes were discovered, for example the plant derived product classes of taxanes (in 1964) and camptothecins (in 1966) or the microbial derived product classes of anthracyclines like doxorubicin and daunorubicin. Best known representatives of the plant derived taxane group are paclitaxel and its semisynthetic

analogue docetaxel. The biological mode of action of taxanes is the stabilization of microtubules, which leads to mitotic cell arrest.[17] The class of camptothecins (e.g. irinotecan) are topoisomerase I inhibitors.[18] Topoisomerase I is responsible for the relaxation of the DNA double-strand by breaking one DNA strand during DNA synthesis. Inhibition of Topoisomerase I leads to DNA double strand breaks and results in apoptosis. The microbial derived anthracyclines are the best known and clinical tested natural product antitumor agents. One representative is doxorubicin which acts as intercalator into DNA strands and, by this, as inhibitor of topoisomerase II as well as generator of free radicals. Topoisomerase II is also responsible for DNA relaxation, but unlike Topoisomerase II it breaks both DNA strands during DNA synthesis. Free radicals damage DNA, the cell membrane and proteins which leads to apoptosis.[19]

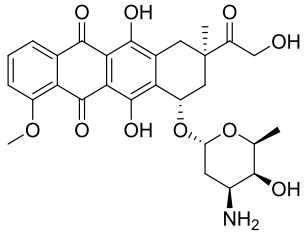

Doxorubicin

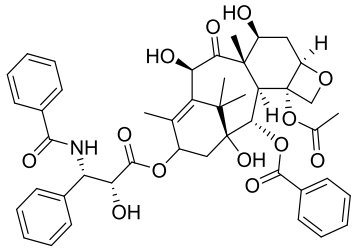

Paclitaxel

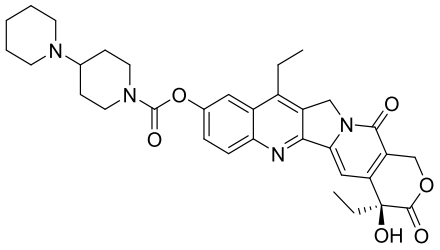

Irinotecan

Metal based anticancer drugs

The discovery of the antiproliferative effects of cisplatin by *Rosenberg et al*. in 1965[20] was the beginning of transition metal based cancer treatment. Having different kinetic properties and mechanisms of action than conventional pure organic drugs, the three platinum based anticancer drugs cisplatin, oxaliplatin and carboplatin approved by the US Food and Drug Administration (FDA) are in worldwide clinical use for the treatment of a broad number of cancer types. Platinum compounds mainly form intrastrang or interstrang DNA adducts like bifunctional alkylating agents, but additionally inhibits enzymes like telomerase.[21] Furthermore, DNA

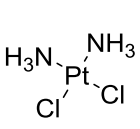

cisplatin

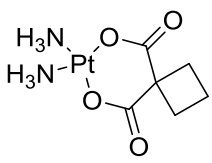

carboplatin

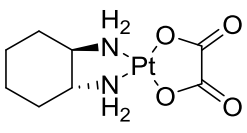

oxaliplatin

damage induces point mutations in the cells genome leading to apoptosis in fast dividing cells. However, as for most of the chemotherapeutic drug, severe side effects like nephrotoxicity (cisplatin), neural toxicity (oxaliplatin) or bone marrow suppression (carboplatin) are dose limiting factors.[21]

Targeted therapeutics

In the last decades the deeper understanding of tumor biology was the key step of changes in paradigm in anticancer research. Recent research focuses on small differences between tumor cells and normal cells, which shall be used to selectively affect neoplastic tissue. The differences of normal cells and cancer cells include changes in a cells phenotype like overexpression of proteins or receptor genes (hallmarks of cancer). Main goal of the so-called targeted therapy is to exploit these phenotypic changes in therapeutic approaches. Famous representatives of targeted therapeutics are the tyrosine kinase inhibitor imatinib (Gleevec®) which is used against different tumor classes like chronic myeloid leukemia (FDA approval in 2001) or gastrointestinal stromal tumor (2012) and the epidermal growth factor receptor (EGFR) inhibitor erlotinib (Tarceva®) used against non-small cell lung cancer (2004) or pancreatic cancer (2005).[22]

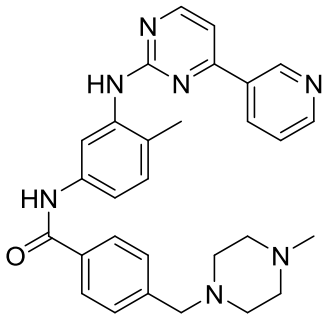

Imatinib

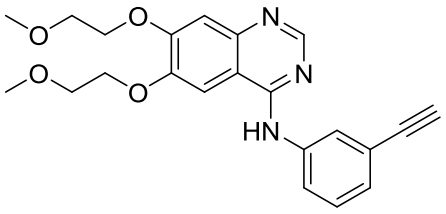

Erlotinib

c. Side effects

Despite the wide range of different cancer treatment approaches, chemotherapy still remains a highly aggressive procedure including adverse effects like nephrotoxicity, cardiotoxicity, nerve toxicity, bone marrow toxicity or strong nausea. Main reason is the lack of selectivity to cancer cells of conventional chemotherapeutics, which mainly act against all fast dividing cells. The expectation on targeted therapeutics was a more specific effect on targets involved in cell-

growth, proliferation or metastasis of cancer cells, and consequently reduced side effects.[22] However, also for this kind of therapeutics, still severe side effects occur, especially adverse effects closely related to the specific targets. For instance, the EGFR is highly overexpressed in various cancer types and, by this, an important target. However, as the EGFR is also expressed during the epidermis differentiation, treatment with EGFR inhibitors lead to severe skin reactions called *papulopustular rash*.[23]

Concluding, cancer development underlies genetic and epigenetic changes of an organism's genome and, by this, there are nearly no completely tumor specific targets to attack and side effects will emerge intrinsically. Thus, strategies to reduce the (severe) side effects of anticancer drug treatment are of high importance.

II. THE PRODRUG CONCEPT

One attempt to reduce adverse effects of common chemotherapeutics is their inactivation in the healthy tissue and selective release at the tumor site. This release can be triggered by various differences between the tumor microenvironment and healthy tissue. The approach of inactivating a drug until specific activation at the desired tissue is called “Prodrug” concept. Several different approaches to specifically release a drug are described in literature like the release due to overexpression of enzymes, reduced oxygen content (hypoxia), low pH values and an altered redox status.[24]

The common structure of a prodrug consists of three different compartments:

1. trigger unit (responsible for the cancer-selective activation of the drug)
2. linker unit (separates the drug from the trigger unit)
3. drug (diagnostic or therapeutic)

The selectivity of the trigger event is the main characteristic of the prodrugs efficiency to decrease the side effects of the active compound. After the trigger event the linker decomposes and releases the active compound spontaneously, evolving the anticancer effect of the drug. Hence, the crucial steps for activation of the prodrug are the trigger event as well as the chemical stability of the linker-drug bonding. Thus, a deeper understanding of the chemical properties of linker and trigger are essential in rational prodrug design and are described in detail below.

a. Linker

Early trials with directly bound drug-trigger conjugates showed disadvantages in stability being either too labile against hydrolysis (e.g. esters) or being too stable (e.g. amides or ethers) to be selectively cleaved at the tumor site. Linker moieties promise an elegant way to attach a trigger and deactivate the drug. The trigger event should induce self-immolation of the coupled linker with release of the drug.[25] Main requirement for linker selection are the release kinetics as well as the choice of functionalities used for coupling between trigger unit and drug. By this, a linker moiety also gives the opportunity to introduce chemical functionalities which are possibly not available at the parent drug e.g. amino, hydroxyl or thiol groups. Self-immolation can be achieved by two different modes of action: cyclisation or elimination. The cyclisation approach is based on a nucleophilic attack of an unmasked nucleophilic functional moiety of the linker unit. The unmasked group can be a hydroxyl group, a thiol or a secondary amine, attacking carboxylic or carbonic esters as well as carbamates or amides. Major force of the drug release is the development of a five- or six-membered ring with a lactamic, lactonic, ureatic or carbamatic moiety. Two cyclisation linker strategies are depicted in Figure 3: (A) a 2-hydroxyphenyl propionic acid based linker[26] which builds an intramolecular lactone during the self-immolation process and (B) an ethylene diamine linker which forms imidazolidinones[27] (B). The second option for self-immolative linkers is based on elimination reactions, also called “electronic cascade linkers”. In contrast to cyclisation strategies this kind of drug release process includes the formation of compounds containing at least one double bond. Electronic

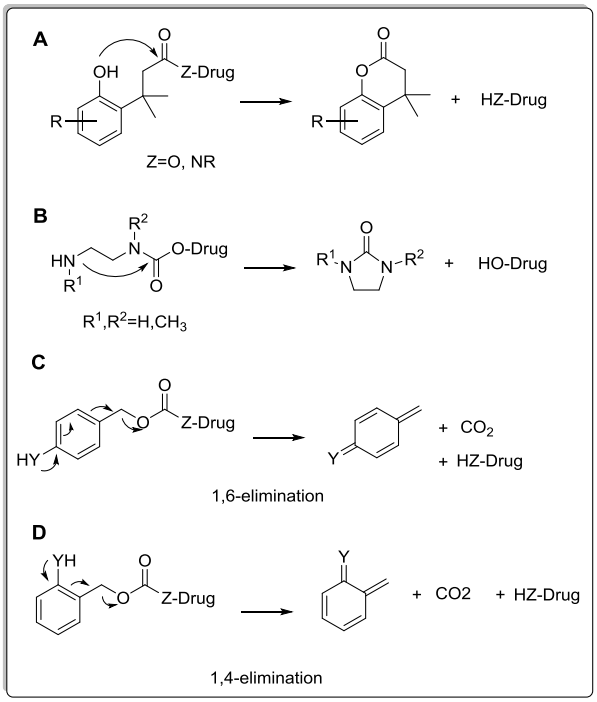

Figure 3 - Self-immolation linker strategies based on cyclisation due to lactonisation (A) or imidazolidinonation (B) and elimination linkers based on 1,6- (C) and 1,4-elimination (D).

cascade linkers are attached to a desired drug by oxycarbonyl groups (free carbamic acids or carbonates) as well as hemiaminals or hemiacetals.[28] Classical self-immolative electronic cascade linkers are based on 1,4- or 1,6-benzyl elimination reactions forming ortho- or para-quinone methides (Figure 3). The formed quinone methides are quenched with nucleophiles like water. One of the most important and efficient self-immolative linker moieties is the *para*-aminobenzyloxycarbonyl (PABC) system which was first described by Katzenellenbogen *et al.* in 1981.[29] PABC is an aniline based linker system which elimination proceeds rapidly under physiological conditions after the trigger activation, making this moiety a valuable tool for prodrug design. To raise the aqueous solubility of the linker molecule, one carbon atom of the ring system can be substituted by a nitrogen atom without diminishing the release kinetics of the system.[30]

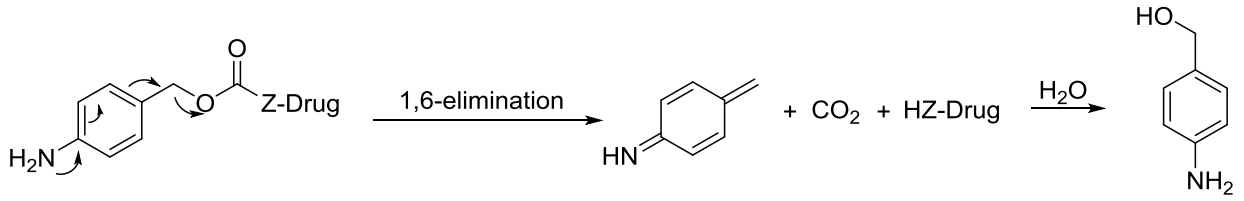

b. Trigger

Since elimination events can be easily triggered by unmasking the nucleophilic groups of the linker moiety, many different kinds of activatable units were reported in literature. However, the trigger moiety should merge the knowledge of tumor biology with chemical drug design. Thus, while many different trigger systems are described in literature, a high selectivity for the tumor tissue is still a challenging task. The currently most promising activation strategies can be divided into several different topics:

Hypoxic activation

Due to insufficient vascularization caused by rapid growth of tumor tissue, in solid tumors often reductive and hypoxic conditions prevail. The state of hypoxia is different for every type of tumor ranging between 30% of the oxygen concentrations of healthy tissue in head and neck cancer down to 5% in pancreatic tumors.[31] The insufficient vascularization leads to low nutrient and oxygen levels and induces the expression of bioreductive enzymes or angiogenic growth factors. A chronic or acute severe hypoxic state seems to be a unique characteristic of tumor cells which can be used for specific drug activation. The activation is caused by enzyme-based electron transfer mechanisms as visualized in Figure 4. For hypoxia-activated prodrug design several different trigger strategies were developed using various activation mechanisms. Most advanced representatives are the class of nitroaromatics which are activated by several non-specific reductases like flavoproteins.[32] The nitro radical anion intermediates of the nitroaromatic reduction can be scavenged by molecular oxygen under normoxic conditions restoring the initial molecule. However, under hypoxic conditions the nitro radical anion is irreversibly reduced to the hydroxylamine ($4e^-$-transfer) or the corresponding amine ($6e^-$-transfer). The reduction potential of nitroaromatic compounds ideally ranges from –450 to –300 mV to be activated by bioreductive enzymes.[32] The most advanced representative of nitroaromatics is the 2-nitroimidazole phosphorus amide mustard TH-302 (Figure 5), currently undergoing clinical phase III trials in combination with gemcitabine against pancreatic cancer.[33]

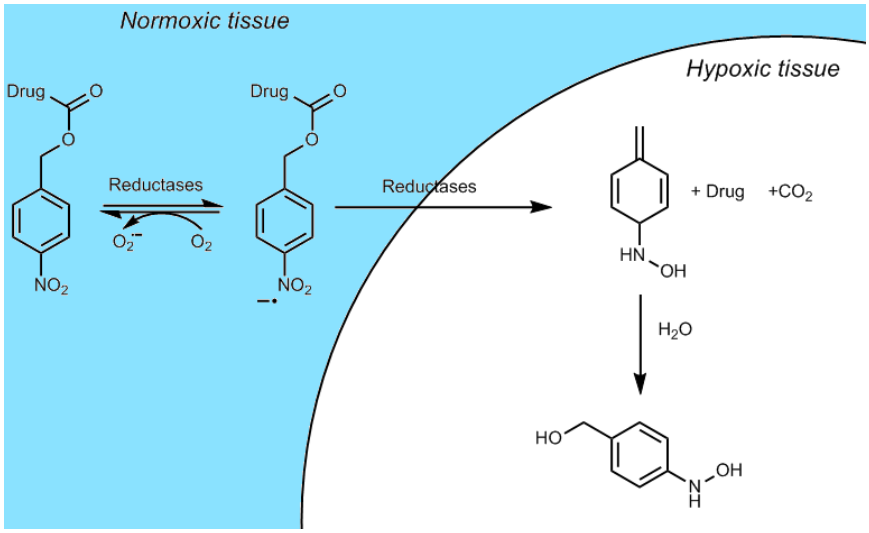

Figure 4 - Schematic activation of hypoxia-activatable prodrugs catalyzed by reductases under normoxic (blue) and hypoxic (white) conditions.

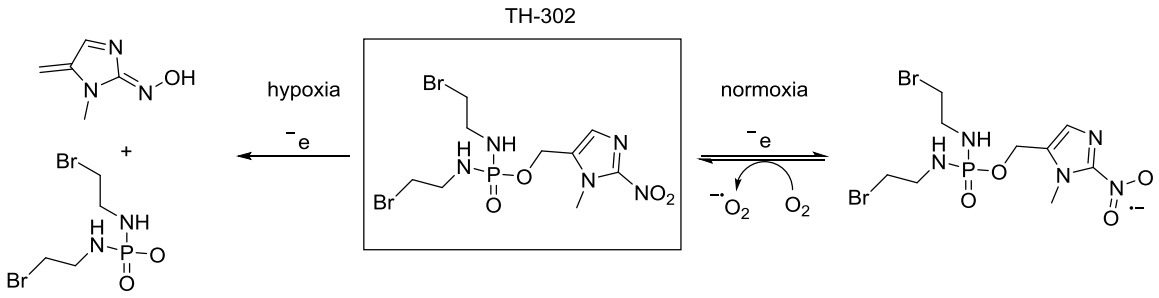

Figure 5 - Reactions of TH-302 under normoxic conditions with oxygen as radical scavenger and under hypoxic conditions undergoing fragmentation

Oxidative activation

Cancer cells are known to exhibit increased oxidative stress leading to high concentrations of reactive oxygen species (ROS) such as peroxides, superoxides or hydroxyl radicals. Usually, the production of ROS occurs in the cell respiratory system of mitochondria. However, their production is highly upregulated in tumor cells e.g. by the activation of oncogenes like *c-myc*[34], cell aging[35] or telomere dysfunction associated with affected mitochondrial functionality[36]. The high levels of ROS can be exploited for oxidative activation of trigger systems, e.g. using boronic acid-based trigger systems schematized in Figure 6.

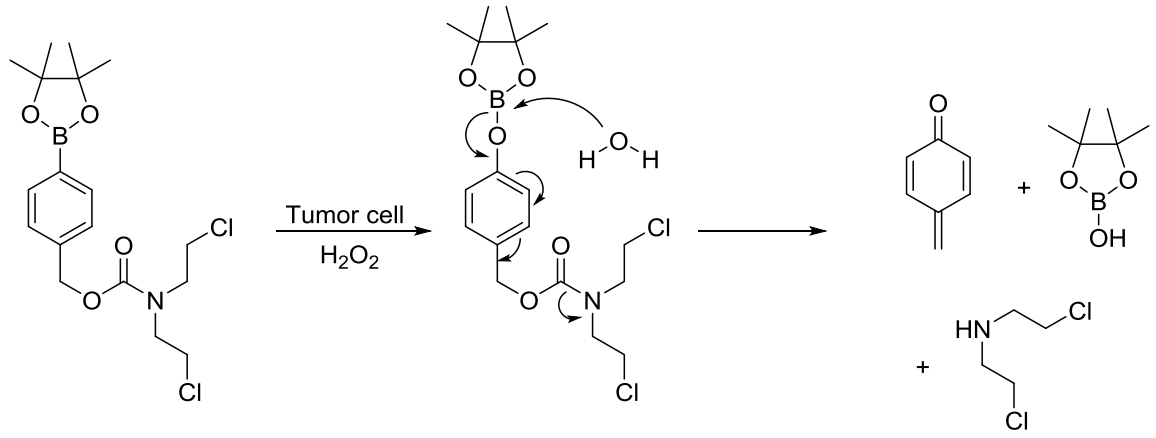

Figure 6 - Oxidative activation of a boronic acid-based trigger system to release a nitrogen drug

pH-dependent activation

Due to anaerobic glycolysis under the hypoxic conditions of the tumor tissue the extracellular environment of cancer cells is often acidic and reaches pH values of 4.5 to 6.5. This decrease of 1.0 to 2.5 pH units can be used in rational prodrug design using acid cleavable bonds (Figure 7). Although, there are several examples evaluated in macromolecular or dendrimeric prodrug design like the human serum albumin directed doxorubicin prodrug aldoxorubicin[37], this type of activation is not reported to be in therapeutic use for small molecules. Most likely the reason is, except for aldoxorubicin-type prodrugs, that it is difficult to find an optimal balance between stability and selective activation.

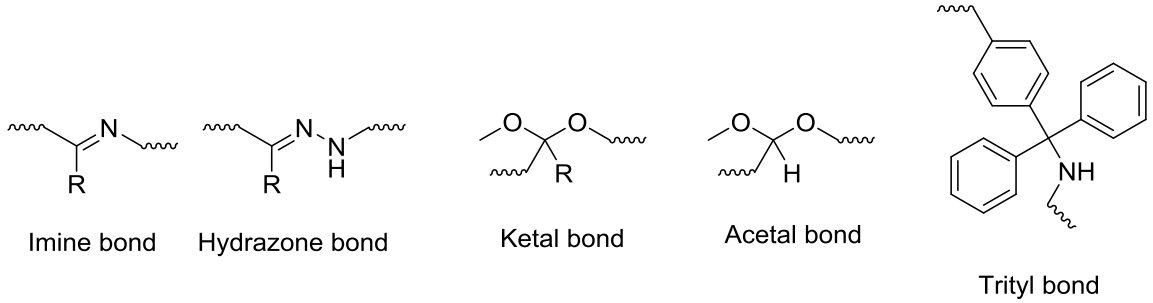

Figure 7 - Acid sensitive chemical bonds applicable for drug targeting of low pH values

Reductive-activatable prodrugs

A further approach is the usage of the thiol containing tripeptide glutathione as trigger. Next to its antioxidative effect, the major biological function is the detoxification of xenobiotics. The glutathione concentration is highly upregulated in some cancer cell lines which is directly related to chemoresistance and tumor progression.[38] Some models of small molecule thiol cleavable

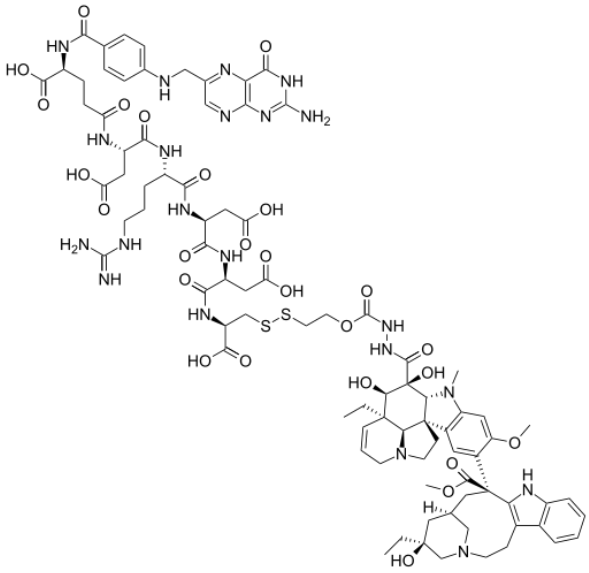

Figure 8 - Structure of vynfinit®

prodrug triggers based on aromatic sulfonic acids[39] or 2-methyl-3-phenacrylate[40]are tested in preclinical evaluations, but up to today there are no examples in clinical trials. However, the use of disulfide bridges which are also activated mainly by glutathione is well established for conjugates in targeted prodrug therapy. One example in clinical investigation is vynfinit® using folic acid as carrier for a Vinca alkaloid linked via a disulfide bond which is cleaved reductively inside tumor cells.

Enzymatic and biocatalytic activation

One famous representative of an enzymatically activated prodrug in cancer treatment is capecitabine, a masked derivative of the antimetabolite 5-fluorouracil, approved by the FDA in 2005 for colorectal cancer and metastasized breast cancer.[41] However, capecitabine is not only activated by tumor-specific enzymes. First the prodrug is metabolized in three steps including deesterification by human carboxylesterases CES1 and CES2 (Figure 4). The so formed carbamic acid spontaneously decomposes to 5'-deoxy-5-fluorocytidine.[42] Further metabolism is performed in the liver or in tumors by the enzyme cytidine deaminase (CDA) to produce 5'-deoxy-5-fluorouridine. Only in the last step for final release of 5-fluorouracil the tumor-related enzyme thymidine phosphorylase (dThdPase) is involved.

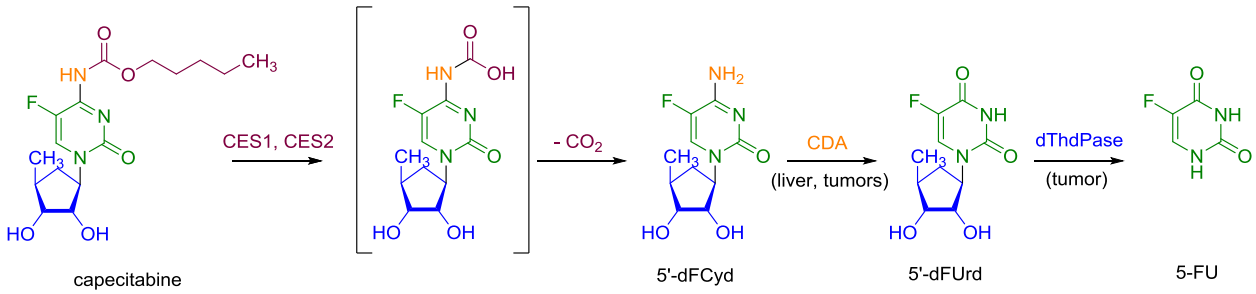

Figure 9 – Degradation steps of capecitabine as example for enzyme activated prodrugs

Recent prodrug approaches focus on the usage of enzymes with higher substrate specificity and high expression in tumor tissue, for example proteases. One example of the therapeutically use of proteases is the cathepsin B cleavable antibody doxorubicin conjugate (ADC) brentuximab

vedotin approved 2011 for treatment of Hodgkin Lymphoma (HL) as well as systemic anaplastic large cell lymphoma.[43] Brentuximab vedotin contains a monoclonal antibody against the CD30-antigen, which is linked to the potent antimicrotubule agent MMAE (monomethyl auristatin E) via a cathepsin B cleavable trigger and a PABC moiety (compare section IIa). Binding of the antibody moiety of brentuximab vedotin to its corresponding antigen leads to internalization of the drug via lysosomes, where cathepsin B releases the drug via proteolytic cleavage. Free MMAE binds to tubulin and disrupts the microtubule network leading to apoptosis.

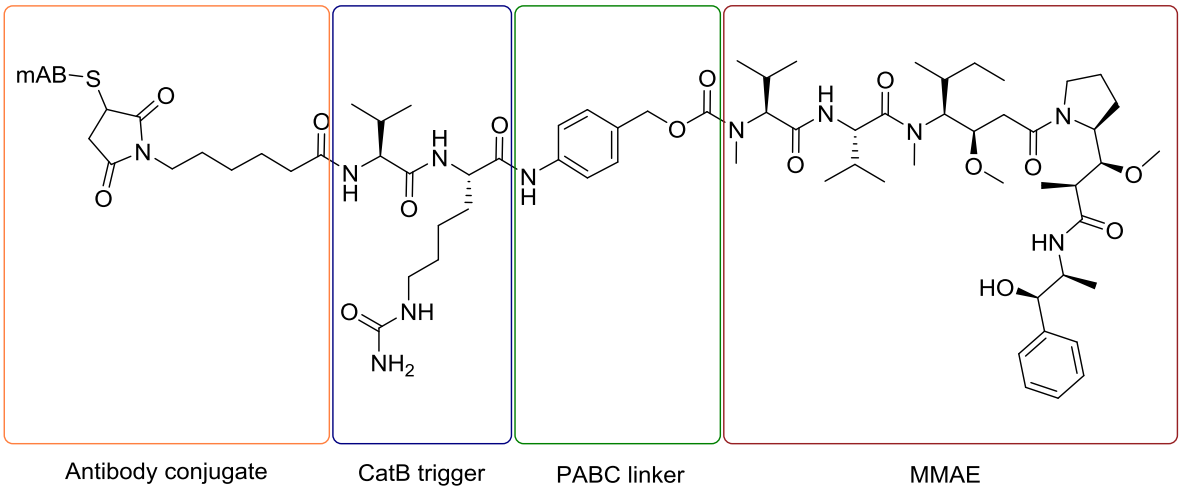

Figure 10 - Structure of brentuximab vedotin®

c. Drugs

As neither the trigger unit nor the linker is able to kill cancer cells, the efficacy of prodrug treatments remain on the masked drug. Main criteria for the use of potentials drugs in prodrug therapy are the cytotoxicity of the drug, its mode of action, potential resistance mechanisms, the activation site of the drug, the ability to effect surrounding cells (bystander effect) as well as, of course, the ability to reach its site of action. A main criterion for the activity of the drug is the activation site of the prodrug. The prodrug can be activated outside of the cell or inside the cell in endosomes, lysosomes or after passive diffusion in the cytosol. Extracellular activation of intracellular active agents without the possibility to enter the cell and vice versa leads to ineffectiveness of the used therapeutic. Cell-uptake can be achieved by several processes including passive diffusion through the cell membrane, endocytosis, pore-forming receptor uptake or phagocytosis. By this, the choice of the right drug according to its activation site is crucial for the activity of the prodrug. Typically, the drug is a cytotoxic compound in the nanomolar range intervening in survival essential processes like proliferation and cell division like cytokines, anti-apoptotic pathways, DNA replication or protein synthesis.

The main challenge in the development of a prodrug is the combination of a suitable trigger with a highly effective drug combined with a stable linker. Though, there are some examples which are already in clinical trials, there is still a high demand for the development of selective tumor activated drugs, especially in the development of selective trigger units. The most interesting questions in future research will be: Are there additional differences between cancer cells and healthy cells which can be utilized in prodrug development? And if yes, are they suitable to be exploited in a selective way?

III. PROTEASES IN CANCER

Developing the potential of invading surrounding tissue and metastasis is the key step of the morbidity and, finally, mortality rates of cancers. The genetic and epigenetic changes of cells promoting these abilities are accompanied with the overexpression or translocalization of enzymes like proteases. Proteases are enzymes which are able to hydrolyze peptide bonds. The class of proteases can be divided into 4 different sub-classes: serine, tyrosine and aspartic proteases as well as metalloproteinases. In cell biology proteases are involved in many physiological processes including digestion, growth, differentiation, cell signaling or apoptosis.

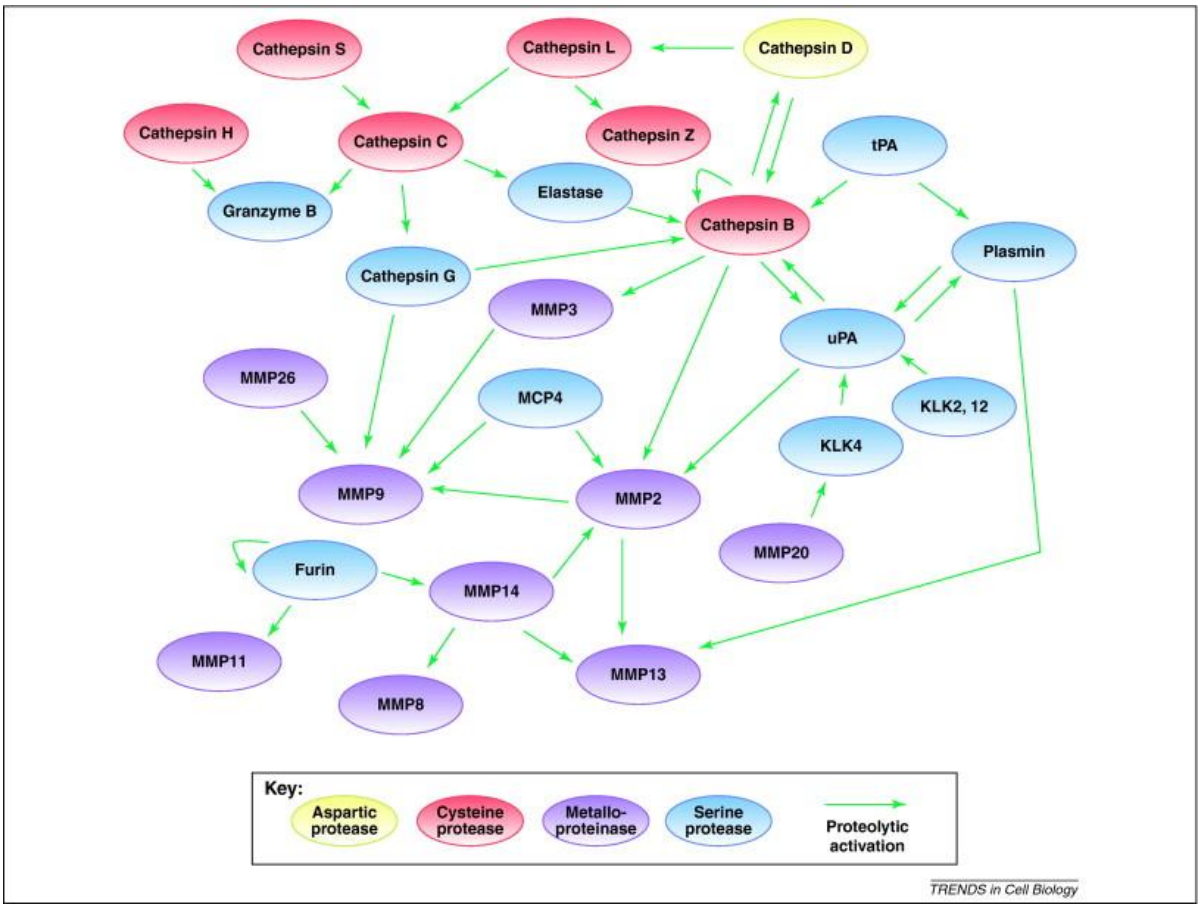

Figure 11 - Overview of the activation interactions network between different kinds of proteases [45]

Altogether, 570 different human proteases[44] are known with a complicated bilateral interaction network (Figure 11). Their activities are regulated in a complex and sensitive activation and

inhibition process, including activation by other proteases, extracellular signal pathways or natural small molecule inhibitors. A small overview of the interplay between the different kinds of proteases is visualized in Figure 11. The best studied representatives of proteases include the families of caspases, cathepsins, matrix metalloproteinases (MMPs) and the urokinase-type plasminogen activator (uPA). Recent research provided evidence that several kinds of proteases show high activity in various cancer types and this is directly related to the expression of cancer related phenotypes (hallmarks of cancer). Thus, these proteases are valuable targets in cancer treatment (for inhibitors) or, more recent, as trigger systems in anticancer prodrug design. The most prominent proteases in different kinds of tumors are the cathepsins B, H, L and S, the MMPs 2, 14 and 22 and uPA.[45]

a. Cathepsins

The class of human cathepsins can be divided into 3 subgroups: aspartic (cathepsin D and E), serine (cathepsin A and G) and cysteine proteases (cathepsin B, C, F, H, K, L, O, S, V, W and Z). The eleven cysteine cathepsins belong to the papain subfamily of cysteine proteases and are relatively small monomeric enzymes with M_w of around 30 kDa, except of cathepsin C (a tetrameric enzyme) with 200 kDa. The active centers consist of an activated cysteine residue with a pK_a of 2.5–3.5 (instead of 8.7 as intrinsic pK_a value of free cysteine). Activation of the cysteine residues are performed by interaction of the thiol groups with imidazole residues of a neighbored histidine resulting into thiolate-imidazolium ion pairs. Originally, the cysteine cathepsins were thought to be primarily located intracellular in lysosomal vesicles and take part in the cellular protein turnover.[46] However, further research on cysteine cathepsins showed crucial differences in location and expression levels of cathepsins. Next to its localization in endosomes and lysosomes, cathepsins were found to be ingredients of membrane microdomains to degrade components of the extracellular matrix (ECM)[47] or secreted (in a proactivated or active form) into the ECM.[48] As an example cathepsin K is secreted into the extracellular space between osteoclasts and bone during bone remodeling processes with collagen as natural substrate. By this, the distinct function of cathepsins and its substrates

might change with its localization. Knockout studies of several cathepsins showed distinct roles for every single cathepsin. While cathepsin B or L are expressed ubiquitous, the expression of some cathepsins seems to be highly regulated in specific cell types like cathepsin K in osteoclasts or cathepsin S in immune cells. Cathepsin B deficient mutants phenotypically sparely differed from wild-type mice, however they showed reduced tumor-necrosis-factor (TNF)-induced apoptosis[49] as well as resistance against experimental pancreatitis[50]. Knockout studies of cathepsin K causes pycnodysostosis, a rare bone disease causing high bone density.[51] Cathepsin L deficient mice showed epidermal dysplasia, periodic hair loss as well as cardiomyopathy in higher ages. While mice with single knockout mutations of any cysteine cathepsin were mobile and fertile, mice deficient in two cathepsins for example B and L died shortly after birth due to severe brain atrophy, indicating redundant cross action of both enzymes in the central nervous system (CNS).[52] Though, not all processes including cathepsins in cell biology are currently known.[53]

b. Substrate Specificity of Cysteine Cathepsins

Substrate specificity and turnover is a crucial characteristic of enzymes in vivo to be involved in specific biological processes. But how can all these different cathepsins specifically cleave different peptide bonds? To investigate this, the interaction between the enzyme's active site and the peptides next to the cleaved bond are of interest. For cathepsins the most important amino acids for specificity range from S_1-P_1 to S_4-P_4 (with S as enzyme residue in the active center, P the corresponding amino acid side chain and the cleavage side between P_1 and P_1`; Figure 12). In 2006 *Craik et al.* investigated the substrate specificity of the family of papain like proteases for the first four amino acids.[54] A small outtake of this study is depicted in Figure 13. These cleavage tests showed significant similarity between the cleavage behaviors in position P_1. The most abundant residues in P_1 are the polar amino acids lysine or arginine for cathepsins B, K and L with addition of glutamine and threonine for cathepsin S.

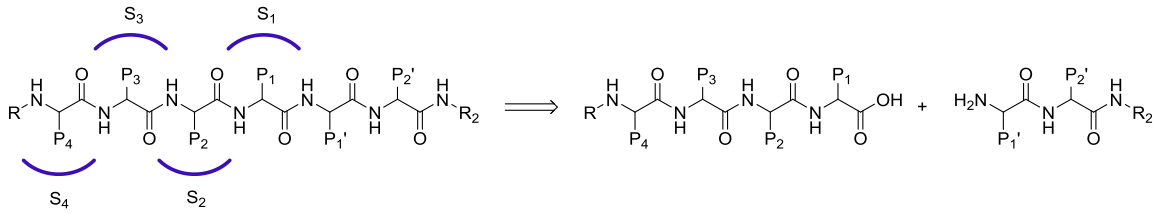

Figure 12 - Hydrolysis of peptide bonds catalyzed by proteases. Interactions of enzyme residues with the peptide chain are symbolized with blue semicircles. S represents enzyme residues, P amino acid side chains.

While the substrate specificity of cathepsin B shows a broad spectrum in P2, cathepsin L prefers aromatic residues like phenylalanine, tryptophan or tyrosine. Cathepsin S and K favor hydrophobic alkane groups in P_2 where cathepsin K has an outstanding preference for proline. While cathepsin K and L shows a broad cleavage array in P_3, substrate specificity of cathepsin B indicates hydrophobic groups and cathepsin S proline or arginine in this position. P_4 seems to be irrelevant for the cleavage specificity of nearly all cathepsins. These results coincide with observations of *Turk et al.* who investigated crystal structures of several cathepsin-substrate complexes and, by this, the structural background of substrate specificity.[55] Cysteine cathepsins are all based on a papain-like structure consisting of two subdomains: R(ight) and L(eft). Detailed investigations of the active centers showed main- and side chain interaction just for the positions S_2, S_1 and S_1'. Furthermore, only position S_2 was revealed to interact with the enzyme through a small pocket determining the S_2 position as crucial for substrate specificity. These studies indicated that the binding pocket is varied in each cathepsin: While in endopeptidases (enzymes cleaving peptide bonds of nonterminal amino acids, like cathepsin K) the whole binding cleft is available for substrate residues, this cleft is blocked at crucial positions in case of the exopeptidases (e.g. cathepsin B at low pH values[56]), which cleave peptide bonds at the end of peptides. Exopeptidases can be categorized into mono- or dipeptidases (e.g. cathepsin C and H) which hydrolyze either single amino acids or blocks of two amino acids in a single cleavage step. For example in case of cathepsin B[57] positively charged histidine residues block the binding cleft (aminopeptidase, hydrolyze peptide bonds from the N-terminus of a peptide), whereas for cathepsin C[58] and cathepsin H[59] these positions are occupied by negatively charged carboxylic groups (carboxypeptidases, hydrolyze peptide bonds from the C-terminus of a peptide).

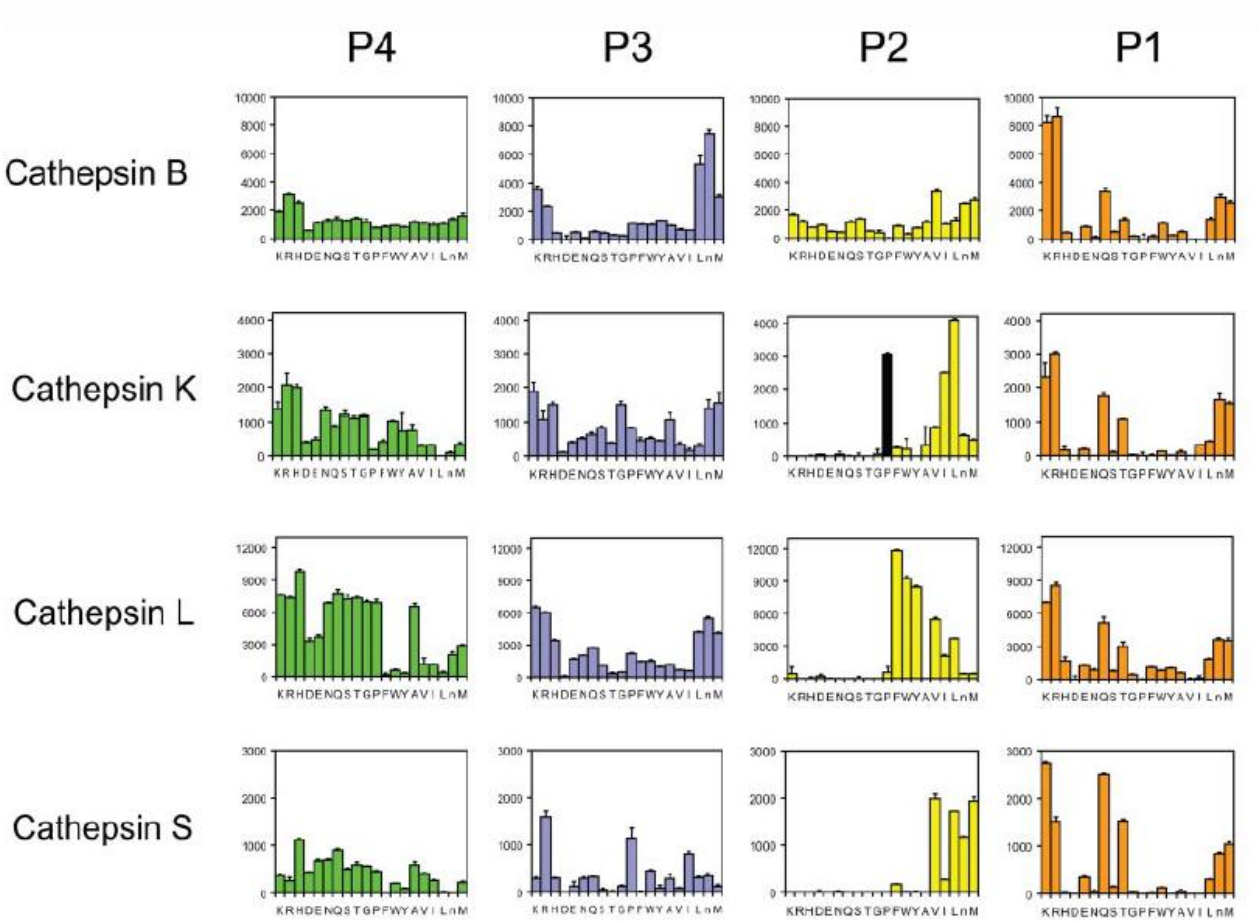

Figure 13 - Substrate specificity studies of cathepsins B, K, L and S. The y-axis represents the picomolar fluorophore amount released after cleavage by the cathepsins per second. The x-axis represents the 20 amino acids in single letter codes with n as norlysin.[54]

c. Cathepsins in Cancer Progression

Cancer development includes several distinct levels from premalignant to the malignant stage. These steps include dysregulation of angiogenesis and invasion, promoted cell proliferation, overcoming apoptosis as well as metastasis. Every mentioned step is related to proteolysis.[45] *Joyce and Hanahan* introduced a mouse model (Rip1-Tag2) for the participation of cathepsins in tumor progression from premalignant to the malignant stage (so far mainly cysteine cathepsins are known to be involved in cancer progression).[60] According to this model (Figure 14), overexpression of cathepsin B and S contribute to premalignant stages by the induction of

angiogenesis due to activation of pro-angiogenic factors or by localized degradation of the basal membrane. In later stages, hyperplasia and the activation/release of pro-growth factors induced by the activity of cathepsin C and Z takes place which lead to exponential tumor growth. Finally, in late stage tumor phases induced by increased activity of cathepsins H and L in cooperation with other cathepsins in addition to enhanced ECM degradation and basement membrane degradation, the proteolysis of cell-cell adhesion proteins like E-cadherin or immunoglubins (Ig) occur. By this, the tumor gains the ability to invade surrounding tissue and transform into invasive tumors. However, currently the distinct roles of every single cathepsin as well as its cross action in cancer progression is not fully understood.

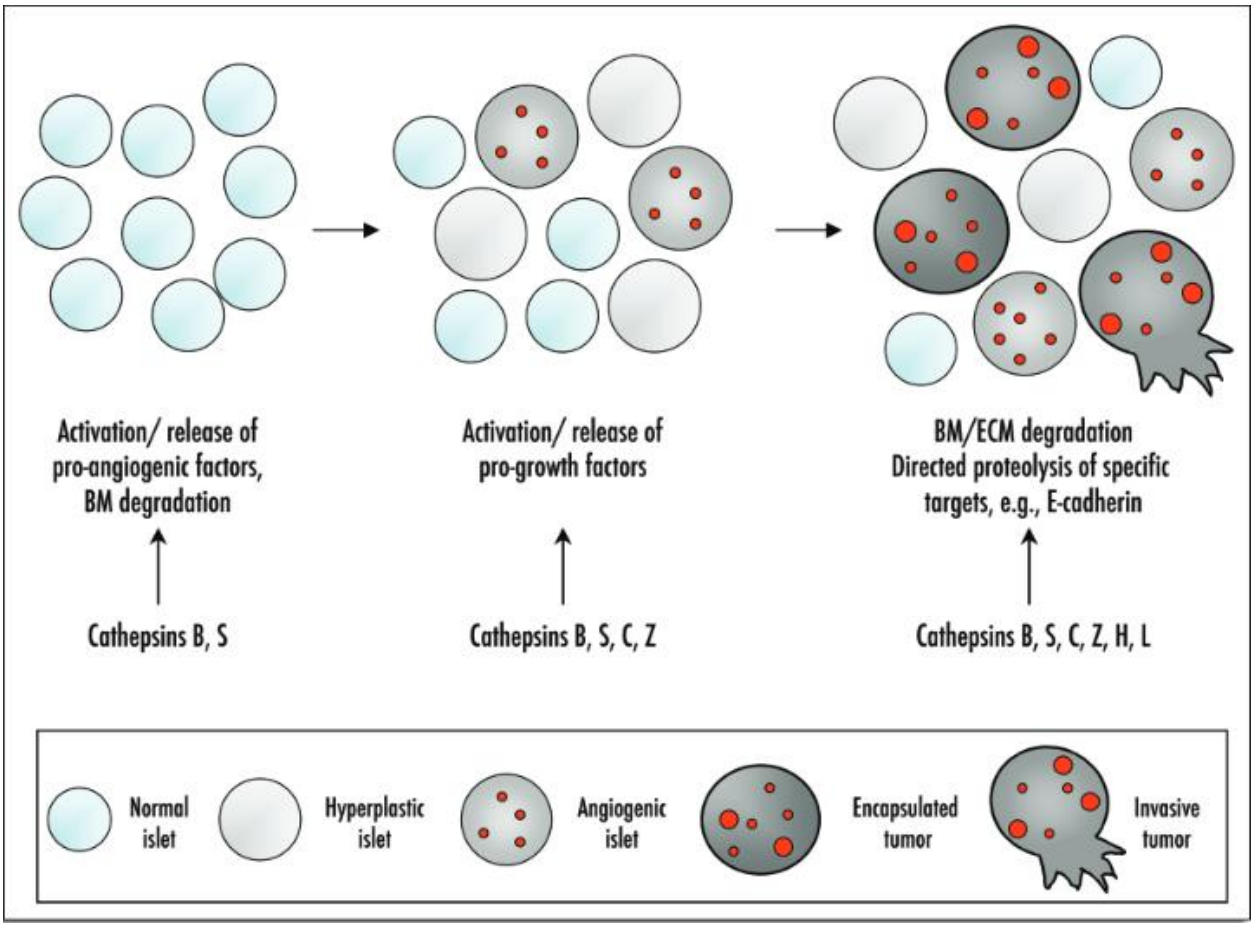

Figure 14 - Tumor formation from normal cells to the malignant state and its correlation with cathepsin overexpression.[60]

IV. AIM OF THE THESIS

The first aim of this master thesis is the development of novel prodrugs with a cathepsin-specific trigger system. As already in detail described in the introduction section IIIb each cathepsin has its preferred amino acid sequence for specific cleavage. To further increase this specificity independently *Turk et al.*[61] and *Bogyo et. al.*[62] used the backbones of cathepsin inhibitors instead of simple amino acids for the development of activity-based probes. Among others, this strategy was described for cathepsin K and cathepsin S.[63] In case of Cathepsin K, the backbone of the clinical investigated inhibitor balicatib (Figure 15A) was used. While the reactive nitrile group at the C-terminal end of the inhibitor balicatib results in a covalent bond with the activated thiol group in the active center of cathepsin K, this functional group was replaced in the activity-based probe (Figure 15B):

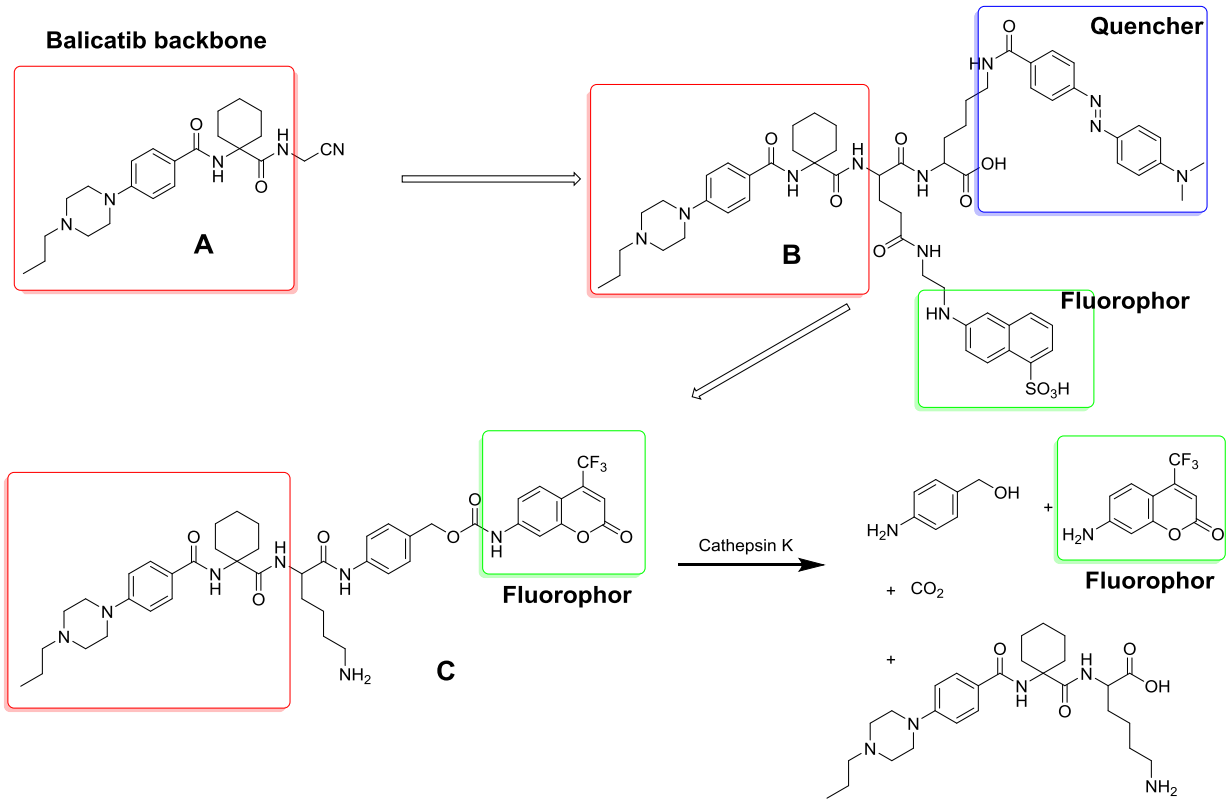

Figure 15 – A) Chemial structure of Balicatib (red); (B) Cathepsin K selective fluorescence probe based on a balicatib backbone (yellow: fluorophore, blue: quencher); (C) strategy for the development of a cathepsine K selective prodrug (red: balicatib backbone, yellow: fluorophore)

On position P1 a fluorophore was attached to a glutamic acid and at P1' a quencher unit to a lysine residue. After selective-cleavage by the cathepsin the quencher is released and the fluorophore is activated. The aim of this master, then, is the modification of this strategy to develop a cathepsin K selective prodrug (Figure 15C). Therefore, again the balicatib backbone was used for high specificity and was coupled to a lysine amino acid as *Craik et al*. showed that lysine and arginine are favored for this enzyme in position P1. In order to provide a spacer between the trigger system and the drug, a para-aminobenzyl alcohol (PABOH) self-immolative linker was implemented in position P1'. Instead of a drug for proof-of-principle studies and later investigations of the release in cancer cells a fluorophore (7-amino-4-trifluoromethylcoumarin) will be used, which fluorescence wavelength is red-shifted after release. Finally, the cleavage behavior of the new "prodrug" with cathepsin K shall be tested by HPLC and fluorescence spectroscopy. The second topic of the master thesis was the development of a general synthetic strategy for the development of prodrugs for the tyrosine kinase inhibitor crizotinib. Crizotinib inhibits the tyrosine kinases anablastic lymphoma kinase (ALK), c-met and ROS1 and was approved for ALK-positive metastatic non-small cell lung cancer (NSCLC) in 2013 by the FDA.[64] Treatment with crizotinib increases the progression-free survival over standard chemotherapy[65], however is also faced with severe side effects. In case of crizotinib, the most common side effects are visual disorders and digestive problems, but also edema, upper respiratory infections and neutropenia.[64] The dose limiting factors are fatigue and increased levels of hepatic transaminases. In order to reduce these adverse effects of single treatment with crizotinib and to provide the possibility of parallel treatment with other kinase inhibitors (which usually results in cumulative toxicities) crizotinib was modified with a para-nitrobenzyl alcohol moiety as a test system for hypoxia-activatable prodrugs.

V. RESULTS AND DISCUSSION

a. Development of a Cathepsin K-selective trigger Unit

Synthesis strategy 1

The synthetic strategy was based on coupling of a homocycloleucine-lysine-PABC fragment (part A) to a piperazinylbenzoic acid to yield the cathepsin K-linker moiety, which finally can be attached to a fluorophore or drug (Scheme 1).

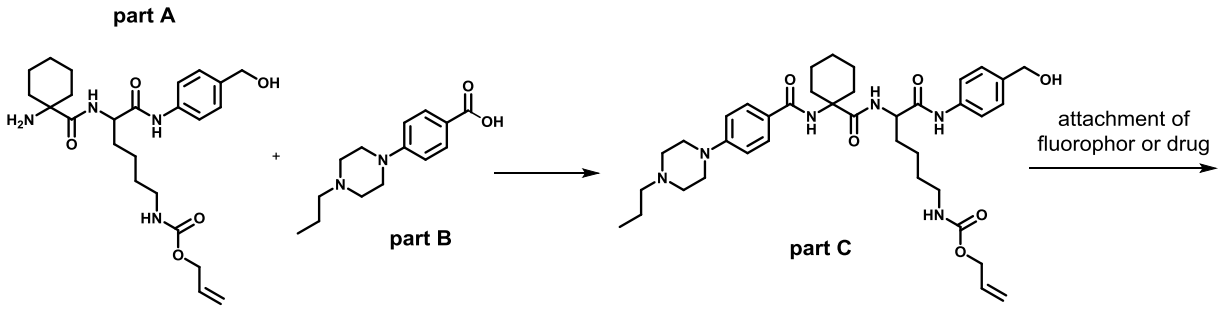

Scheme 1 - Coupling strategy of building blocks A and B to yield the cathepsin K trigger system (part C) which finally can be attached to a fluorophore or drug

Synthesis of part A:

First, for the synthesis of part A, 1-aminocyclohexanecarboxylic acid (**1**; H_2N-Ac6-OH) was protected with di-tert-butyldicarbonat (DiBOC) at the amino position (Scheme 2). The Boc-protected amino acid **2** (Boc-Ac6-OH) was then transformed to the hydroxysuccinimide active ester **3** using a standard coupling protocol with dicyclohexyl carbodiimide (DCC). Coupling with commercially available ε-alloc-protected lysine under basic conditions led to the dipeptide **4** (Boc-Ac6-Lys(alloc)-OH; with only ~30% after purification via column chromatography, the product yield of this reaction was quite low). Afterwards, *para*-aminobenzyl alcohol (PABOH) was coupled with DCC / hydroxyl benzotriazole (HOBt) resulting in the self immolative linker containing dipeptide **5** (Boc-Ac6-Lys(alloc)-PABOH), which was again purified by column

chromatography (~40% yield). Subsequently, compound **5** was deprotected with 4M HCl resulting in the free amine H2N-Ac6-Lys(alloc)-PABOH (**6**) (^{1}H-NMR see Figure 16).

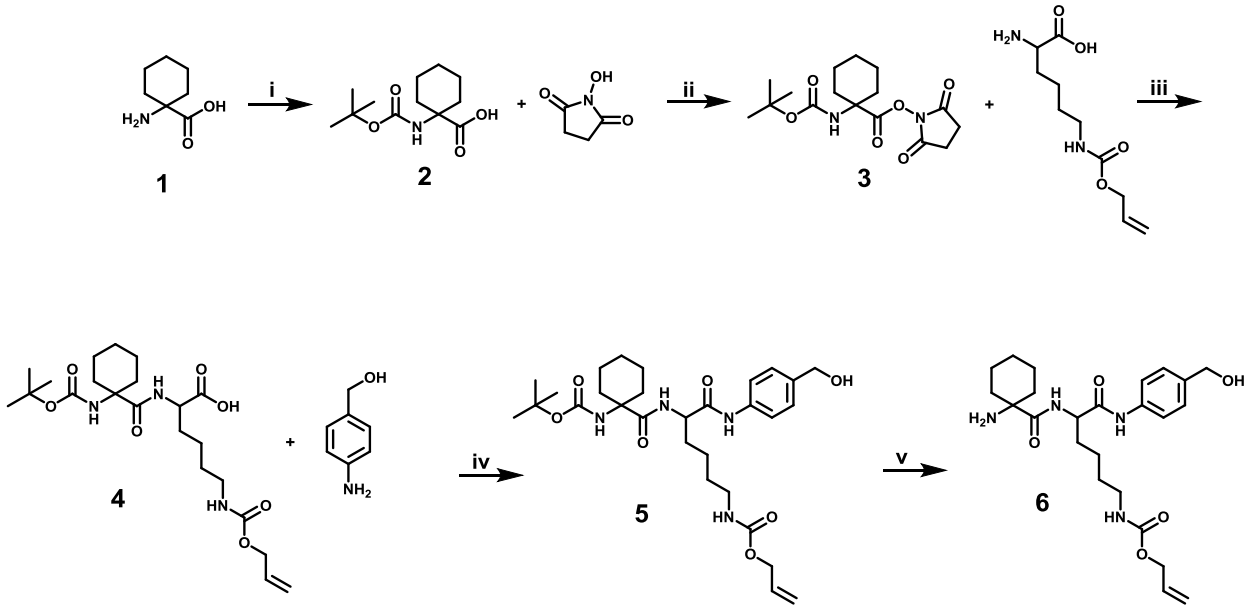

Scheme 2 - Synthesis route of part A. i: DiBOC, NaOH(2M), Dioxane, r.t., 16h; ii: DCC, THF, 0°C, 15min, r.t., 16h; iii: Na_2CO_3, THF, 16h; iv: DCC, HOBt, THF, 16h; v: HCl(4M), THF, 1h.

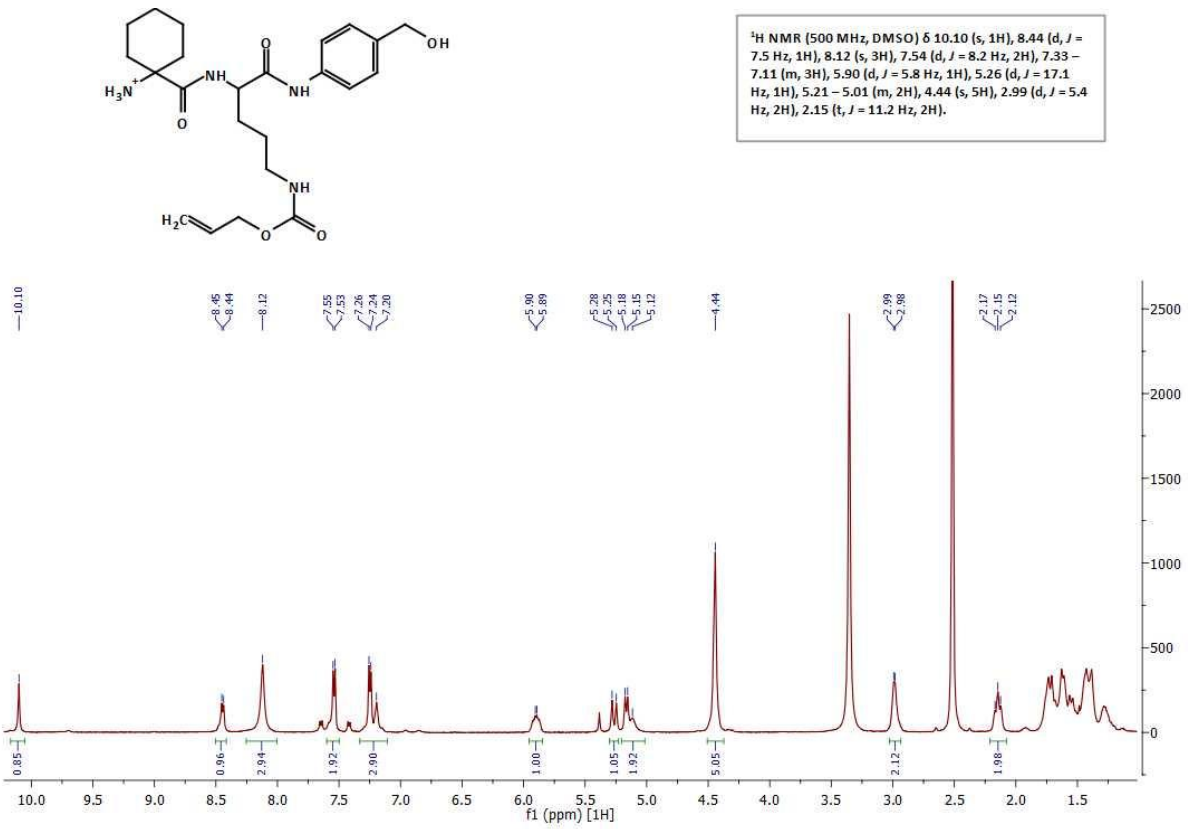

Figure 16 - ^{1}H-NMR spectrum of the deprotected amine 6 in d_6-DMSO

Synthesis of part B:

Next, part B (**9**; 4-(4-propylpiperazin-1-yl)benzoic acid) was tried to synthesize according to a patent of *Kobayashi et al.*[66]. Therefore, commercially available 4-(piperazin-1-yl)-benzoic acid ethyl ester (**7**) was propylated with 1-bromopropane in DMF to obtain compound **8** (Scheme 3) and without purification directly hydrolyzed by refluxing with sodium hydroxide in an ethanol/water mixture (1:1).

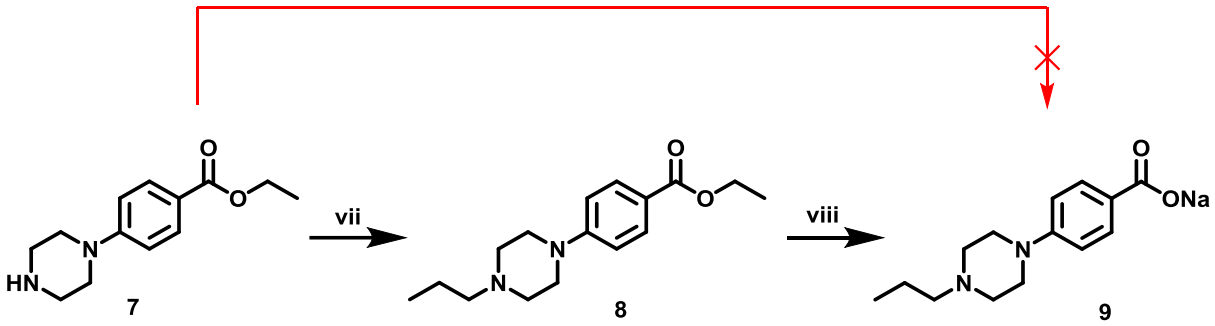

Scheme 3 - Synthesis of 4-(4-propylpiperazin-1-yl)benzoic acid. Vii: 1-bromopropane, DMF, TEA; viii: NaOH, EtOH/H_2O, 80 °C, 16h;

However, the NMR spectrum of our product indicated a mixture of two compounds. According to integral analysis, already the propylation reaction did not occur in quantitative yield. In detail, a second set of signals appeared in the piperazinylic range between 2.5 and 3.5 ppm and the integrals at 0.8 ppm, 1.5 ppm and 2.35 ppm which represent the propyl residue do not reach the supposed ratio of 3:2:2. Thus, the second species most likely originates from the non-alkylated but deprotected carboxylic acid. The corresponding ^{1}H-NMR is depicted in Figure 16.

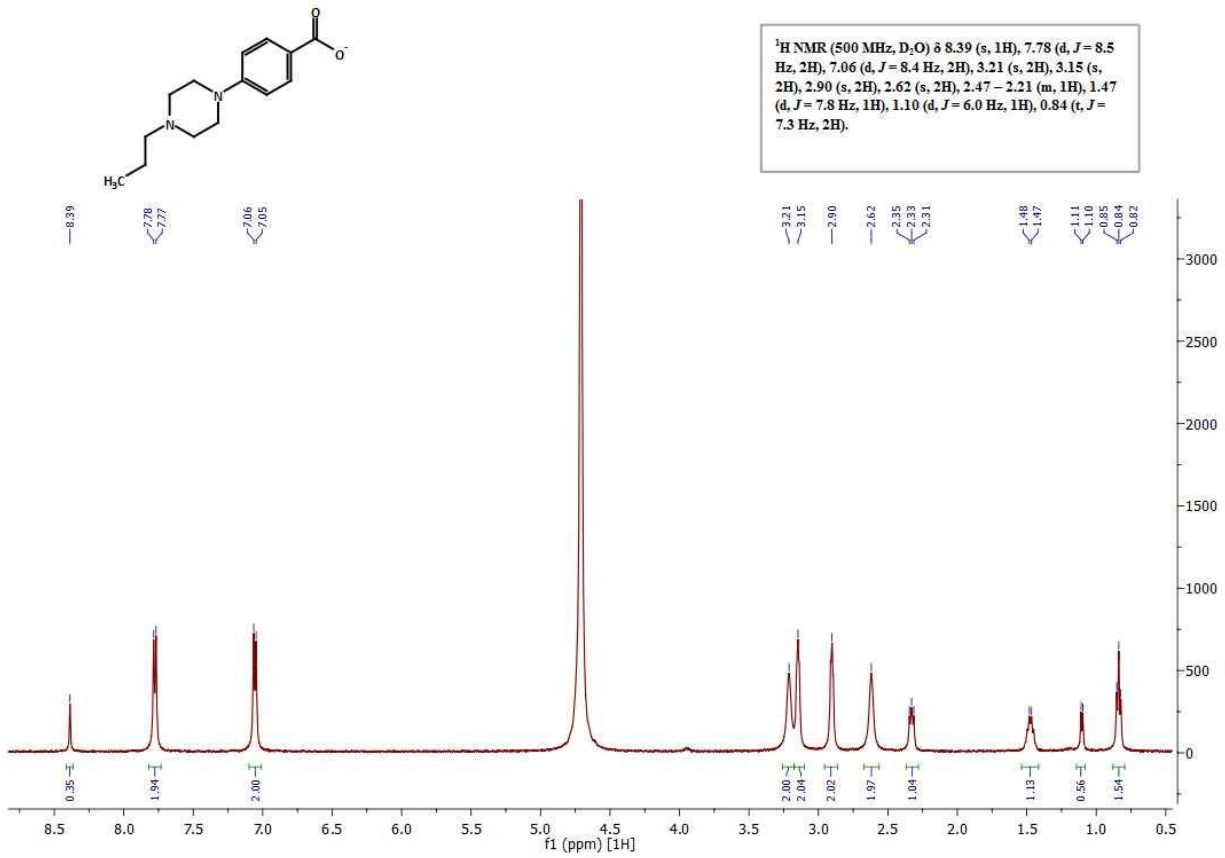

Figure 16 - ^{1}H-NMR (D_2O) spectrum of the reaction product of the synthesis route of compound 9 as described by Kobayashi et al.

Therefore, the synthesis procedure of Kobayashi was modified and split into two steps: first the propylation reaction with purification via column chromatography (~50% yield) and, subsequently, the alkaline hydrolysis of the ethyl ester yielding the sodium salt **9**. The last step occurred in quantitative yields and, thus, the product was used without further purification (Figure 17).

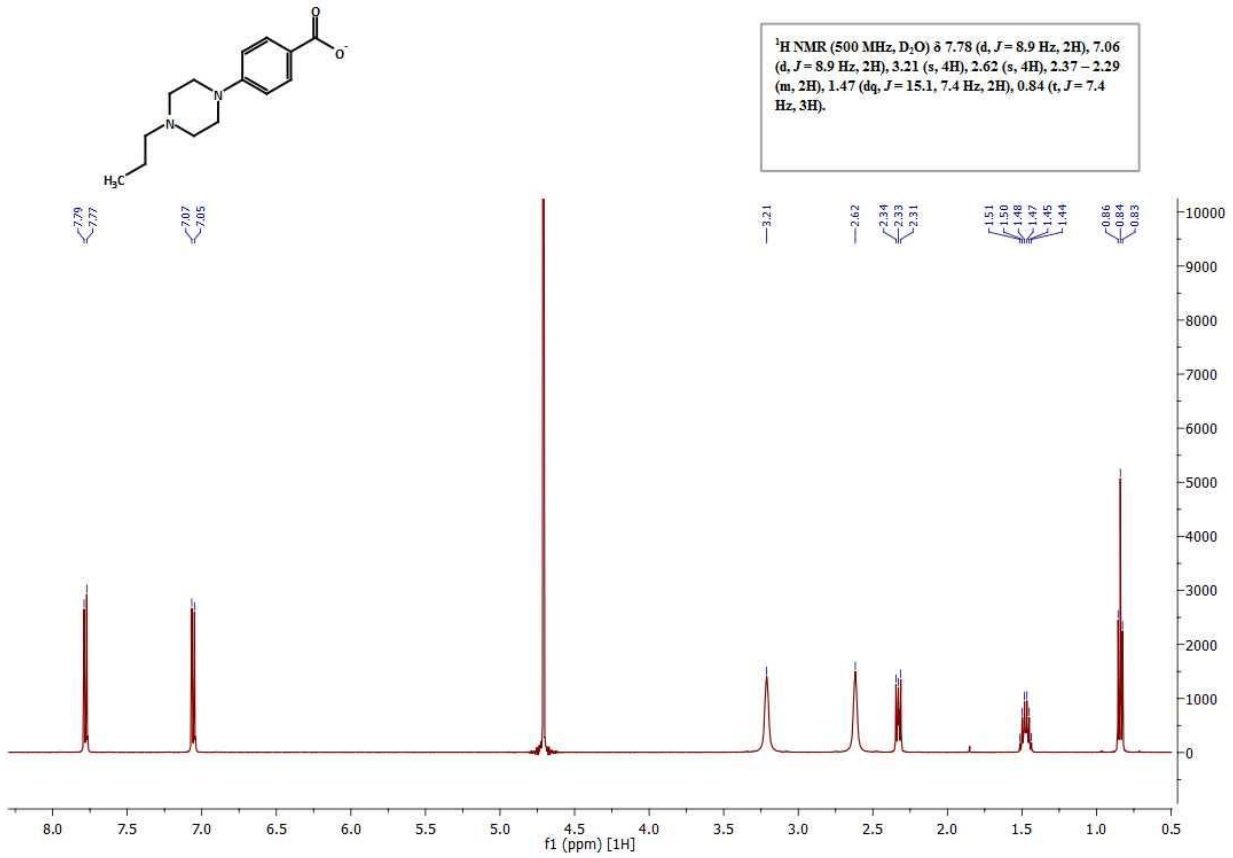

Figure 17 - ^{1}H-NMR in D_2O spectrum of compound 9 after purification via column chromatography and alkaline deprotection

Part A and part B should subsequently be coupled to obtain the cathepsin K specific trigger moiety (part C, **13**) as visualized in Scheme 4. The first reaction was tried with a standard coupling procedure based on TBTU (O-(Benzotriazol-1-yl)-N,N,N‘,N’-tetramethyluronium tetrafluoroborat). As TBTU requires basic conditions to form the activated ester of the carboxylic acid, directly the sodium salt (**9**) was used. As this coupling procedure provided the product only in very small amounts, the coupling agent was changed to EEDQ (N-Ethoxycarbonyl-2-ethoxy-1,2-dihydroquinoline). Mechanistically, EEDQ requires a proton at the carboxylic acid moiety. Thus, the hydrochloric acid salt **10** (Scheme 4) of part B was generated in situ and reacted with **6**. Unfortunately, also this procedure did not provide any product. Now, the same reaction was also performed with the internal salt **12**, which was obtained via addition of one equivalent of acetic acid. Again, no product formation could be observed.

Furthermore, a carbodiimide-based coupling strategy was tried with activation of the acid using diisopropyl carbodiimide (DIC) in presence of HOBt (hydroxyl benzotriazole) without success. Finally, the coupling was tried with the corresponding acid chloride **12**. The acid chloride was prepared according to literature as described by *Lopez* by stirring of the sodium salt **9** in pure oxalyl chloride overnight. However, also the usage of the acid chloride did not lead to acceptable amounts of product.

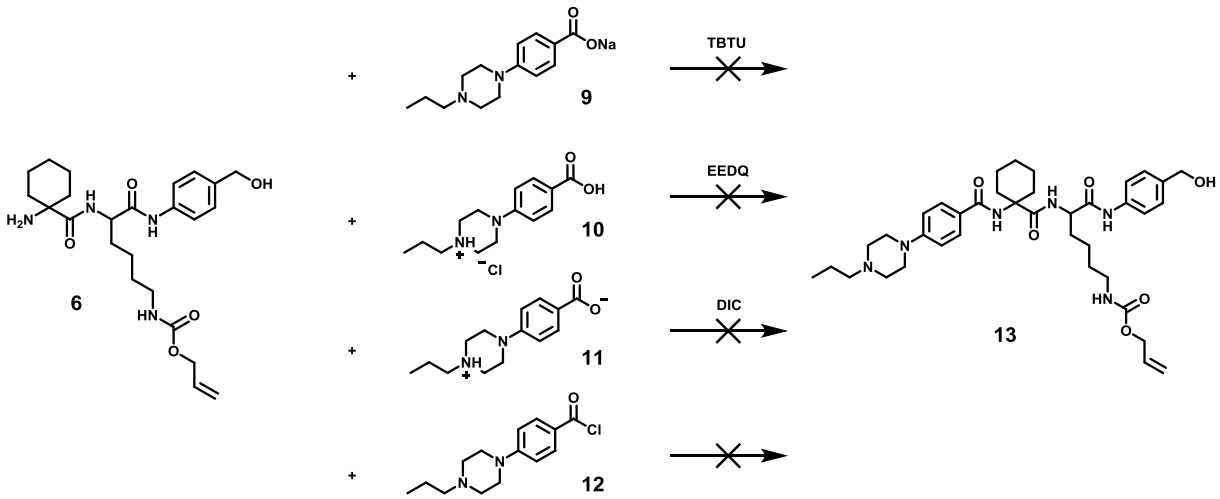

Scheme 4 - Final coupling of acid to free amine 6

Due to these disappointing results from the coupling trials of part A and part B a new synthetic strategy was developed.

Synthesis strategy 2

This second synthesis route focused on an early coupling of 4-(4-propylpiperanzinyl)benzoic acid moiety to the 1-amino-1-cyclohexylcarboxylic acid (part D) which represents the cathepsin K selective dipeptide. Furthermore, the fluorophore and linker containing moiety (part E) shall represent a building block which can also be used to attach selective moieties for other cathepsins.

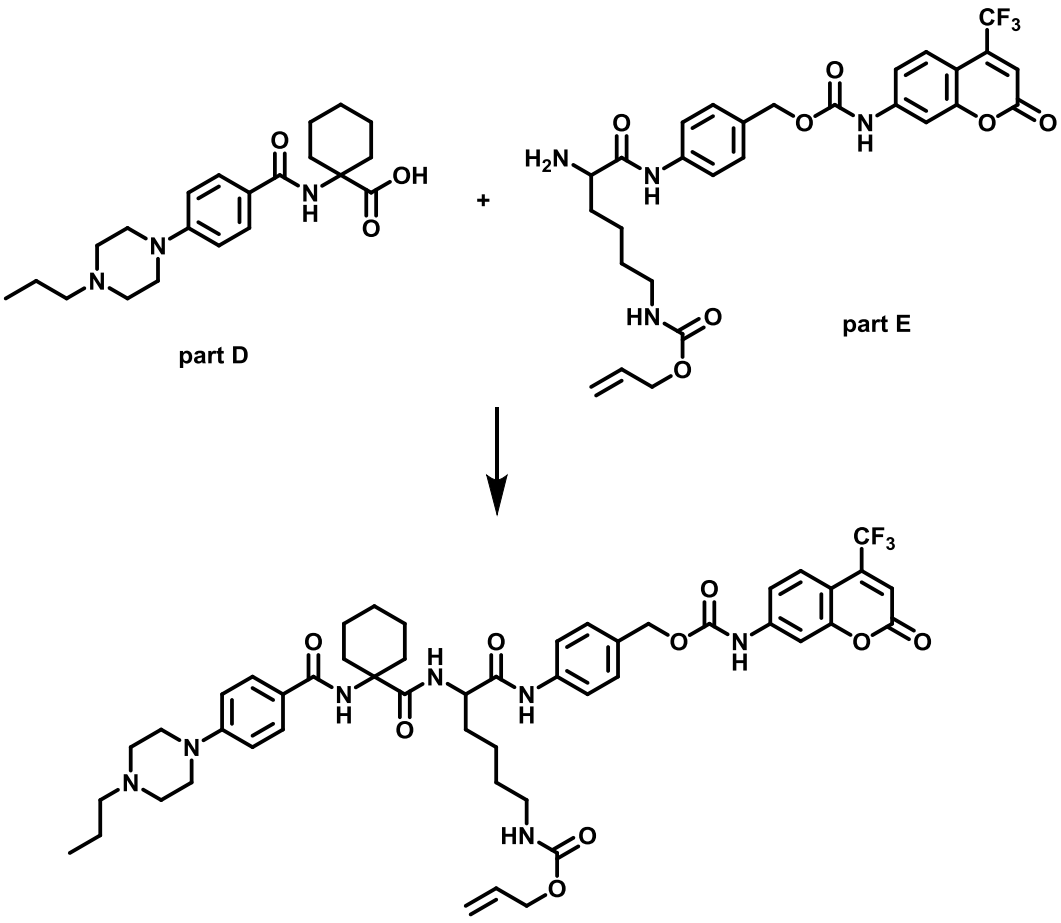

Scheme 5 - Coupling procedure of the cathepsin K specific building block (part D) with the fluorophore containing build block (part E) to obtain the prodrug system.

Synthesis of part D:

The novel synthetic route for part D is depicted in Scheme 6.

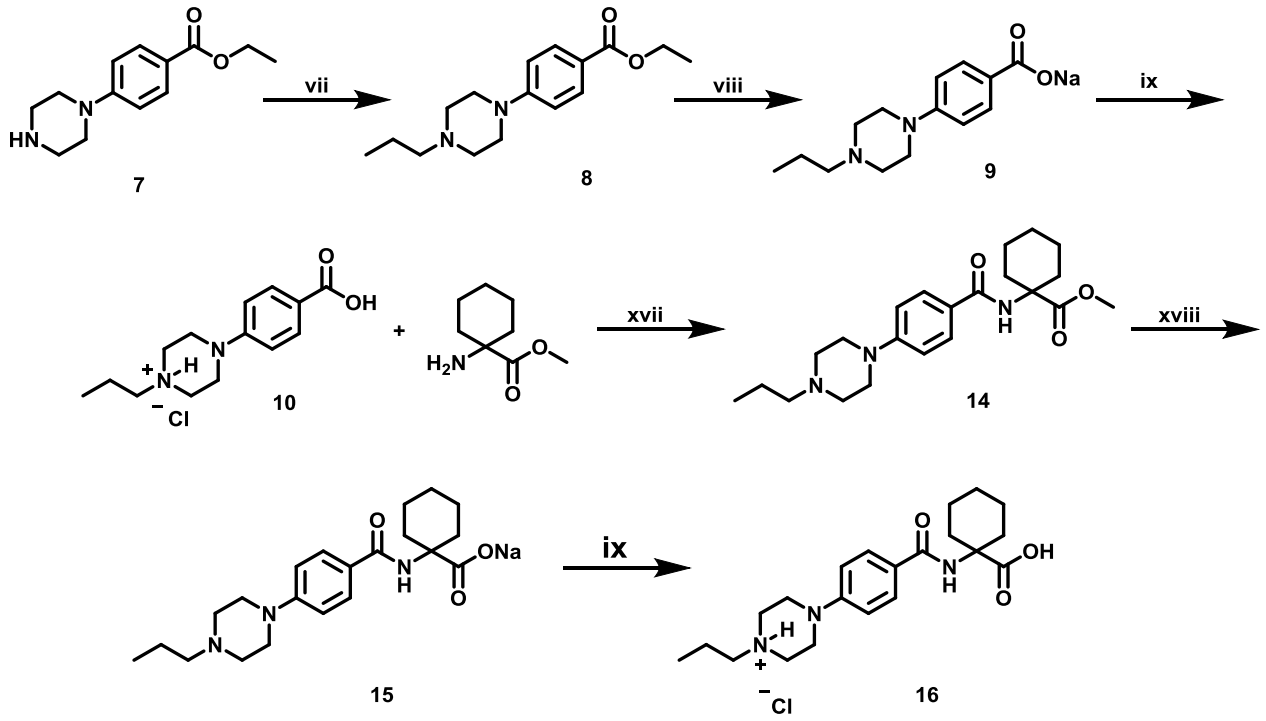

Scheme 6 - Synthesis of part D. vii: 1-bromopropane, DMF, triethylamine, 16h; viii: sodium hydroxide, ethanol/water, 80 °C, 16h; ix: 5 equiv. hydrochloric acid; xvii: EDC*HCl, HOBt, DMF, triethylamine, 16h; xviii: Sodium hydroxide (aq, 3 equiv.), THF; ix: Hydrochloric acid, water

The synthesis of **9** was performed as described for part B (Scheme 3). The deprotected sodium salt **9** was acidified to pH 3 with 1M HCl and, by this, converted into the hydrochloride salt **10**. This salt was then coupled with the carbodiimide-based coupling reagent 1-Ethyl-3-(3-dimethylaminopropyl)carbodiimide (EDC) in presence of HOBt in DMF to obtain the methyl ester **14** of the balicatib backbone. As described in literature by *Kobayashi et al.*[66], hydrolysis of the ester was performed with 3M hydrochloric acid under reflux for six hours. However, since mass spectrometry did not indicate product formation, the hydrolysis protocol was changed to alkaline conditions with three mole equivalents of sodium hydroxide in THF (80% yield). Finally, the corresponding deprotected sodium salt **15** was acidified with 1M HCl yielding the HCl salt

16. Resulting sodium chloride of the acidification was removed by dissolving the product in ethanol and subsequent filtration. The ^{1}H-NMR spectrum of **16** can be seen in Figure 18 and the product was later used without further purification.

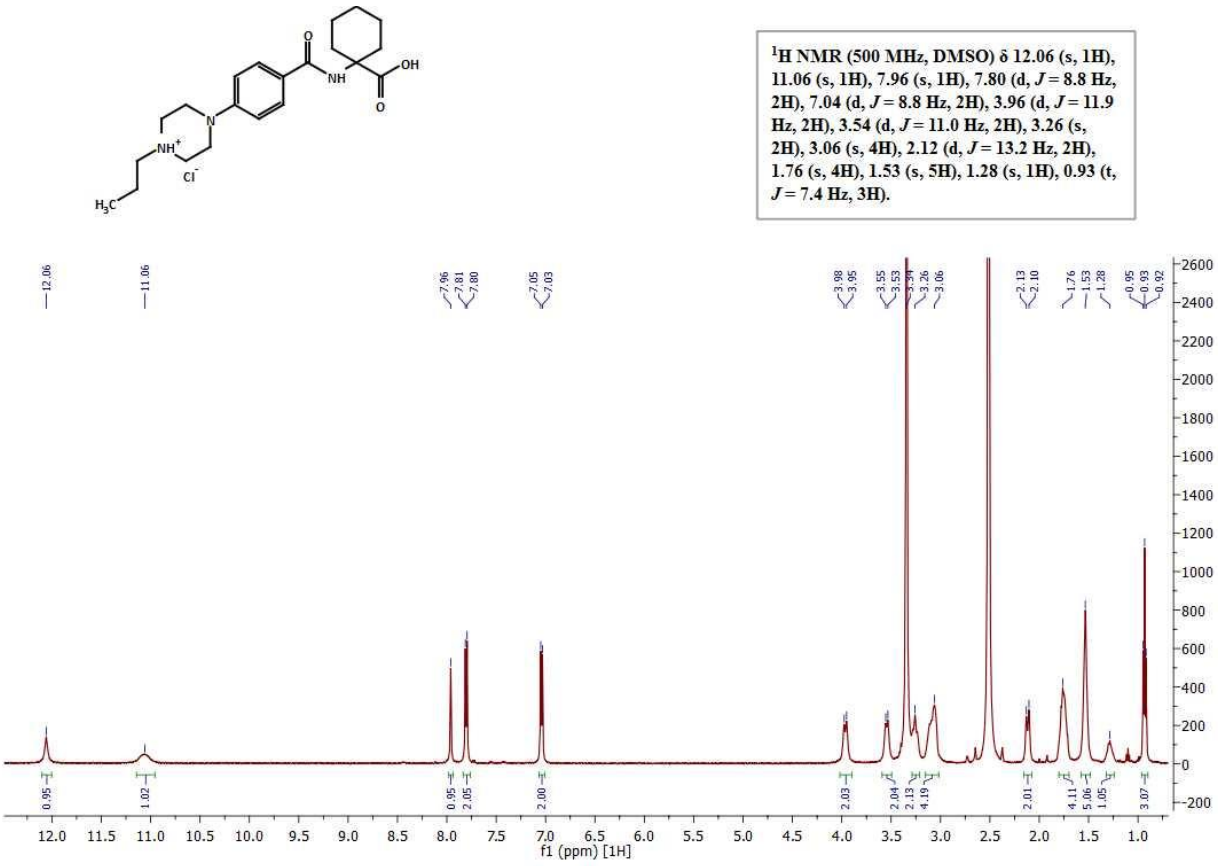

Figure 18 – ^{1}H-NMR spectrum of compound 16 in d_6-DMSO (part D)

Synthesis of part E:

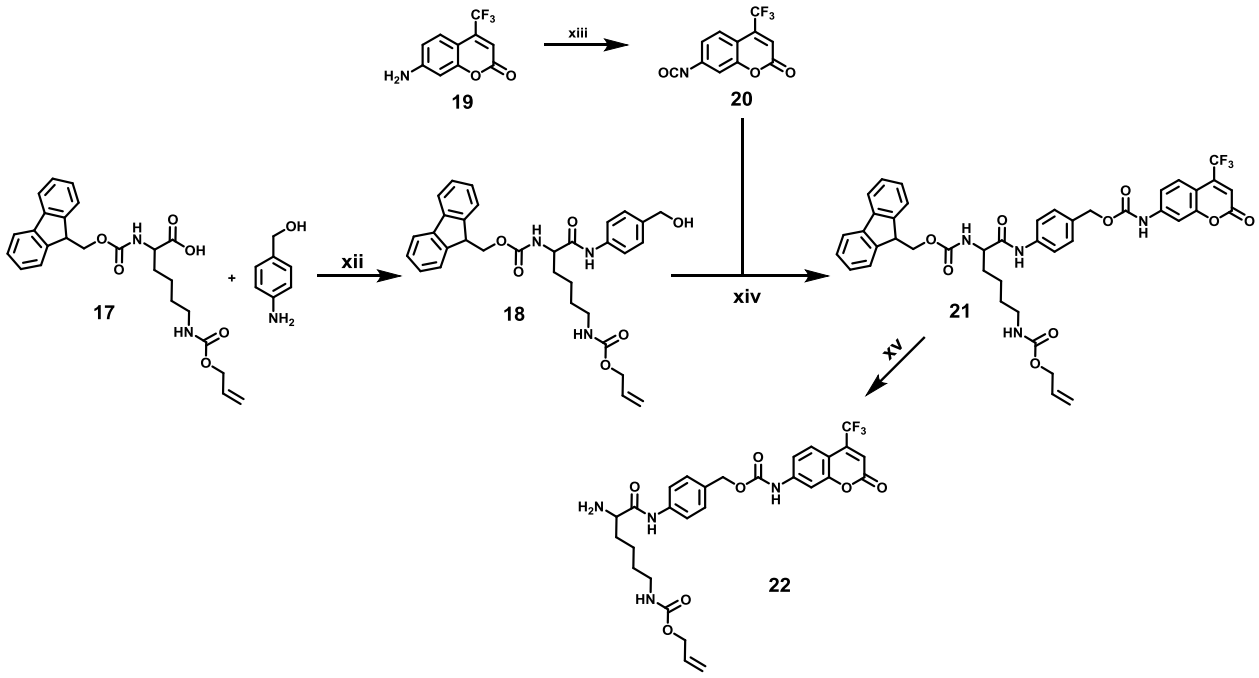

Scheme 7 – Synthesis of part E. xii: EEDQ, THF, 16h; xiii: phosgene, toluene, 120°C, 16h; xiv: THF, 80 °C, 2h; xv: piperidine (20%) in DMF, 1h

First, commercially available α-Fmoc-ε-alloc-protected lysine (**17**) was coupled to *para*-aminobenzyl alcohol with EEDQ in THF to obtain Fmoc-Lys(alloc)-PABOH (**18**) in very good yields (80%). Easy workup was provided by simply precipitation of the product with diethyl ether. The next step was the coupling of compound **18** with the fluorophore moiety. However, the synthesis of compound **21** proved to be extremely challenging. First, the formation of the carbamate containing compound **21** was tried by activation of the hydroxyl group of **18.** Therefore **18** was first reacted with *para*-nitrophenyl chloroformate and this activated carbonate was further treated with the acyl-group carrier 4-dimethylamino pyridine (4-DMAP). This generates a highly reactive species in situ which shall finally react with the amino group of coumarin (the whole reaction mechanism is depicted in Scheme 8).

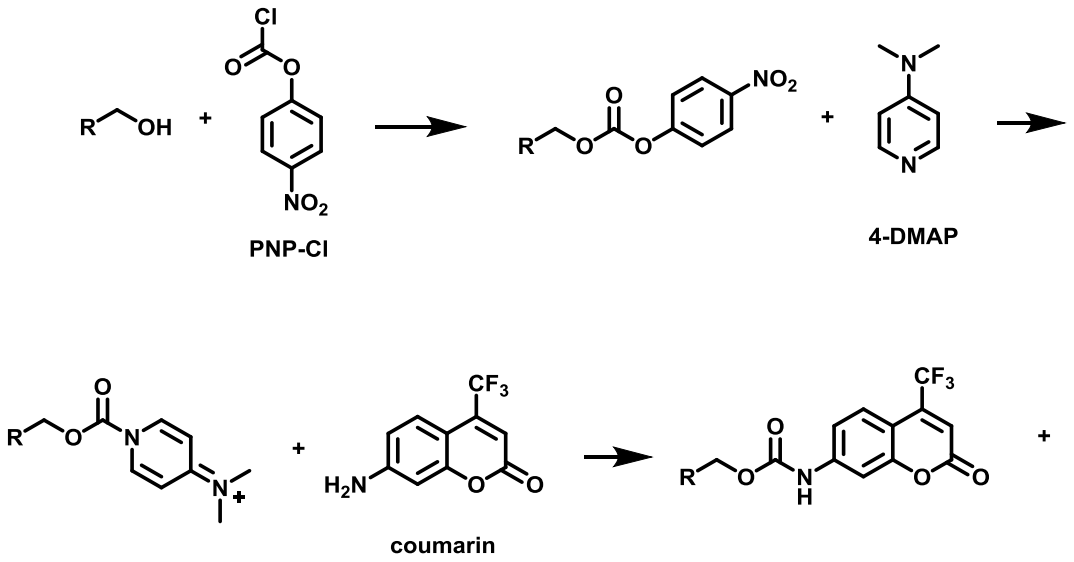

Scheme 8 - Reaction scheme for the coupling of 18 and coumarin via a carbonate (PNP-Cl: *para*-nitrophenyl chloroformate, 4-DMAP: 4-dimethylamino pyridine)

Unfortunately, this synthetic route did not provide any product. Thus, the idea was the activation of the coumarin for coupling to the alcohol **18**. Therefore coumarin has to be transformed into the isocyanate derivative (Scheme 9).

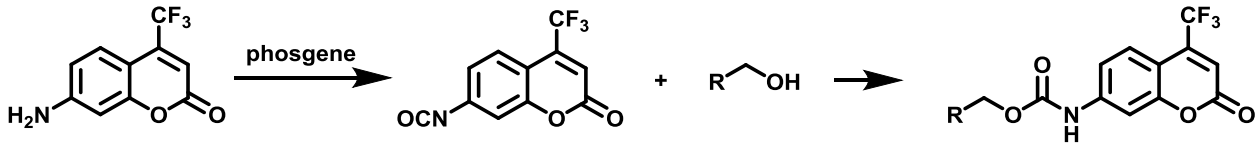

Scheme 9 - Reaction scheme for the coupling of 18 and coumarin via an isocyanate

The formation of the isocyanate was initially tried with triphosgene at 0°C in dichloromethane (DCM) as described in literature[67]. Thereby, the isocyanate should be generated in situ and the carbamate **21** shall be formed by simple addition of the Fmoc-Lys(alloc)-PABOH conjugate **18**. Indeed, ^{1}H-NMR investigations of the crude product indicated complete turnover of **18** as indicated by a shift of the methylene group of the benzylic alcohol as well as complete vanish of the hydroxyl group peak (the mass spectrum was not meaningful as this compound is hardly

ionized). However, after purification via column chromatography, no peaks of the coumarin moiety were found in the aromatic region. Trials to repeat the activation reaction at different temperatures remained unsuccessful equally as trials with another activation procedure using di-tertbutyldicarbonate in presence of 4-DMAP in acetonitrile[68]. Most likely, the amino group of coumarin was not converted into the isocyanate and the triphosgene presumably reacted with the hydroxyl group of **18** instead, generating the symmetric carbonate as depicted in Figure 19.

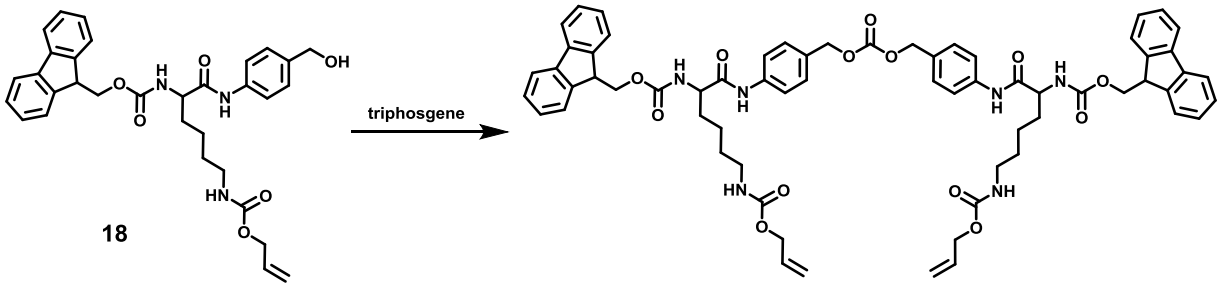

Figure 19 - Possible reaction product of the coupling procedure using triphosgene

Most likely, the absent of conversion to the isocyanate is due to the very low nucleophilicity of the anilinic amino group of coumarin, which may be further decreased by the electron withdrawing intramolecular ester group in meta-position as well as the trifluoromethyl group. Consequently, a more potent reagent has to be used to form the isocyanate of coumarin. According to literature, phosgene is 130-fold more reactive than triphosgene in the formation of chloroformates from methanol[69] and was subsequently used for the activation reaction.

Excursion: Phosgene is a highly toxic gaseous reagent with a median LC_{50} value of 500 ppm/ min in humans and was used as warfare agent during World War I. Once inhaled, at high concentrations phosgene leads to choking. At lower concentrations, it attacks amino acids and enzymes of the respiratory system, subsequently suppressing essential metabolism processes. Furthermore, phosgene reacts with the humidity present in the lungs and forms HCl and CO_2. The formed HCl attacks cells of the lung epithelium and by this suppress the respiratory system. Even very low concentrations (5 ppm/min) can lead to lethal lung edema up to forty-eight

hours after exposition. Due to the high danger arising from phosgene gas, all reactions have to be carried out in a fume hold, containing an apparatus which carries unreacted rests of phosgene gas into a NaOH containing bubbler.

Notably, also the solid triphosgene releases phosgene during the reaction and thus exactly the same safety precautions have to be considered.

Finally, isocyanate formation was achieved with a protocol published for 7-amino-4-methylcoumarin by refluxing **19** with phosgene (20%) in toluene for 16 h at 115°C.[70]

All different tested reactions and their conditions to synthesize the isocyanate are summarized in Table 1.

Table 1 - Strategies for the synthesis of the isocyanate 20 and coupling to the alcohol generating 21

Reaction	Solvent	Reactant	Temperature	t_i [h]	t_c [h]	Yield
Activation of peptide	THF	PNP	0 °C to r. t.	1,5	16	/
	THF	PNP / 4-DMAP	0 °C to r. t.	1,5	16	/
Activation of coumarin	DCM	triphosgene	0 °C	2	16	/
	DCM	triphosgene	0 °C to r. t.	2	16	/
	DCM	triphosgene	r. t.	2	16	/
	ACN	DiBoc	0 °C to r. t.	0.08	16	/
	toluene	phosgene	115°C	16	2	40%

PNP – para-nitrophenyl chloroformate; 4-DMAP – 4-dimethylaminopyridine); t_i: reaction time of formation of the isocyanate, t_c: reaction time of coupling of the isocyanate with 18

The isocyanate **20** was directly used without isolation and refluxed with **18** in THF at 80 °C to obtain compound **21** as indicated by mass spectrometry and ^{1}H-NMR spectroscopy. Trials to

purify the product via extraction or column chromatography remained difficult, due to the comparable lipophilicities of the product, educts and side products. Thus, the crude product was directly deprotected to compound **22** using 20% piperidine in DMF, which then was successfully purified by column chromatography in an overall yield of ~40%.

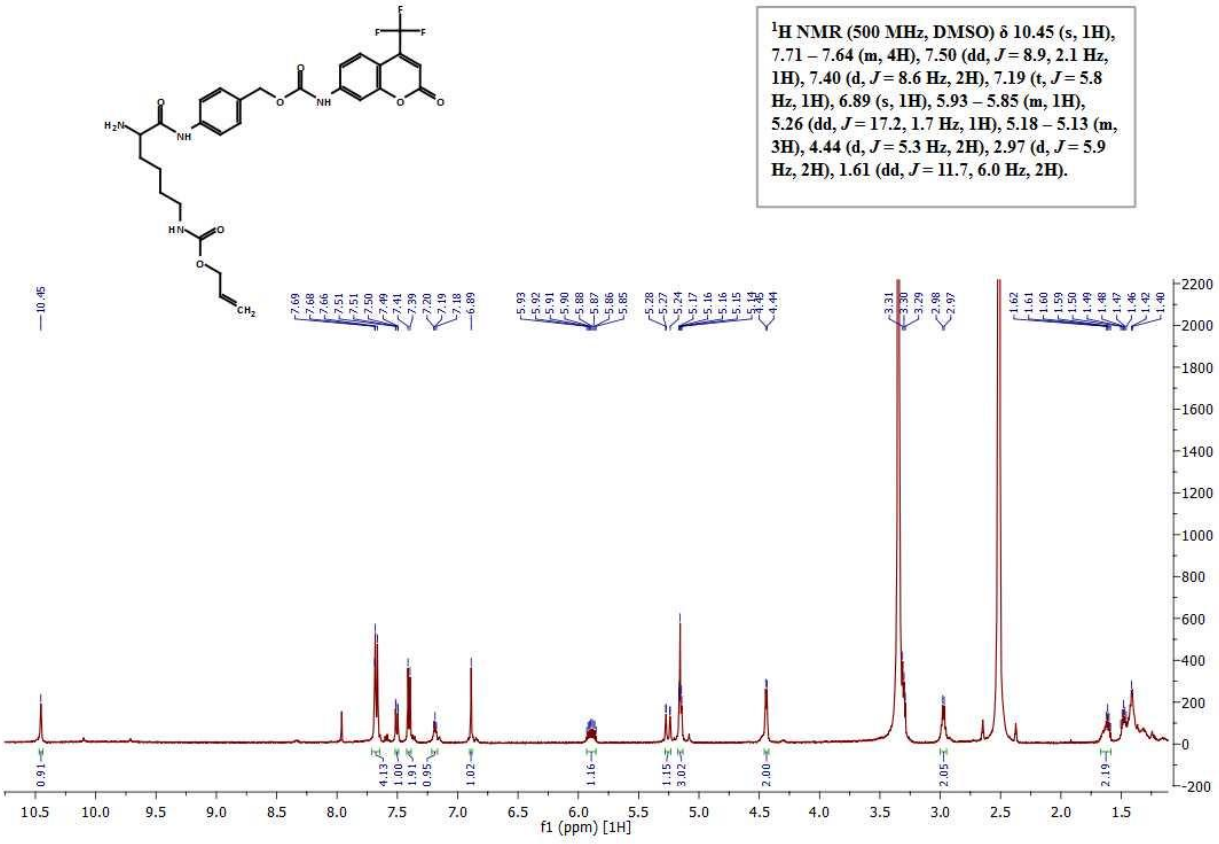

Figure 20 – ^{1}H-NMR spectrum of compound 22 in d_6-DMSO (part E)

Coupling of part D and part E:

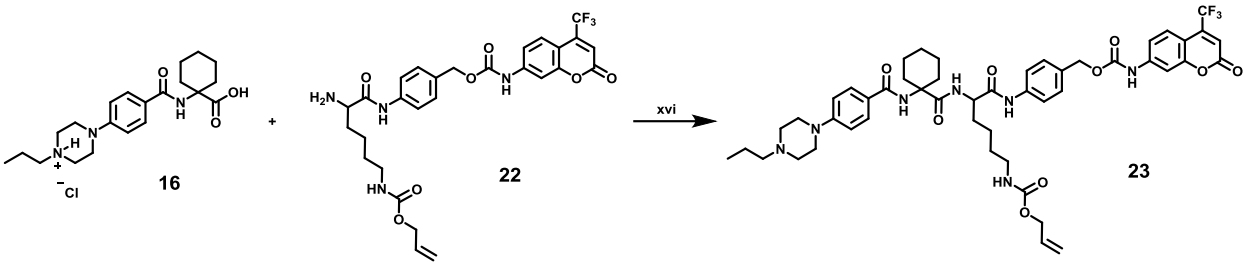

Figure 21 - Final coupling of the cathepsin K specific dipeptide (part D) with the fluorophore containing residue (part E).

In order to synthesize the final cathepsin K selective conjugate (Figure 21) coupling of part D (**16**) with part E (**22**) was initially tried with a standard TBTU / HOBt procedure. Thus, acid **16** was activated with TBTU in presence of HOBt for thirty minutes and amine **22** was added. The reaction was allowed to stir for 16 h. Mass spectrometry investigations showed the presence of educts as well as the formation of one product with the wrong mass of 689 in positive ion mode (Figure 22). Thus, TBTU seems to form side products with the applied amine which can be explained by investigating its reaction mechanism (Figure 23).

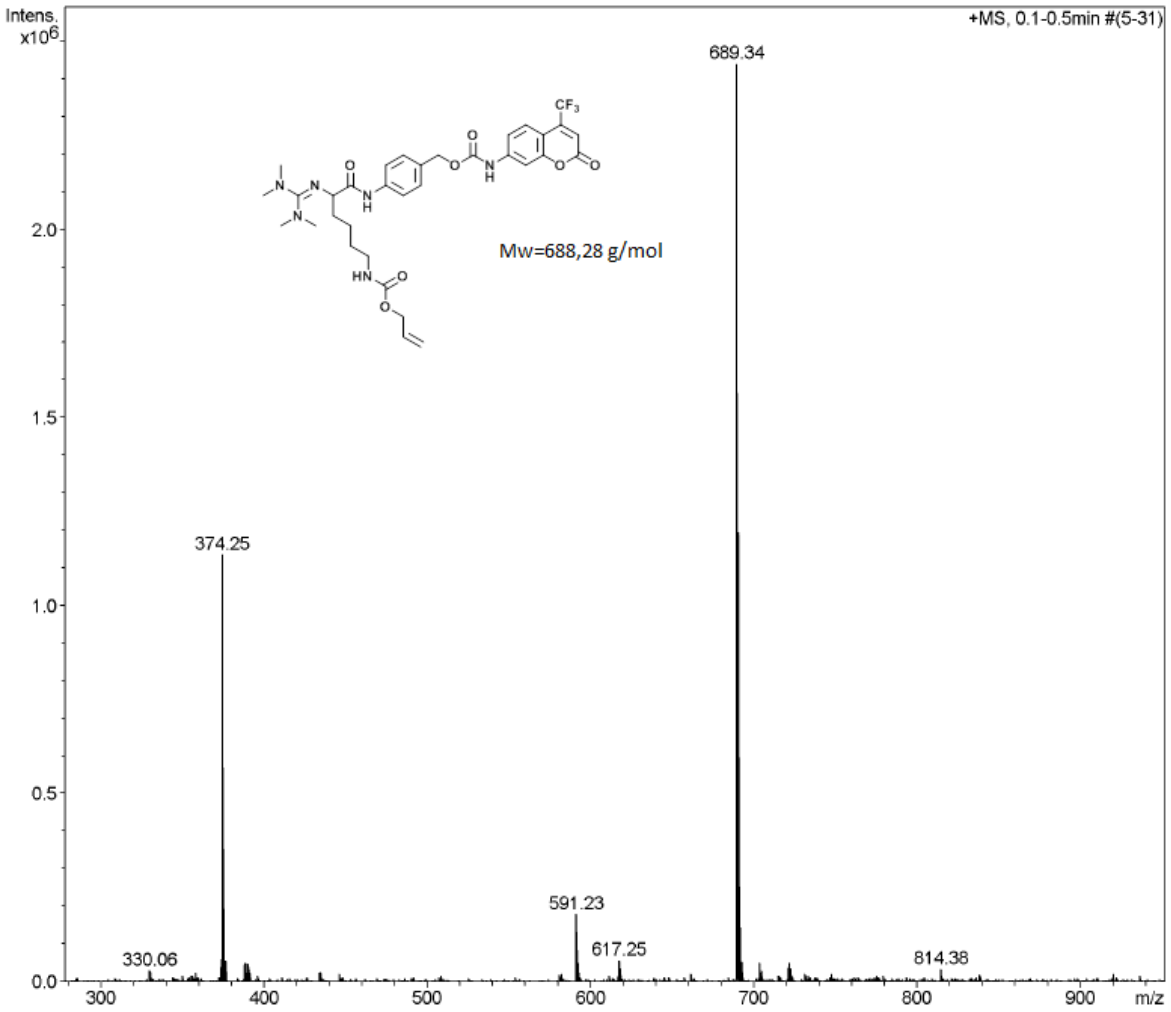

Figure 22 – The mass spectrum of the initial trial to synthesize 23 using TBTU shows the formation of a guanidine side product (M_w=689,28 g/mol). Further signales indicates educts (16 at M_w=374,25 g/mol and 22 at M_w=591,23 g/mol)

By this, the deprotonated carboxylic acid gets activated by TBTU and subsequently forms the hydroxybenzotriazole active ester. Addition of the amine should finally result in the desired peptide bond. If the carboxylic acid is not activated, the amine attacks the uronium salt of TBTU and forms a guanidine side product. In case of amine **22**, the guanidine side product has a molar weight of 688 g/mole which belongs to the observed mass peak. By this, the coupling procedure has to be changed to species which are inert to amines.

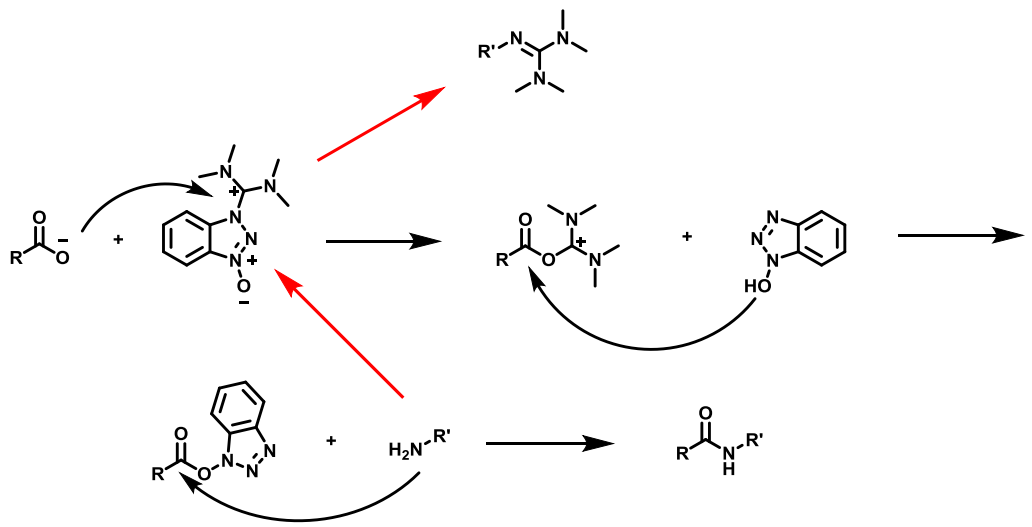

Figure 23 - Peptide coupling mechanism with TBTU/HOBt (black arrows) and the side reaction yielding the formation of the guanidine

The coupling was finally accomplished using a carbodiimide/HOBt protocol with 1-ethyl-3-(3-dimethylaminopropyl)carbodiimide hydrochloride (EDC). Mass spectrometry indicated the formation of **23** and purification was performed with preparative HPLC (ACN/H_2O (1% HCOOH)) in yields of ~30% (NMR and analytical HPLC indicate that still very small amounts of impurities are present).

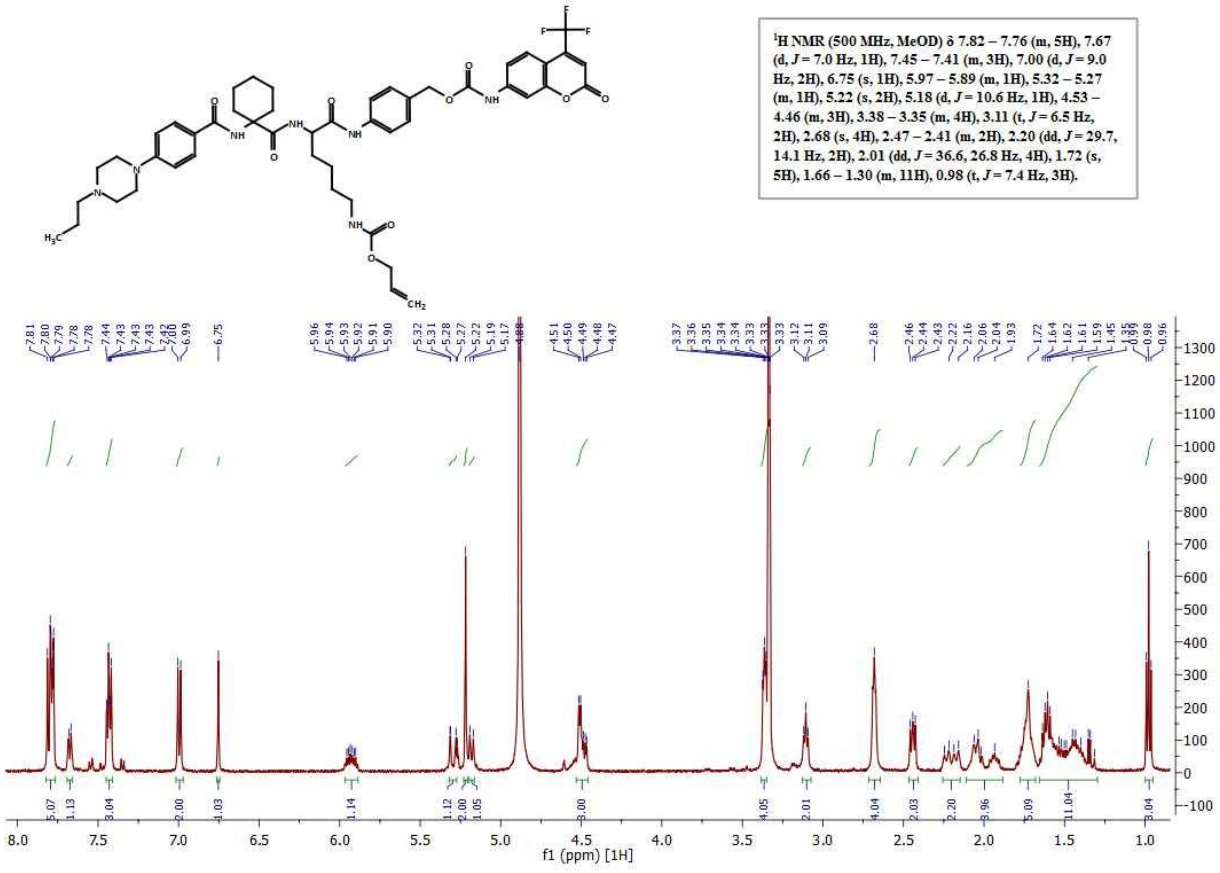

Figure 24 - ^{1}H-NMR spectrum of compound 23 in MeOD after purification via preparative HPLC

Cleavage test

Finally, the prodrug activation was tested by a cleavage assay of **23** by cathepsin K. Cathepsin K is postulated to cleave the peptide trigger between the peptide bond of the lysine and the PABC residue as visualized in Figure 25. The cleavage progress can be monitored via fluorescence spectroscopy by the release of the fluorophore moiety, 7-amino-4-trifluoromethylcoumarin.

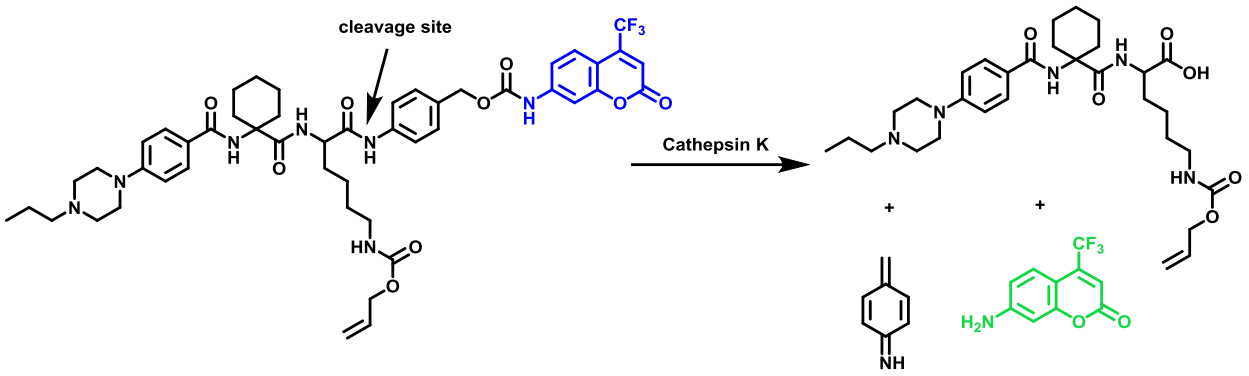

Figure 25 - Scheme of the cleavage of the novel prodrug system by cathepsin K

Therefore, the prodrug was incubated with cathepsin K in acetate buffer solution at pH 5.5. Upon release, the emission wavelength of the fluorophore is red-shifted. With an excitation wavelength of 395 nm the emission intensity of the free fluorophore was measured in an interval range between 490–510 nm, showing a maximum at 497 nm[71]. The time-dependent change of the emission intensity is plotted in Figure 26.

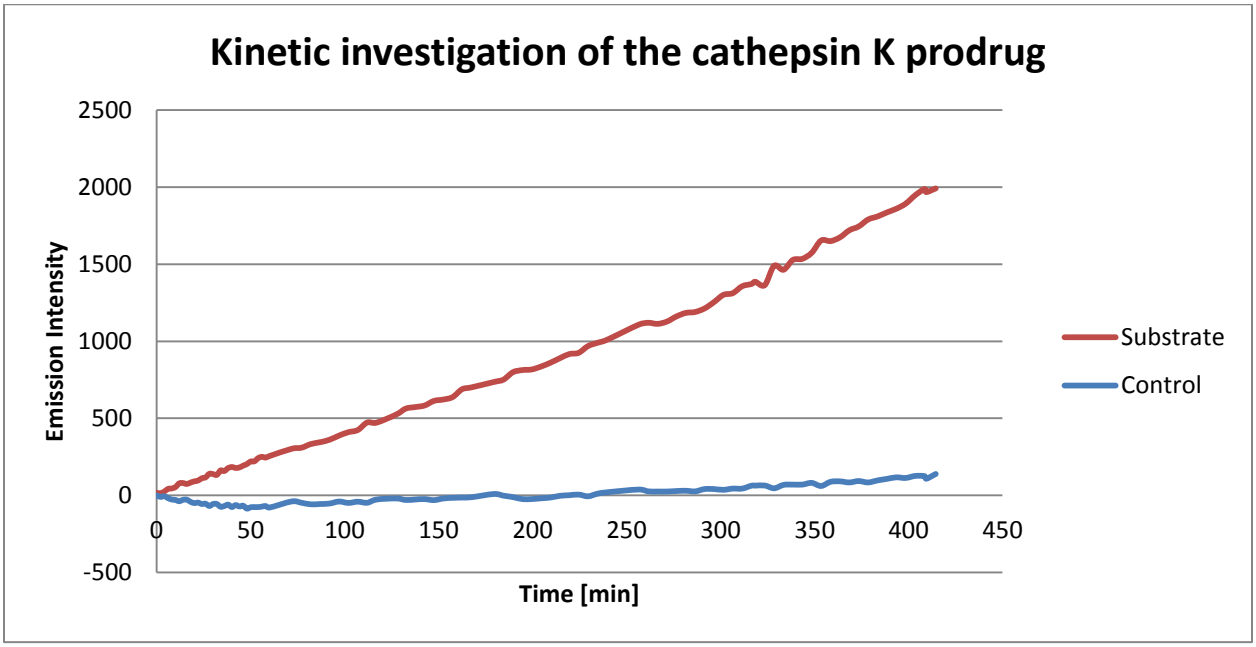

Figure 26 - Plotted graph of the emission intensity of the cathepsin prodrug in presence of cathepsin K (red) and without cathepsin K (blue) as function of time at emission wavelength of 495 nm with an excitation wavelength of 395 nm

The increasing intensity at the emission wavelength of 497 nm proves the release of free fluorophore and by this, activation of the prodrug **23** by cathepsin K. Thus, these first data indicate that the new prodrug concept indeed is a promising platform for further investigations.

b. Development of a Tyrosine Kinase Inhibitor Prodrug

General information

Second topic of this master thesis was the development of a prodrug strategy for an already clinically approved tyrosine kinase inhibitor (TKI). TKIs belong to the class of targeted therapeutics which interacts with distinct cancer-related molecular targets. Despite their partially improved properties over standard chemotherapy, still severe side effects can occur during treatment. Additionally, to overcome drug resistance against single TKIs, drug combinations (often with another TKI) would be of high interest. Some of these drug combinations show exciting tumor regression in animal models[72]. However, some clinical studies revealed, that a huge problem of such drug combinations are accumulated toxicities, which frequently result in study termination or at least dose reduction for both compounds[73]. In turn, the required pharmacological concentrations are often no longer reached leading to ineffectiveness of the given combination therapy. Hence, there is urgent need for strategies to reduce the side effects of TKIs in order to enable combined therapy regiments. One option is the development of prodrugs for this class of compounds. By this, aim of this part of the master thesis was the synthesis of a prodrug of the tyrosine kinase inhibitor crizotinib (Figure 27).[74]

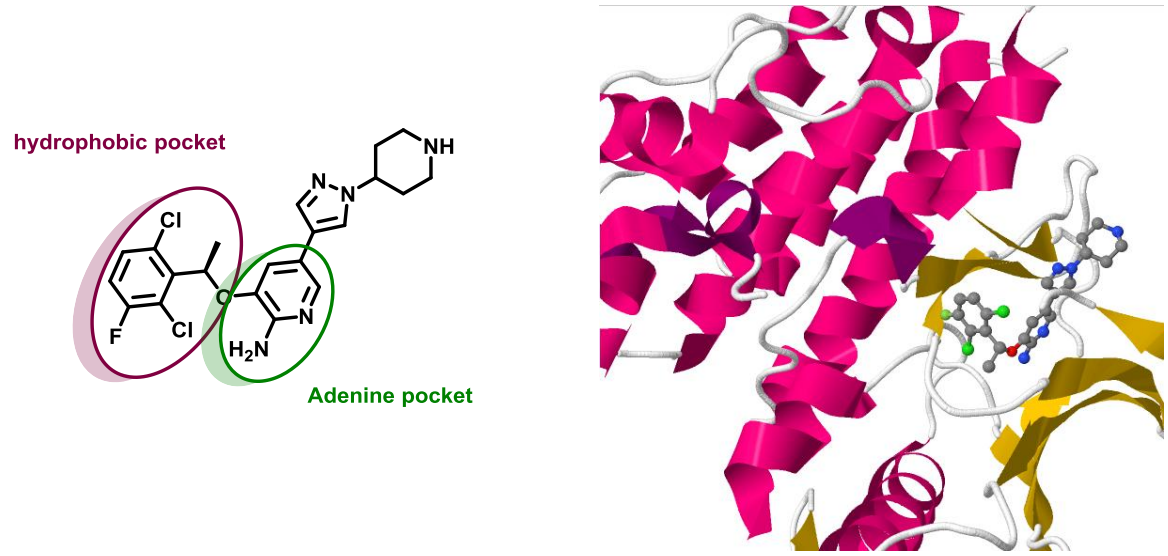

Figure 27 - Structure of crizotinib and its interaction with the ALK protein (gray-carbon, blue-nitrogen, red-oxygen, green-halides)[75]

Crizotinib was developed by Pfizer and belongs to the 3-benzyloxy-2-aminopyridine class of TKIs. With IC_{50} values of 5-20 nM for the hepatocyte growth factor receptor (c-met) and 25-50 nM for the anablastic lymphoma kinase (ALK), crizotinib inhibits the phosphorylation and subsequently the activation of these enzymes[76]. ALK and c-met are known to be involved in carcinogenesis and cancer progression (especially, ALK was identified as fusion partner for oncoproteins in many different cancer types[77]). ALK occurs in about 4% of the incidences of non-small cell lung cancer (NSCLC) patients accounting to 45,000 incidents per year worldwide. Crizotinib was approved in 2013 as the first ALK-inhibitor for ALK-positive metastatic non-small cell lung cancer.[78]

Developing a prodrug strategy for crizotinib

In order to convert crizotinib into a prodrug the chemical structure of crizotinib has to be modified in a way that interaction with its natural binding site of the tyrosine kinase is impossible. Hence, the interaction of crizotinib with the ALK oncoprotein has to be prevented. As shown in Figure 27, the interaction of crizotinib with ALK mainly affects the aminopyridine and halogenated phenyl moiety, whereas the piperidine structure sticks out of the binding pocket. Due to the higher nucleophilicity of the secondary amine of the piperidine structure

compared to the anilinic amine, the former has to be deactivated. Thus, we first methylated this position, which should not change the binding ability of crizotinib to the ALK protein.

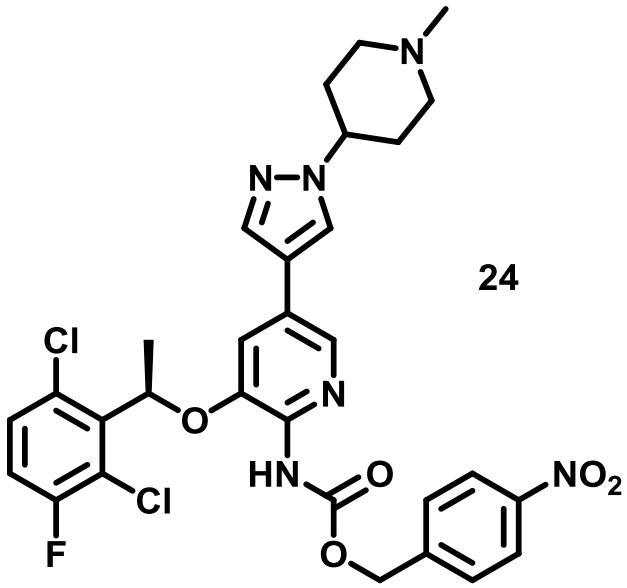

Figure 28 - Structure of the hypoxia activatable crizotinib prodrug

Now the trigger moiety can be selectively connected to the anilinic amino group. As trigger system *para*-nitrobenzyl alcohol was used. Although, the reduction potential of the benzylic nitro groups is too low to be activated at physiological conditions, this system is well described in literature as prodrug system activated by nitroreductases of *Escherichia coli*. Thus, this trigger moiety is used in so-called antibody-directed enzyme prodrug therapy (ADEPT) concepts[79]. For us the *para*-nitrobenzyl prodrug is only a test substance to investigate the stability and activation ability of crizotinib prodrug systems in general.

Syntheses

First, as already mentioned, the secondary amine functionality of the piperazinyl group of crizotinib was methylated using methyliodide in DMF. Purification of the "methylcrizotinib" was performed via column chromatography over alumina (EtOAc/MeOH 9:1) with fair yields of 50%.

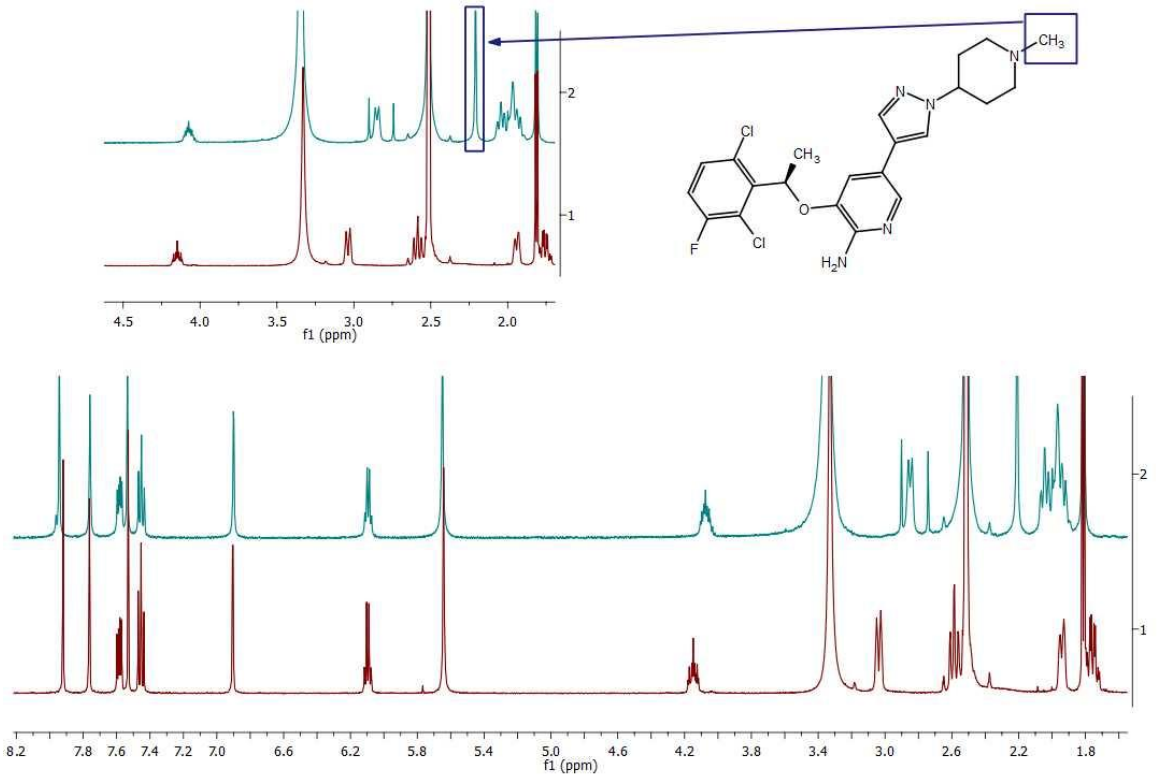

Figure 29 – Comparison of the ^{1}H-NMR spectra in d_6-DMSO of the commercially available crizotinib (red) and the methylated methylcrizotinib (green)

The next step was the attachment of the *para*-nitrobenzyl alcohol moiety. As there were no reactions described in literature (and crizotinib is quite expensive) first 2-aminopyridine was used as test system. In order to provide a synthetic strategy which can also be applied to other trigger systems like peptides for cathepsin cleavage, the formation of chloroformates of the trigger system was excluded (harsh reaction conditions and expected high amount of side reactions). Therefore, the first trials were coupling of 2-aminopyridine (**25**) with 4-nitrobenzyl(4-nitrophenyl) carbonate (**26**) to generate the desired carbamate **27** as visualized in Scheme 10. A comparable reaction was already described in literature[80]. Furthermore, addition of one equivalent of HOBt was tried to create a highly reactive acylating carbonate species in situ.

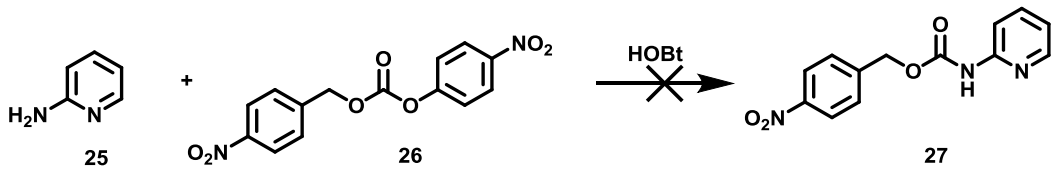

Scheme 10 - Reaction pathway of activated para-nitrobenzyl alcohol with 2-aminopyridine

Unfortunately, both reactions did not provide any product and the synthesis strategy was changed to the activation of the anilinic amine. Due to the pyridinic nitrogen atom next to the amine group of 2-aminopyridine (**25**), this compound class provides interesting capabilities in the formation of carbamates: the so called transesterifications. *Shinde et al.* could prove that Boc-protection of 2-aminopyridine in methanol resulted in the formation of the methyl carbamate (**30**) instead of the Boc-protected derivative (**28**) (Scheme 11).[81] Noteworthy, the reactions of 3-aminopyridine and 4-aminopyridine under the same reaction conditions yielded in the expected Boc-protected amines.

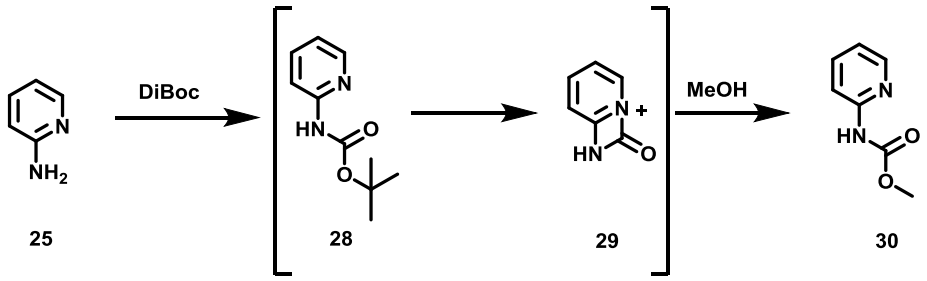

Scheme 11 - Transesterification of Boc-protected 2-aminopyridines in methanol to the methyl carbamate

For 2-aminopyridine the authors proposed the formation of a highly reactive four-membered ring system (**29**) in situ which can be attacked by hydroxyl groups. While *Shinde et al.* used Boc to form the reactive intermediate **29** and methanol (in excess) as nucleophile to perform the transesterification step, we developed the idea that this reaction might also be possible in an inert solvent like DMF using an active carbamate containing a good leaving group. Finally,

transesterification with the *para*-nitrobenzyl alcohol moiety forms the desired carbamate **27** (Scheme 12).

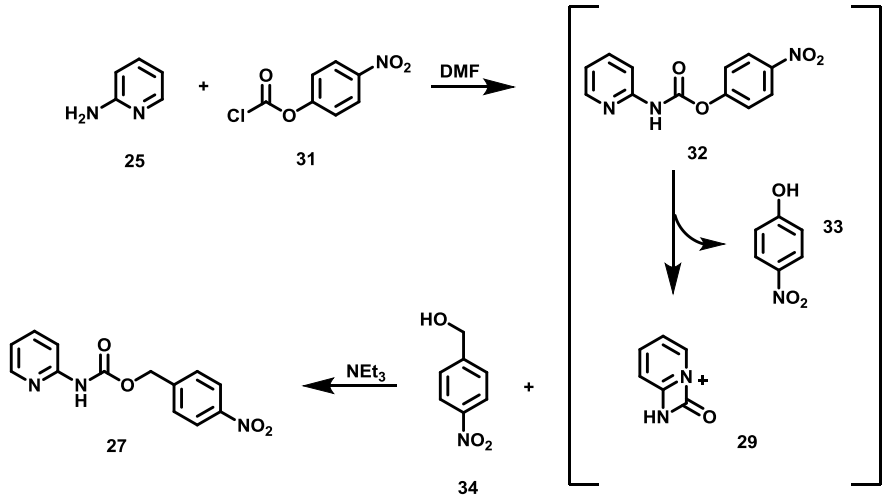

Scheme 12 - Reaction scheme of the activation reaction of 2-aminopyridine with 4-nitrophenyl chloroformate and substitution with 4-nitrobenzyl alcohol

For the synthesis of the "active" carbamate *para*-nitrophenyl chloroformate (**31**) was used. Since *para*-nitrophenol (**33**) is a good leaving group, the pyridine nitrogen atom should be able to attack the carbamate to form the active species **29**. Final addition of the benzyl alcohol **34** should result in the desired compound **27**. In detail, *para*-nitrophenyl chloroformate was added to 2-aminopyridine in DMF at 0°C with formation of **32**. After 15 minutes, the benzyl alcohol **34** was added and the reaction mixture was stirred overnight. As the analysis of the reaction clearly showed the formation of the desired compound **27** (indirectly proving formation of intermediate **32**), the strategy was transferred to methylcrizotinib. The same reaction procedure yielded after purification with preparative HPLC in 35% of the methylcrizotinib prodrug **24** (Figure 28). The final product was characterized by ^{1}H-NMR spectroscopy, mass spectrometry (1 Peak at M-H^{+}: 643) and HPLC analysis (single peak at 3.4min in ACN/H_2O 20-55%).

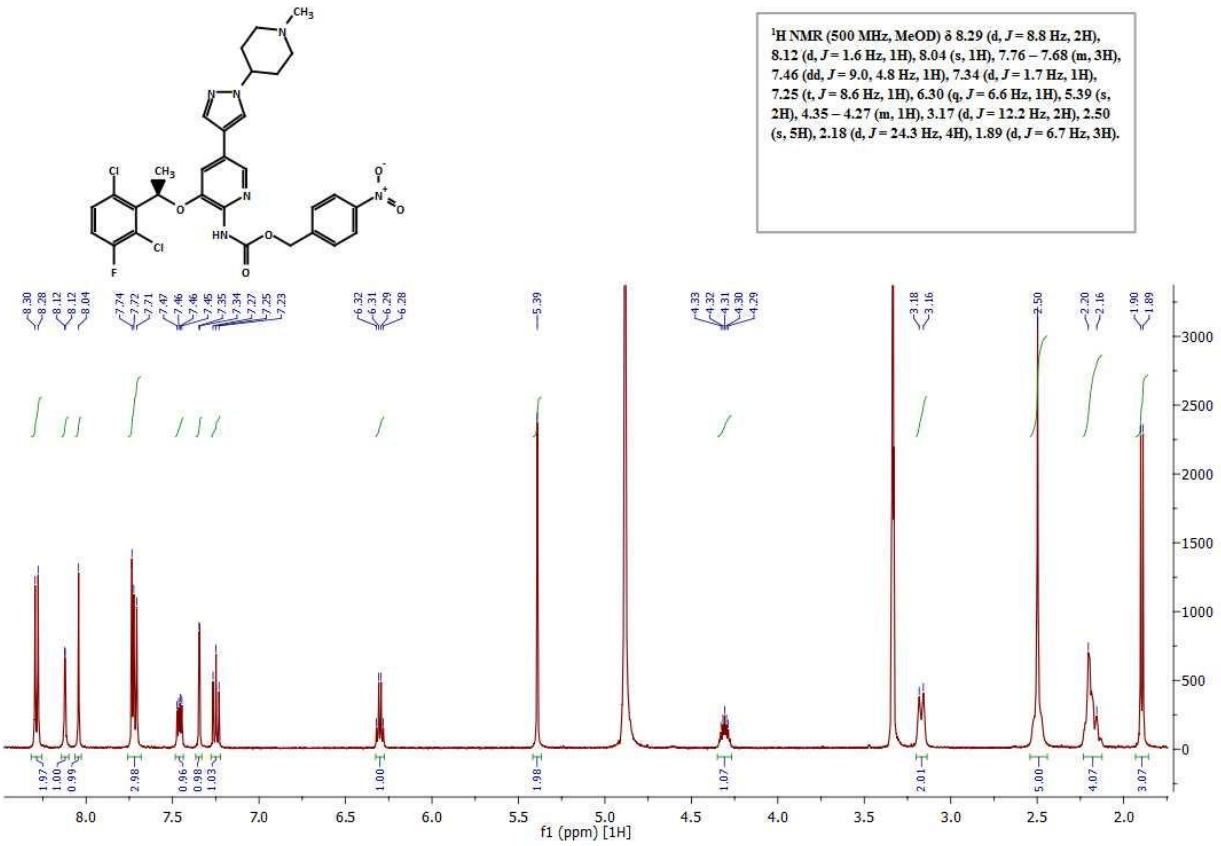

Figure 30 - ^{1}H-NMR of the nitrobenzyl-prodrug of crizotinib in d_4-MeOD

Cleavage test

To test if the crizotinib prodrug **24** indeed releases the compound after activation of the trigger unit a cleavage assay was performed. Therefore *E. coli* nitroreductase and NADH were incubated with **24** and the turnover of the prodrug into free crizotinib was detected by the decrease of product peak as well as the increase of the free crizotinib. As visualized in Figure 31, crizotinib has a retention time of ~4.6 min (1) while the prodrug elutes at ~6.8 minutes (2). After addition of the enzyme, the free drug was nearly fully release already after 30 min (3). The reaction seems to reach a steady-state, as still a small amount of educts was visible after 1 h (4). By this, the release of free crizotinib could be verified and the general applicability of this prodrug system was proven. Thus, this synthesis strategy can now be applied to other already established trigger systems like nitroimidazoles.

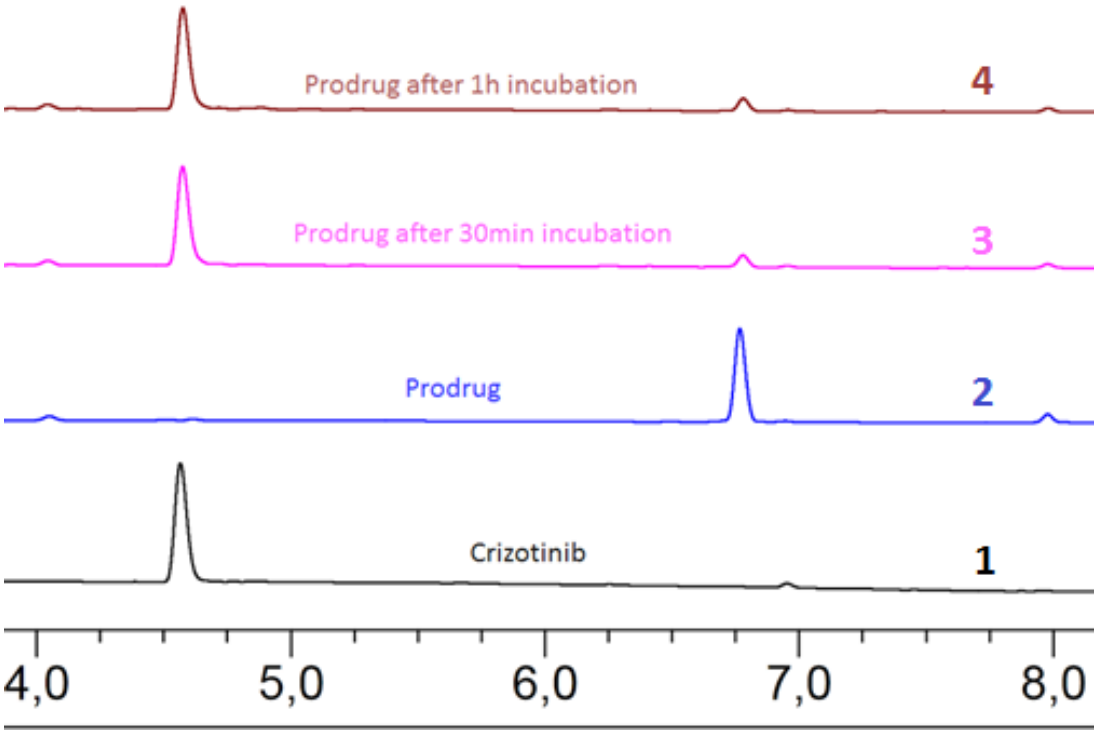

Figure 31 - Results of the cleavage assay of prodrug 24 of crizotinib.

VI. SUMMARY AND OUTLOOK

The area of tumor-activated prodrugs is a promising and multifaceted field in anticancer therapy research. Main goal of this concept is the selective release of a drug in the tumor tissue, overcoming the often severe side effects of anticancer drugs. In general, there is a great potential for the development of prodrugs with the possibility to use different triggers, linker moieties and drugs. In order to develop a new trigger system, the first aim of this thesis was the synthesis of a cathepsin K-selective moiety. Main target of this trigger system are tumors that overexpress cathepsin K like bone cancer cells or metastases. The synthesis could be successfully established using the backbone of the highly selective cathepsin K inhibitor balicatib, a self-immolative linker and a fluorophore as test moiety (Figure 32). Indeed, incubation of the novel compound with cathepsin K results in the release of the attached fluorophore. The next steps will be:

- to test the selectivity of this trigger system against other cathepsins
- in vitro investigations of the release in cancer cell lines overexpressing cathepsin K
- attachment of an appropriate anticancer drug
- exploiting the same synthetic strategy for the synthesis of other cathepsin-selective trigger units like cathepsin S

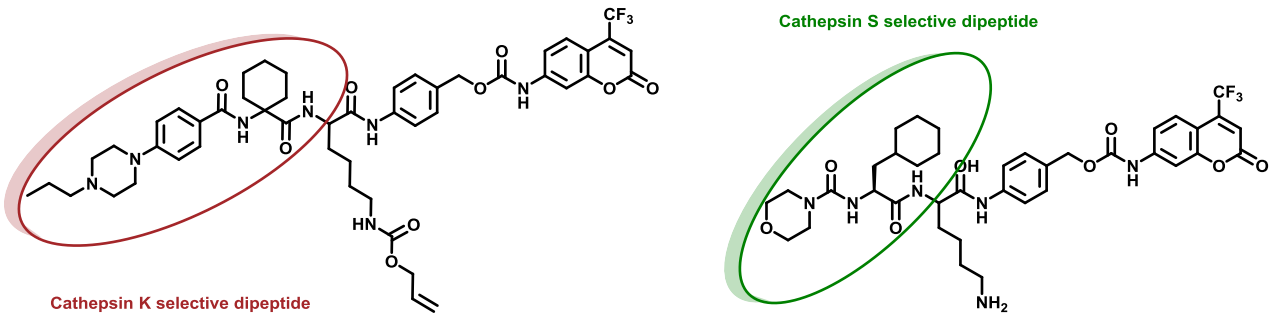

Figure 32 - Cathepsin S and Cathepsin K selective trigger systems

Aim of the second project of this master thesis was the development of a general synthetic prodrug strategy for the clinically approved ALK inhibitor crizotinib. Therefore, as a model system *para*-nitrobenzyl alcohol was attached to the NH_2 moiety crucial for binding of crizotinib to the ALK protein. After successful synthesis of the prodrug, the corresponding cleavage study clearly showed the release of free crizotinib and consumption of the prodrug. Due to these promising results, the next step will be the attachment of an already established trigger unit like the hypoxia activatable class of nitroimidazoles. Finally, this concept hopefully will enable the combined therapy of crizotinib with other TKIs in clinical use without occurrence of severe side effects.

VII. EXPERIMENTAL SECTION

a. Materials and instrumentation

Chemicals

All solvents and reagents were obtained from commercial suppliers and used without further purification. Anhydrous DMF, THF and toluene were bought from Sigma-Aldrich over molecular sieves. For column chromatography silica gel 60 from Sigma-Aldrich (particle size 35–70 µm) was used. 4-(piperazin-1-yl)-benzoic acid ethyl ester was purchased from CHESS fine organics. Crizotinib was purchased from Ontario Chemicals, Inc. Cathepsin K, OmniCathepsin® and the cathepsin K reference was purchased from Enzo Life Sciences. All other chemicals, if not further specified were purchased from Sigma-Aldrich, Acros, Fisher-TCI or AlfaAesar.

ATTENTION:

Phosgene

This master thesis includes several reactions with phosgene or triphosgene as reactant. Phosgene is a highly toxic respiratory poison. Reactions with phosgene should be performed in a closed system with an appended gas destruction module containing sodium hydroxide. After every reaction, argon should be bubbled through the reaction mixture to remove rests of unreacted phosgene. Subsequent removal of the solvent of these reactions mixtures should be performed under reduced pressure in a fume hood.

Instrumentation

Mass Spectrometry

ESI-MS spectrometry was carried out with a Bruker Esquire 3000 ion trap spectrometer (Bruker Daltonic, Bremen, Germany). Expected and experimental isotope distributions were compared.

NMR Spectroscopy

NMR spectra were recorded in d_6-DMSO, D_2O, MeOD or $CDCl_3$, referring to the respective solubilities of the synthesized compounds, with a Bruker FT-NMR Avance III 500 MHz spectrometer at 500.10 (^1H). Chemical shifts (ppm) were referenced internal to the solvent residual peaks. For the description of the spin multiplicities the following abbreviations were used: s = singlet, d = duplet, t = triplet, sx = sextet, m = multiplet.

Preparative RP-HPLC

Preparative RP-HPLC was performed on an Agilent 1200 Series system controlled by Chemstation software. The experimental conditions were as follows: stationary phase: silica-based C18 gel; column: XBridge BEH C18 OBD Prep Column (130 Å, 5 µm, 19 mm x 250 mm); flow rate: 17.00 ml/min, injection volume: 5–7 ml; column temperature: 25°C.

b. Syntheses

4-(4-propylpiperazinyl)benzoic acid ethyl ester (8)

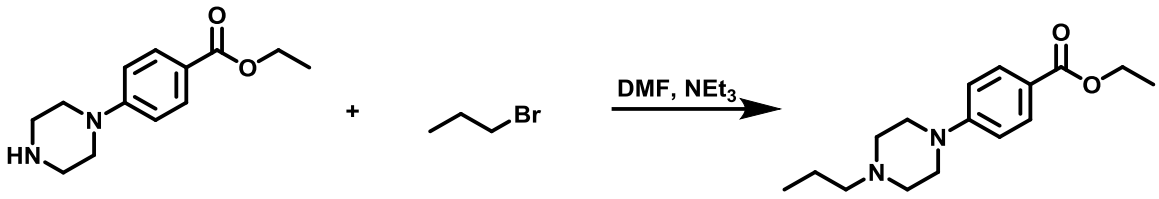

7 8

4-piperazin-1-yl benzoic acid ethyl ester **7** (300 mg, 1.28 mmol) was dissolved in DMF abs. (6 mL), triethylamine (355µL, 2.56 mmol) and 1-bromopropane (128 µL, 1.41 mmol) was added. The reaction mixture was stirred overnight. DMF was removed under reduced pressure and the crude product was dried in vacuo overnight. Purification was performed with column chromatography using EtOAC/MeOH (37:3) containing 1% triethylamine to obtain product **8**.

Yield: 293 mg (50%)

Characterization:

^{1}H NMR (500 MHz, DMSO): δ = 7.79 (d, *J* = 9.0 Hz, 2H), 6.98 (d, *J* = 9.1 Hz, 2H), 4.24 (d, *J* = 7.1 Hz, 2H), 3.32 – 3.28 (m, 4H), 2.49 – 2.46 (m, 4H), 2.30 – 2.24 (m, 2H), 1.48 (d, *J* = 7.4 Hz, 2H), 1.30 (t, *J* = 7.1 Hz, 3H), 0.88 (t, *J* = 7.4 Hz, 3H)

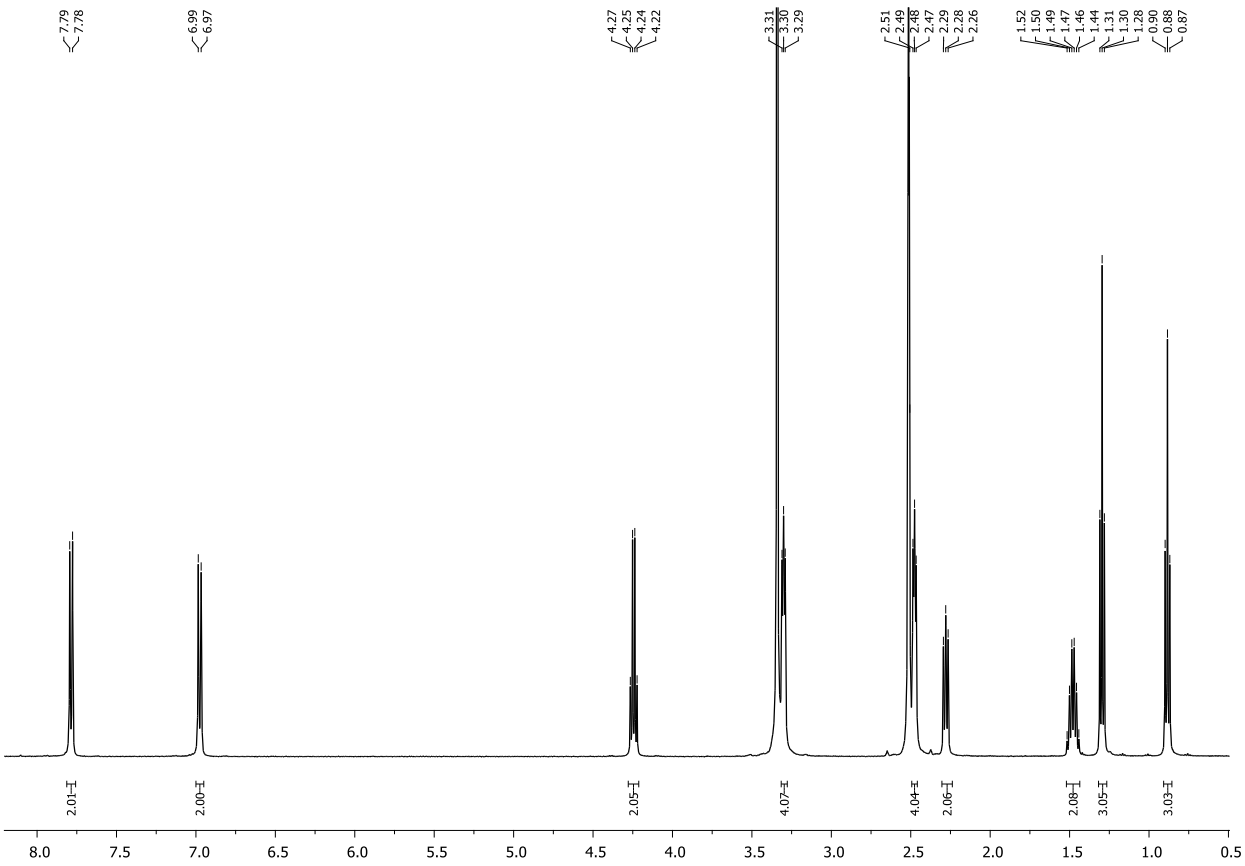
7.79
7.78
6.99
6.97
4.27
4.25
4.24
4.22
3.31
3.30
3.29
2.51
2.49
2.48
2.47
2.29
2.28
2.26
1.52
1.50
1.49
1.47
1.46
1.44
1.31
1.30
1.28
0.90
0.88
0.87
2.01
2.00
2.05
4.07
4.04
2.06
2.08
3.05
3.03
8.0
7.5
7.0
6.5
6.0
5.5
5.0
4.5
4.0
3.5
3.0
2.5
2.0
1.5
1.0
0.5

4-(4-carboxyphenyl)-1-propylpiperazin-1-ium chloride (10)

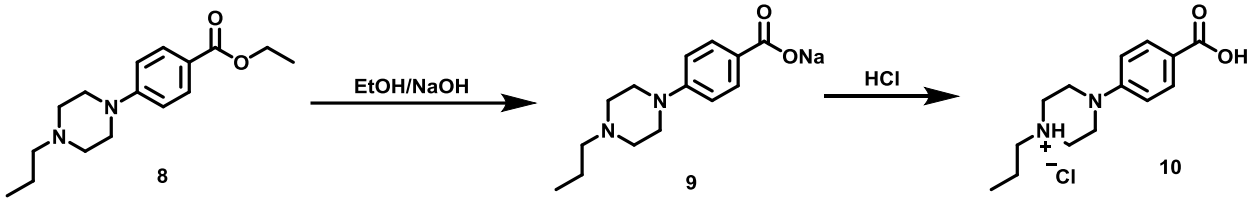

Ethyl 4-(4-propylpiperazin-1-yl)benzoate **8** (250 mg, 0.905 mmol) was dissolved in 4 mL of ethanol/water (1:1) at 70 °C and hydrolyzed by addition of 2 equiv. of sodium hydroxide. The reaction mixture was refluxed for 2 h and cooled down to room temperature. After acidification to pH 3 with 1M hydrochloric acid, the solvent was reduced to 3 mL which resulted in precipitation. The precipitate was filtered, washed with diethyl ether several times and dried in vacuo overnight to obtain pure product **10**.

Yield: 209 mg (81%)

Characterization:

^{1}H NMR (500 MHz, DMSO): δ = 12.45 (bs, 1H), 10.85 (bs, 1H), 7.83 (d, *J* = 8.7 Hz, 2H), 7.06 (d, *J* = 8.8 Hz, 2H), 4.02 (d, *J* = 12.9 Hz, 2H), 3.55 (d, *J* = 11.3 Hz, 2H), 3.27 (t, *J* = 12.6 Hz, 2H), 3.15 – 3.01 (m, 4H), 1.76 (sx, *J* = 15.6, 7.6 Hz, 2H), 0.93 (t, *J* = 7.3 Hz, 3H)

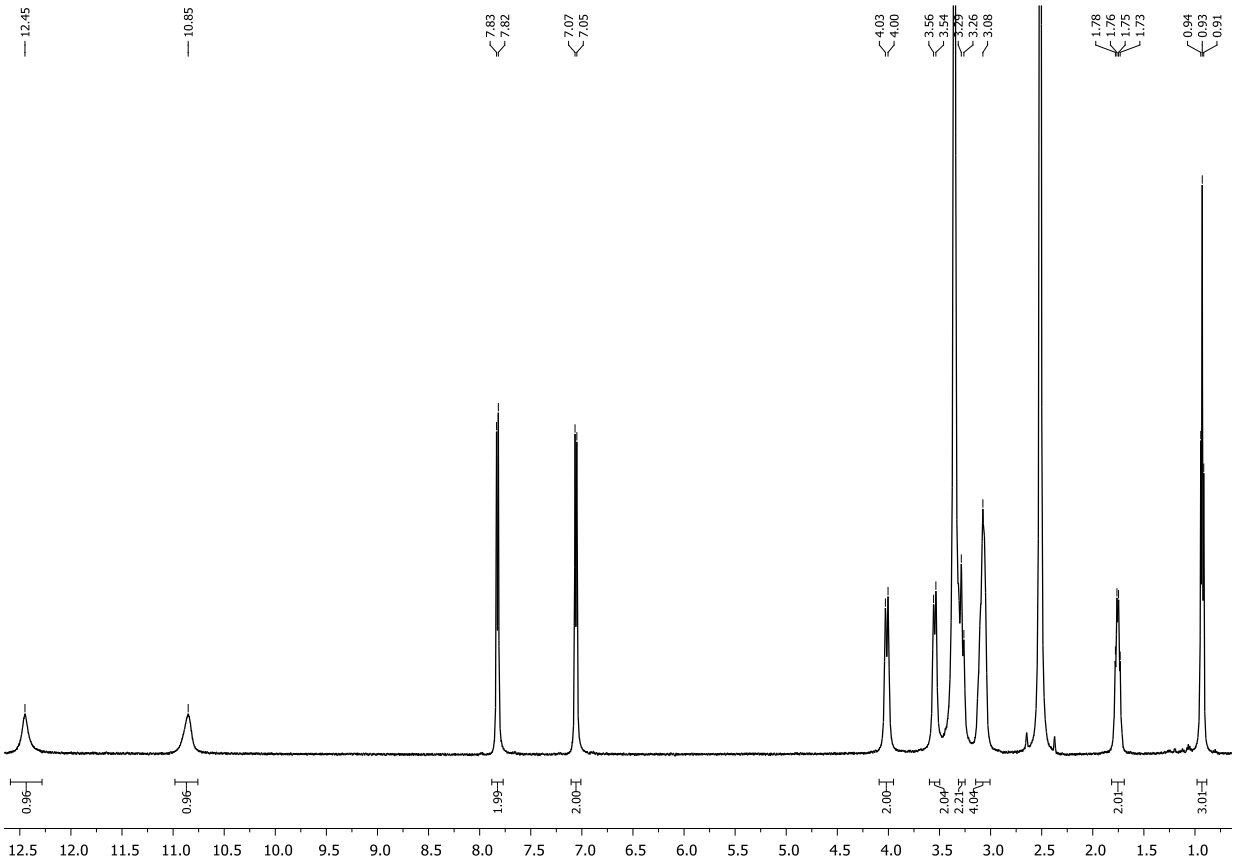
12.45
10.85
7.83
7.82
7.07
7.05
4.03
4.00
3.56
3.54
3.29
3.26
3.08
1.78
1.76
1.75
1.73
0.94
0.93
0.91
0.96
0.96
1.99
2.00
2.00
2.04
2.21
4.04
2.01
3.01
12.5 12.0 11.5 11.0 10.5 10.0 9.5 9.0 8.5 8.0 7.5 7.0 6.5 6.0 5.5 5.0 4.5 4.0 3.5 3.0 2.5 2.0 1.5 1.0

Methyl 1-(4-(4-propylpiperazin-1-yl)benzamido)cyclohexane-1-carboxylate (14)

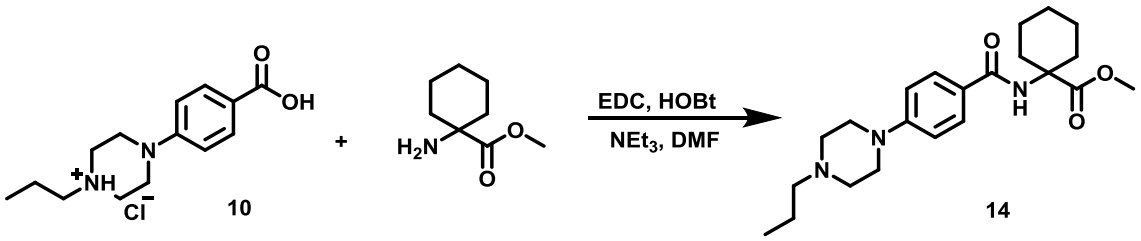

4-(4-carboxyphenyl)-1-propylpiperazin-1-ium chloride **10** (150 mg, 0.527 mmol) was dissolved in DMF (4mL) and H_2N-Ac6-OMe (83 µL, 0.553mmol), triethylamine (73 µL, 0.527 mmol) and hydroxybenzotriazole (86 mg, 0.56 mmol) were added. After 5 min 1-ethyl-3-(3-dimethylaminopropyl)carbodiimide (EDC, 107.3 mg, 0.56 mmol) was added and the reaction mixture was stirred overnight (color changed from colorless to slight orange). After dilution with $NaHCO_3$, the reaction mixture was extracted with ethyl acetate three times. The combined organic phases were dried over Na_2SO_4 and the solvent was removed. Purification was performed via column chromatography (EtOAc/MeOH 8:2) to obtain product **14**.

Yield: 109 mg (54%)

Characterization:

^{1}H NMR (500 MHz, DMSO): δ = 8.03 (s, 1H), 7.74 (d, *J* = 9.0 Hz, 2H), 6.95 (d, *J* = 9.0 Hz, 2H), 3.57 (s, 3H), 3.27 – 3.22 (m, 4H), 2.49 (t, *J* = 5.2 Hz, 4H), 2.32 – 2.25 (m, 2H), 2.07 (d, *J* = 13.3 Hz, 2H), 1.76 (t, *J* = 11.2 Hz, 2H), 1.60 – 1.44 (m, 8H), 0.89 (t, *J* = 7.4 Hz, 3H)

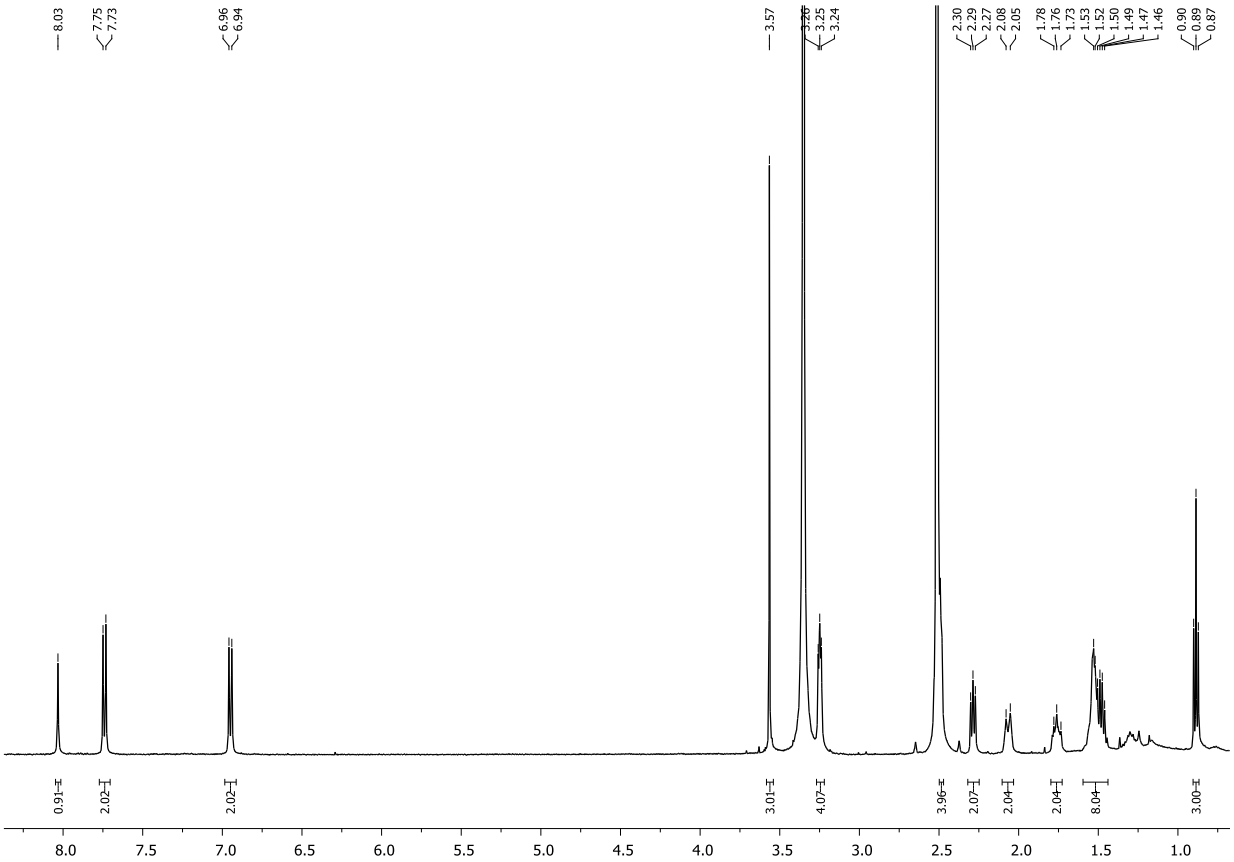
8.03
7.75
7.73
6.96
6.94
3.57
3.26
3.25
3.24
2.30
2.29
2.27
2.08
2.05
1.78
1.76
1.73
1.53
1.52
1.50
1.49
1.47
1.46
0.90
0.89
0.87
0.91
2.02
2.02
3.01
4.07
3.96
2.07
2.04
2.04
8.04
3.00
8.0
7.5
7.0
6.5
6.0
5.5
5.0
4.5
4.0
3.5
3.0
2.5
2.0
1.5
1.0

4-(4-((1-carboxycyclohexyl)carbamoyl)phenyl)-1-propylpiperazin-1-ium chloride (16)

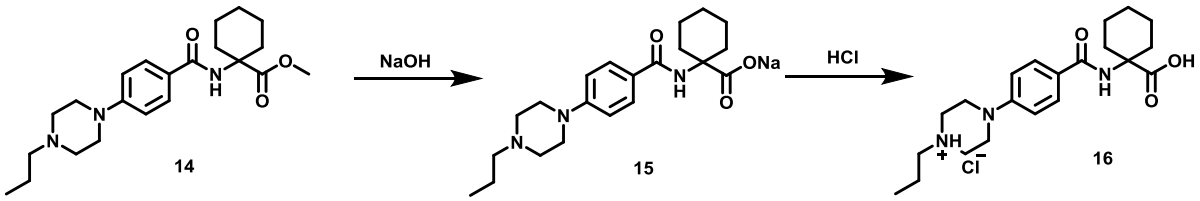

Methyl 1-(4-(4-propylpiperazin-1-yl)benzamido)cyclohexane-1-carboxylate **14** (50 mg, 0.281 mmol) was dissolved in water (1 mL) containing three equivalents of sodium hydroxide (34 mg, 0.843 mmol) and THF (1.5 mL). The reaction mixture was refluxed overnight. The mixture was cooled down to room temperature and the solvent was removed under reduced pressure. The crude product was dissolved in water, adjusted to pH 4 with 1M hydrochloric acid and extracted with EtOAc three times. The aqueous phase was evaporated and the product was dissolved in a small amount of THF. After precipitation with Et_2O, the product was dissolved in ethanol to remove rests of sodium chloride. The solid was filtered, solvent was removed and the product was dried in vacuo overnight to obtain pure **16**.

Yield: 42,5 mg (80%)

Characterization:

^{1}H NMR (500 MHz, DMSO): δ = 12.06 (s, 1H), 11.06 (s, 1H), 7.96 (s, 1H), 7.80 (d, *J* = 8.8 Hz, 2H), 7.04 (d, *J* = 8.8 Hz, 2H), 3.96 (d, *J* = 11.9 Hz, 2H), 3.54 (d, *J* = 11.0 Hz, 2H), 3.26 (s, 2H), 3.06 (s, 4H), 2.12 (d, *J* = 13.2 Hz, 2H), 1.76 (s, 4H), 1.53 (s, 5H), 1.28 (s, 1H), 0.93 (t, *J* = 7.4 Hz, 3H).

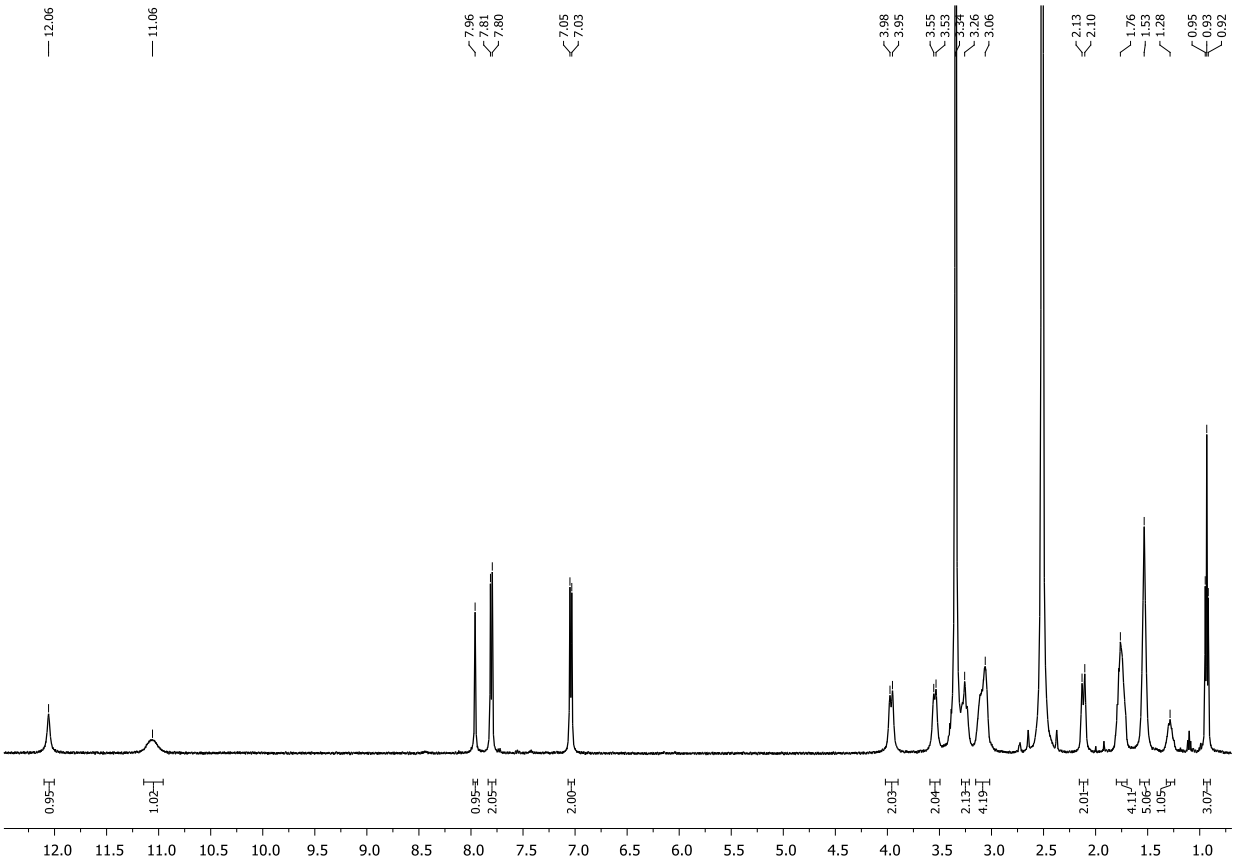
12.06
11.06
7.96
7.81
7.80
7.05
7.03
3.98
3.95
3.55
3.53
3.34
3.26
3.06
2.13
2.10
1.76
1.53
1.28
0.95
0.93
0.92
0.95
1.02
0.95
2.05
2.00
2.03
2.04
2.13
4.19
2.01
4.11
5.06
1.05
3.07
12.0 11.5 11.0 10.5 10.0 9.5 9.0 8.5 8.0 7.5 7.0 6.5 6.0 5.5 5.0 4.5 4.0 3.5 3.0 2.5 2.0 1.5 1.0

(9H-fluoren-9-yl)methyl allyl (6-((4-(hydroxymethyl)phenyl)amino)-6-oxohexane-1,5-diyl)dicarbamate (18)

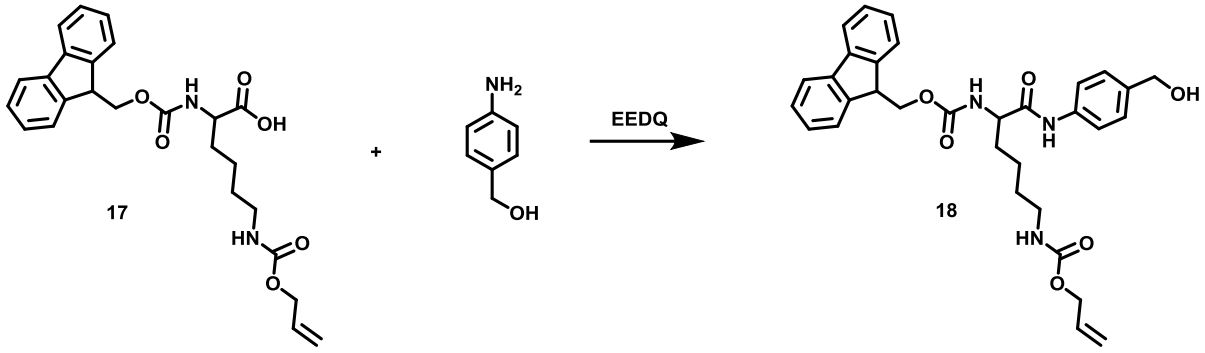

Fmoc-Lys(alloc)-OH (300 mg, 0.663 mmol) **17** and *para*-aminobenzyl alcohol (86mg, 0.7 mmol) were dissolved THF (5.5 mL) and ethoxycarbonyl-2-ethoxy-1,2-dihydroquinoline (EEDQ, 175 mg, 0.7 mmol) was added. The reaction mixture was stirred for 16 h. The solvent was removed under reduced pressure at 30 °C and the remaining residue was triturated with diethyl ether and suspended with an ultrasonic bath. The precipitation was filtered and dried in vacuo overnight to obtain **18**.

Yield: 332,2 mg (90%)

Characterization:

^{1}H NMR (500 MHz, DMSO): δ = 9.97 (s, 1H), 7.90 (d, *J* = 7.5 Hz, 2H), 7.75 (t, *J* = 6.7 Hz, 2H), 7.62 (d, *J* = 7.9 Hz, 1H), 7.56 (d, *J* = 8.4 Hz, 2H), 7.43 (t, *J* = 6.6 Hz, 2H), 7.34 (dd, *J* = 12.2, 7.1 Hz, 2H), 7.25 (d, *J* = 8.4 Hz, 2H), 7.19 (t, *J* = 5.5 Hz, 1H), 5.90 (ddd, *J* = 22.4, 10.7, 5.4 Hz, 1H), 5.26 (d, *J* = 17.2 Hz, 1H), 5.16 (d, *J* = 10.4 Hz, 1H), 5.10 (t, *J* = 5.7 Hz, 1H), 4.44 (d, *J* = 5.4 Hz, 4H), 4.31 – 4.27 (m, 2H), 4.24 (dd, *J* = 12.5, 5.6 Hz, 1H), 4.13 (dd, *J* = 13.9, 8.7 Hz, 1H), 2.99 (d, *J* = 5.6 Hz, 2H), 1.66 (dt, *J* = 18.3, 9.2 Hz, 2H), 1.47 – 1.25 (m, 4H)

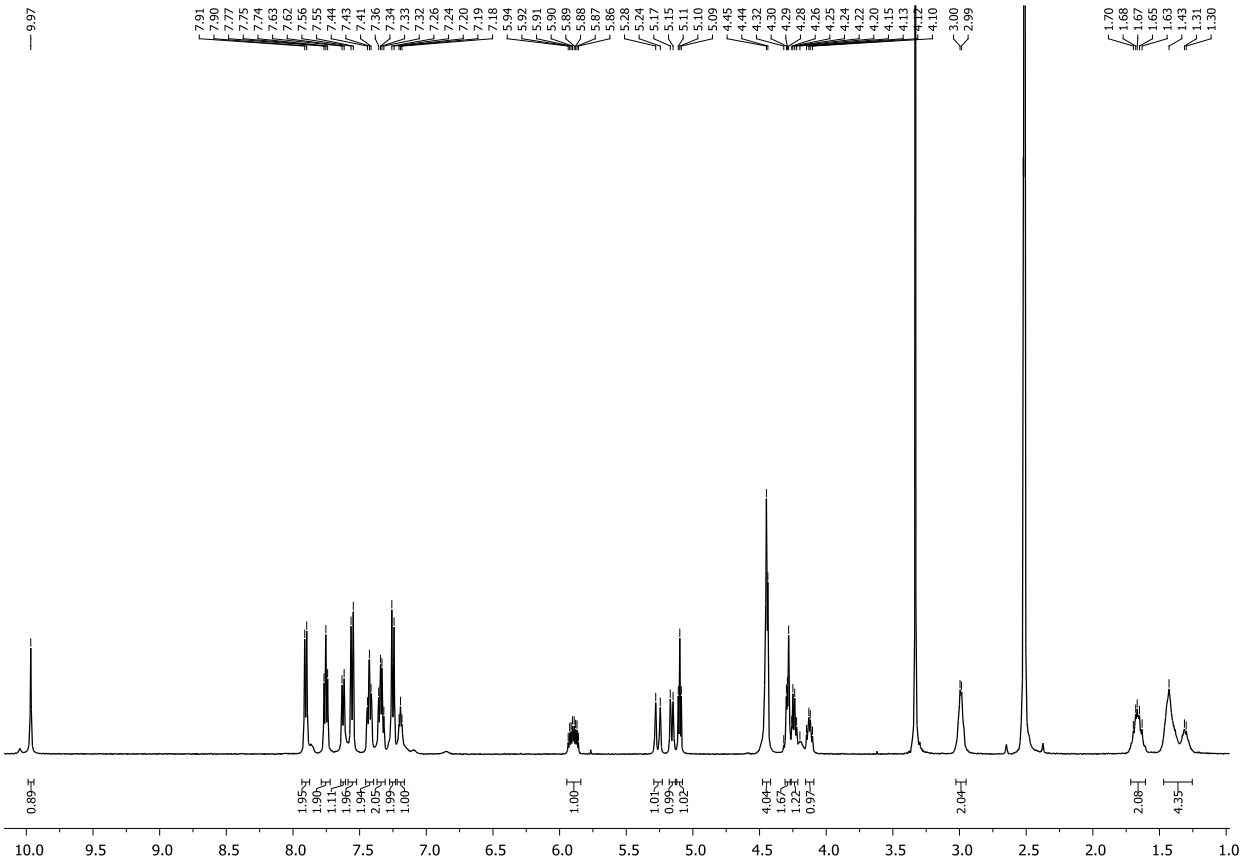
9.97
7.91
7.90
7.77
7.75
7.74
7.63
7.62
7.56
7.55
7.44
7.43
7.41
7.36
7.34
7.33
7.32
7.26
7.24
7.20
7.19
7.18
5.94
5.92
5.91
5.90
5.89
5.88
5.87
5.86
5.28
5.24
5.17
5.15
5.11
5.10
5.09
4.45
4.44
4.32
4.30
4.29
4.28
4.26
4.25
4.24
4.22
4.20
4.15
4.13
4.12
4.10
3.00
2.99
1.70
1.68
1.67
1.65
1.63
1.43
1.31
1.30
0.89
1.95
1.90
1.11
1.96
1.94
2.05
1.99
1.00
1.00
1.01
0.99
1.02
4.04
1.67
1.22
0.97
2.04
2.08
4.35
10.0
9.5
9.0
8.5
8.0
7.5
7.0
6.5
6.0
5.5
5.0
4.5
4.0
3.5
3.0
2.5
2.0
1.5
1.0

(9H-fluoren-9-yl)methyl allyl (6-oxo-6-((4-((((2-oxo-4-(trifluoromethyl)-2H-chromen-7-yl)carbamoyl)oxy)methyl)phenyl)amino)hexane-1,5-diyl)dicarbamate (22)

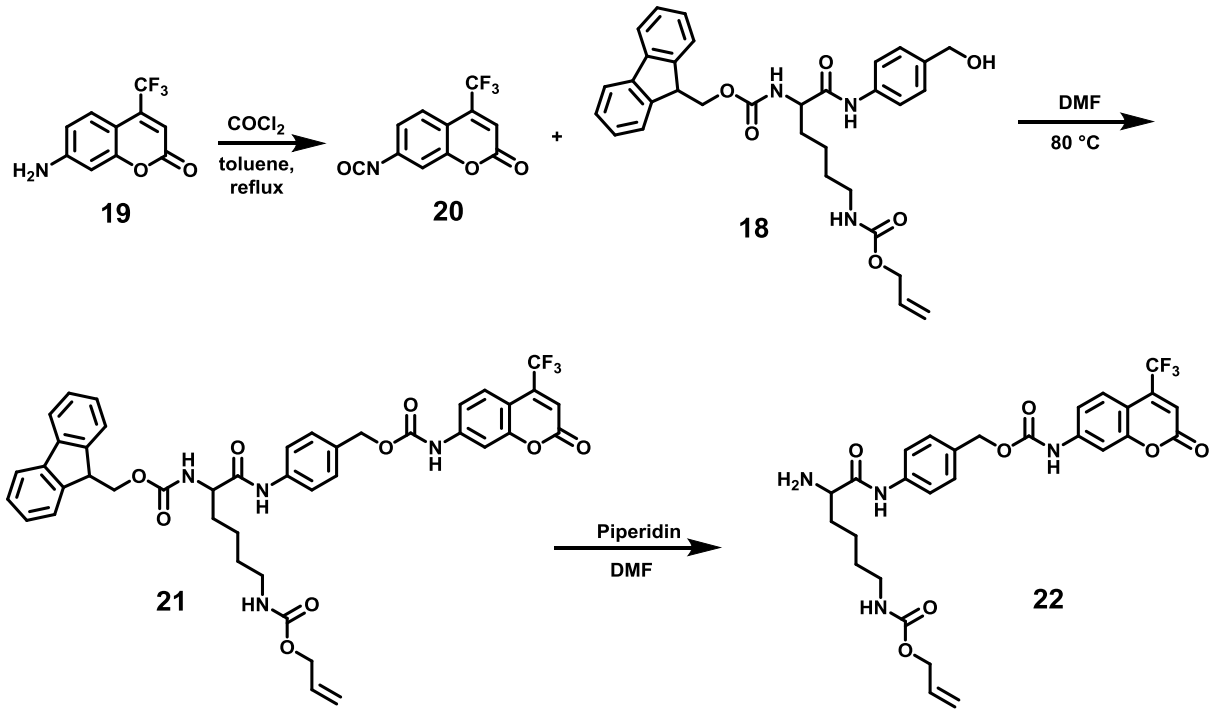

Coumarin (200 mg, 0.873 mmol) **19** was suspended in 1 mL of toluene and a 20% solution of phosgene in toluene (4 mL) was added. The reaction mixture was stirred for 16 h at 120 °C. Argon was bubbled through the reaction mixture to remove rests of phosgene. The solvent was removed under reduced pressure and the product was dried in vacuo. Fmoc-Lys(alloc)-PABOH **18** (195 mg, 0.349 mmol) was dissolved in DMF abs. (5 mL) and crude isocyanate **20** (222.8 mg, 0.873 mmol) in DMF abs. (3 mL) was added. The reaction mixture was stirred at 80 °C for 2 h and solvent was removed under reduced pressure. The product was dissolved in a small amount of THF and precipitated with petrol ether. The precipitate was dried in vacuo overnight and used without further purification in the deprotection step.

Fmoc-Lys(alloc)-PABOH-Coumarin **21** (110 mg, 0.135 mmol) was dissolved in DMF (1.6 mL) and 20% piperidine in DMF (1.6 mL, 3.375 mmol) was added. The reaction mixture was stirred for 30 min. After addition of piperidine the color of the reaction mixture changed to orange and

back to yellow again. The solvent was removed under reduced pressure and the product was dried in vacuo overnight. Purification was performed via column chromatography (EtOAC/PE: 4:6 pre-eluting, EtOAc/MeOH 9:1 elution of product) to obtain product **22**.

Characterization:

^{1}H NMR (500 MHz, DMSO): δ = 10.45 (s, 1H), 7.71 – 7.64 (m, 4H), 7.50 (dd, *J* = 8.9, 2.1 Hz, 1H), 7.40 (d, *J* = 8.6 Hz, 2H), 7.19 (t, *J* = 5.8 Hz, 1H), 6.89 (s, 1H), 5.93 – 5.85 (m, 1H), 5.26 (dd, *J* = 17.2, 1.7 Hz, 1H), 5.18 – 5.13 (m, 3H), 4.44 (d, *J* = 5.3 Hz, 2H), 2.97 (d, *J* = 5.9 Hz, 2H), 1.61 (dd, *J* = 11.7, 6.0 Hz, 2H).

ESI-MS in MeOH: m/z (positive) 591 (H_2N-Lys(alloc)-PABC-Coumarin – H^+)

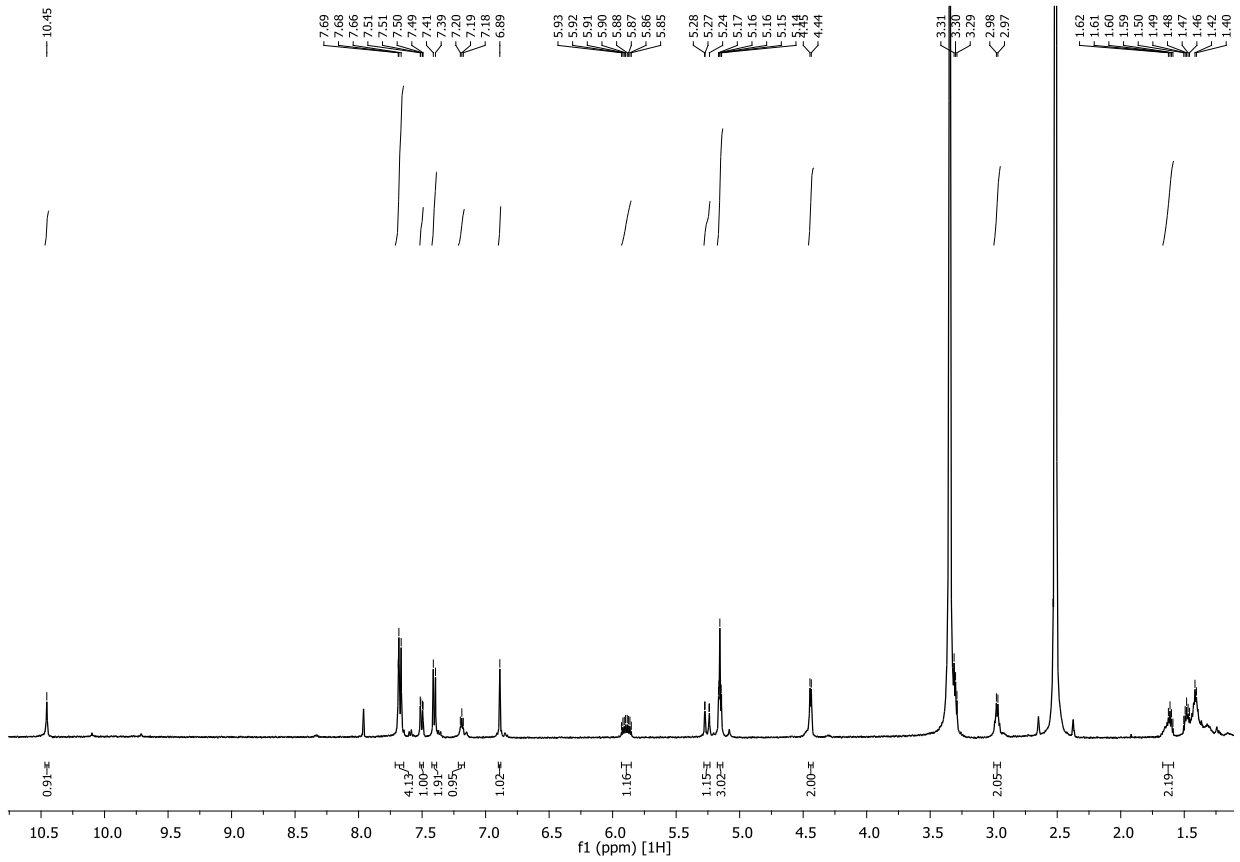

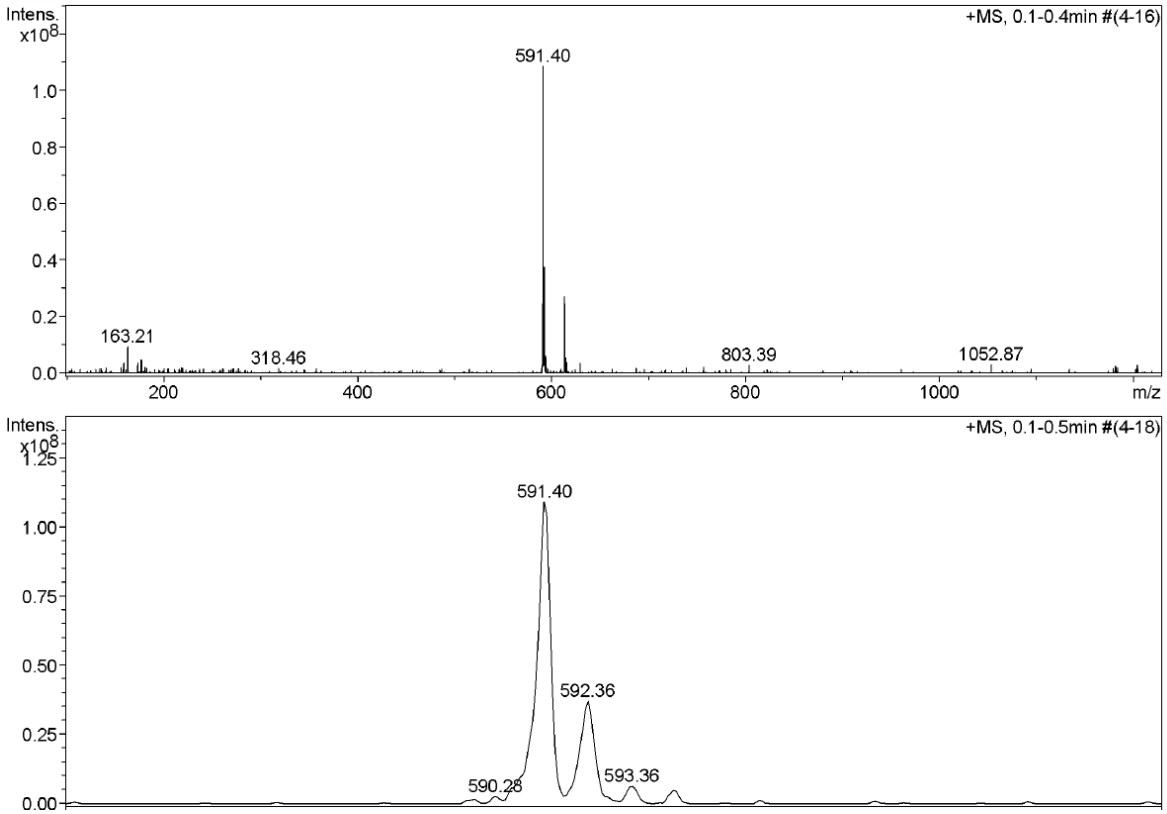
Intens.
x10^8
+MS, 0.1-0.4min #(4-16)
591.40
1.0
0.8
0.6
0.4
0.2
163.21
318.46
803.39
1052.87
0.0
200
400
600
800
1000
m/z
Intens.
x10^8
+MS, 0.1-0.5min #(4-18)
1.25
591.40
1.00
0.75
0.50
592.36
0.25
590.28
593.36
0.00

Allyl (6-oxo-6-((4-((((2-oxo-4-(trifluoromethyl)-2H-chromen-7-yl)carbamoyl)oxy)methyl) phenyl)amino)-5-(1-(4-(4-propylpiperazin-1-yl)benzamido)cyclohexane-1-carboxamido)hexyl) carbamate (23)

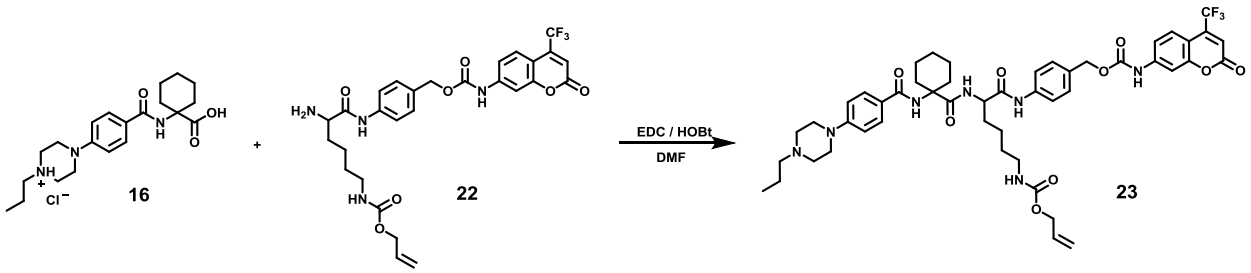

Compound **16** (36.1 mg, 0.088 mmol) was dissolved in DMF (2 mL) and hydroxybenzotriazole (15 mg, 0.097 mmol) and EDC (19 mg, 0.097) were added. The reaction mixture was stirred for 30 min and H_2N-Lys(alloc)-PABC-Coumarin **22** (52.2 mg, 0.088 mmol) and *N,N*-diisopropylethylamine (15 µL, 0.088 mmol) in DMF (1 mL) were added to the solution. The reaction mixture was stirred overnight. The solvent was removed under reduced pressure, the product was dissolved in EtOAc and washed with aqueous $NaHCO_3$ (5%), twice with water and dried over Na_2SO_4. The solvent was removed under reduced pressure and the product was dried in vacuo overnight. Further purification was performed with preparative HPLC using ACN/H_2O (0.1% formic acid) as eluent to obtain product **23**.

Yield: 8 mg (10%)

Characterization:

^{1}H NMR (500 MHz, MeOD): δ = 7.82 – 7.76 (m, 5H), 7.67 (d, *J* = 7.0 Hz, 1H), 7.45 – 7.41 (m, 3H), 7.00 (d, *J* = 9.0 Hz, 2H), 6.75 (s, 1H), 5.97 – 5.89 (m, 1H), 5.32 – 5.27 (m, 1H), 5.22 (s, 2H), 5.18 (d, *J* = 10.6 Hz, 1H), 4.53 – 4.46 (m, 3H), 3.38 – 3.35 (m, 4H), 3.11 (t, *J* = 6.5 Hz, 2H), 2.68 (s, 4H), 2.47 – 2.41 (m, 2H), 2.20 (dd, *J* = 29.7, 14.1 Hz, 2H), 2.01 (dd, *J* = 36.6, 26.8 Hz, 4H), 1.72 (s, 5H), 1.66 – 1.30 (m, 11H), 0.98 (t, *J* = 7.4 Hz, 3H).

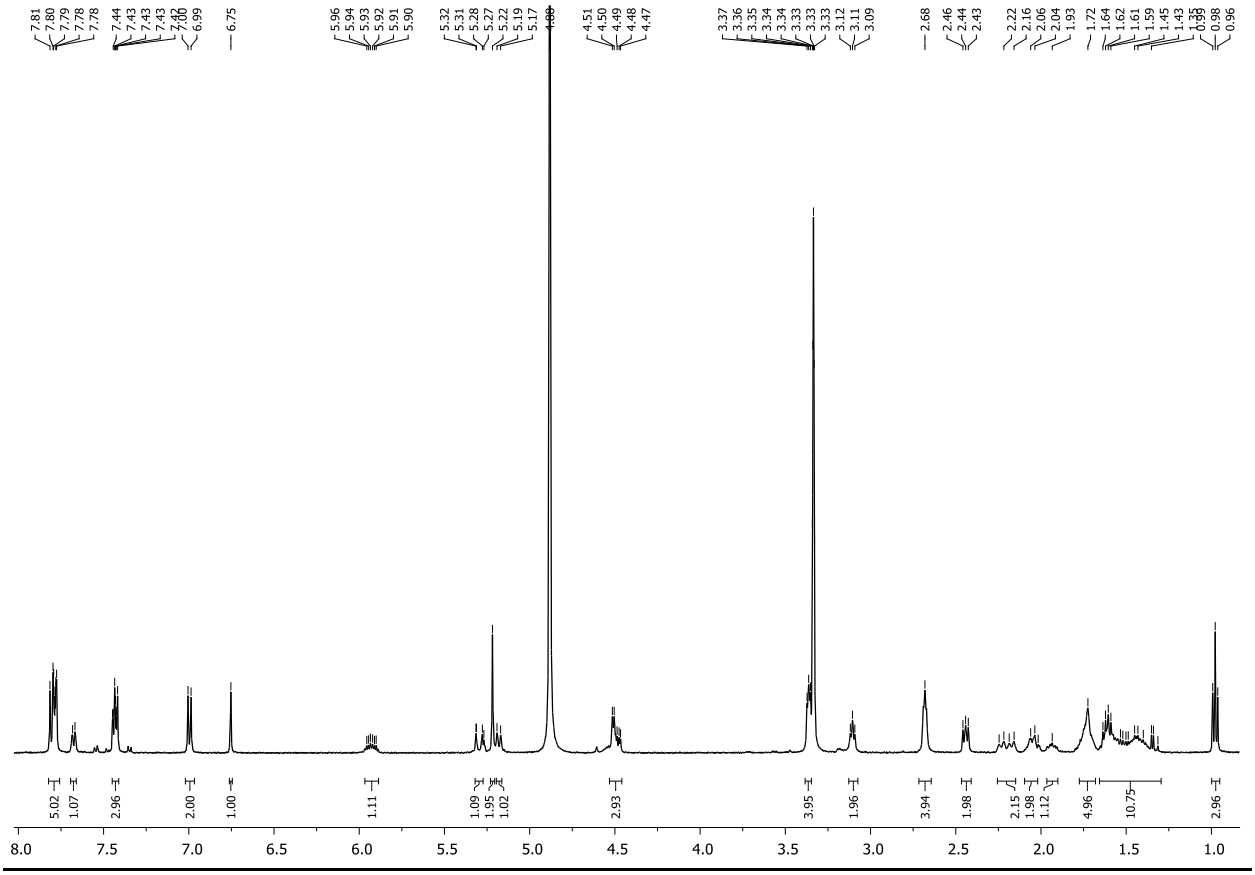

(R)-3-(1-(2,6-dichloro-3-fluorophenyl)ethoxy)-5-(1-(1-methylpiperidin-4-yl)-1H-pyrazol-4-yl)pyridin-2-amine

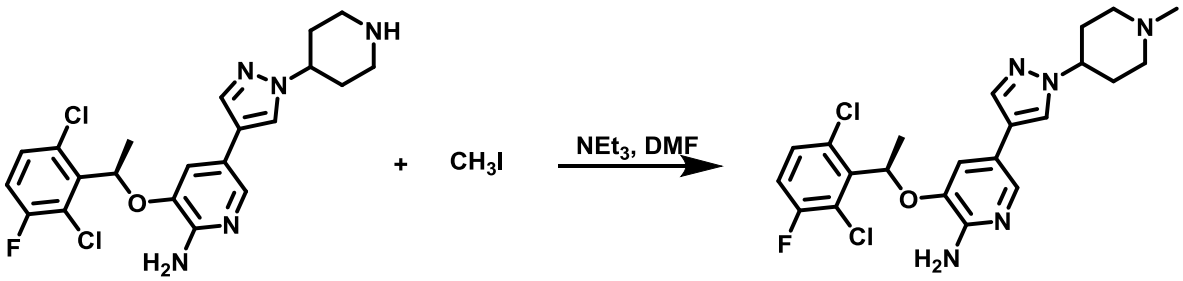

Crizotinib (250 mg, 0.56 mmol) was dissolved in DMF abs. (4 mL) and triethylamine (82.2 mg, 0.83 mmol, 112.2 µL) was added. After cooling down the reaction mixture to 0 °C, a solution of methyl iodide (118.2 mg, 0.83 mmol, 52.1 µL) in DMF abs. (247,9 µL) was added portion wise (3 x 100µL). The reaction mixture was allowed to stir at room temperature overnight. The reaction mixture was diluted with water (6 mL) and extracted with ethyl acetate 5 times. All organic portions were combined, washed with brine, dried over sodium sulfate (anhydrous) and the solvent was removed under reduced pressure. The product was dried in vacuo overnight and purification was performed via column chromatography (aluminum oxide, EtOAc/MeOH 9:1).

Yield: 127 mg (49%)

Characterization:

^{1}H NMR (500 MHz, DMSO) δ 7.94 (s, 1H), 7.76 (d, *J* = 1.7 Hz, 1H), 7.58 (dd, *J* = 9.0, 4.9 Hz, 1H), 7.54 (s, 1H), 7.45 (t, *J* = 8.7 Hz, 1H), 6.90 (s, 1H), 6.09 (q, *J* = 6.5 Hz, 1H), 5.65 (s, 2H), 4.12 – 4.04 (m, 1H), 2.85 (d, *J* = 11.4 Hz, 2H), 2.21 (s, 3H), 2.08 – 1.89 (m, 7H), 1.81 (d, *J* = 6.6 Hz, 3H)

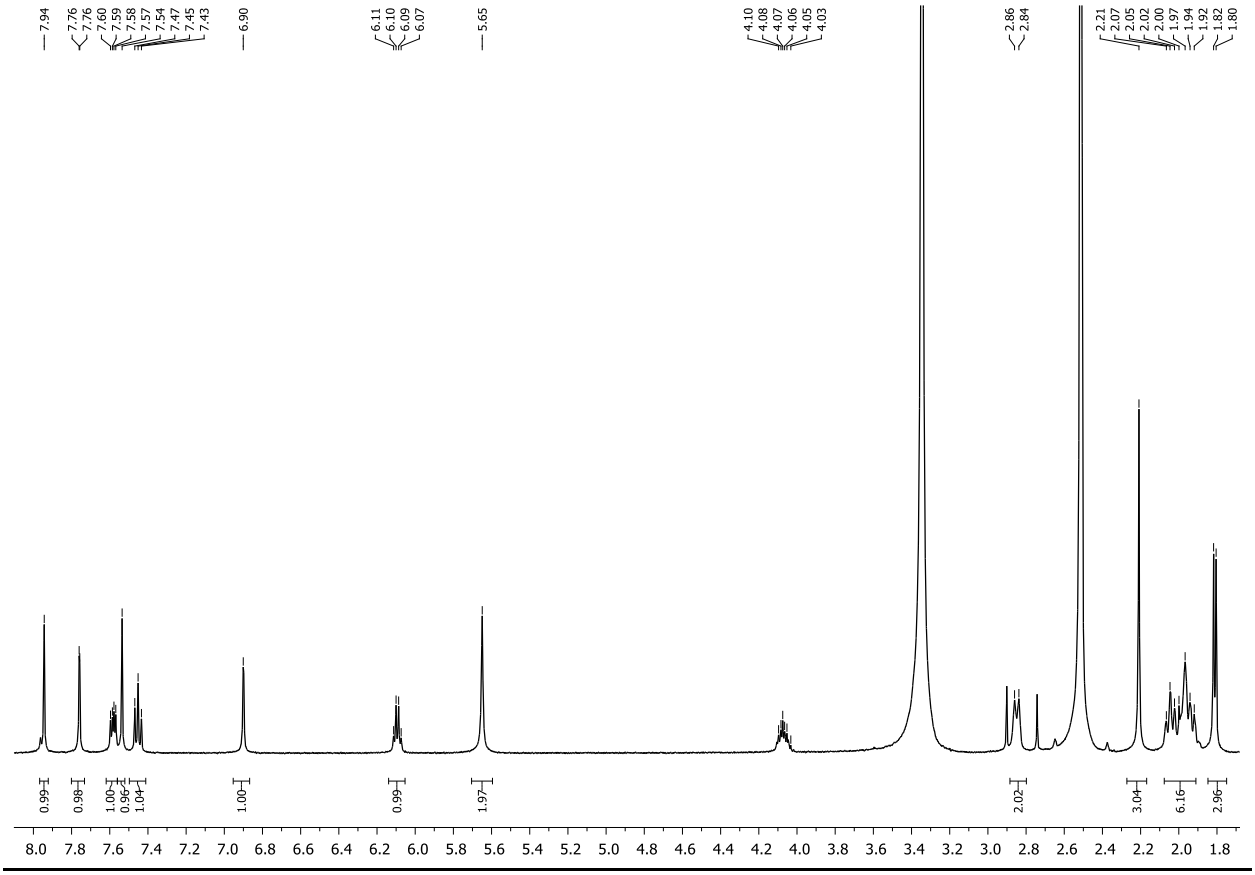
7.94
7.76
7.76
7.60
7.59
7.58
7.57
7.54
7.47
7.45
7.43
6.90
6.11
6.10
6.09
6.07
5.65
4.10
4.08
4.07
4.06
4.05
4.03
2.86
2.84
2.21
2.07
2.05
2.02
2.00
1.97
1.94
1.92
1.82
1.80
0.99
0.98
1.00
0.96
1.04
1.00
0.99
1.97
2.02
3.04
6.16
2.96
8.0 7.8 7.6 7.4 7.2 7.0 6.8 6.6 6.4 6.2 6.0 5.8 5.6 5.4 5.2 5.0 4.8 4.6 4.4 4.2 4.0 3.8 3.6 3.4 3.2 3.0 2.8 2.6 2.4 2.2 2.0 1.8

4-nitrobenzyl (R)-(3-(1-(2,6-dichloro-3-fluorophenyl)ethoxy)-5-(1-(1-methylpiperidin-4-yl)-1H-pyrazol-4-yl)pyridin-2-yl)carbamate (24)

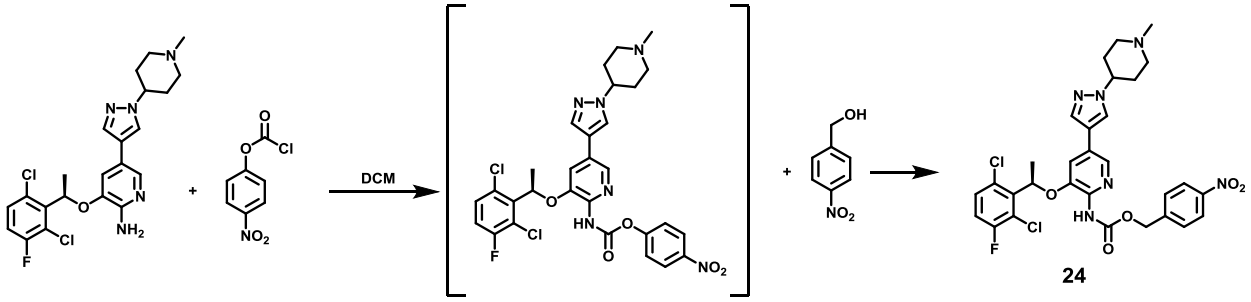

Methylcrizotinib (20 mg, 0.043 mmol) was dissolved in DCM abs. (2 mL) under argon atmosphere and cooled to 0 °C. Then, *para*-nitrophenyl chloroformate (8.7 mg, 0.043 mmol) and pyridine (16.8 mg, 0.043 mmol, 3.5 µL) were added. The reaction mixture was stirred for 15 min at 0 °C and the ice bath was removed. *Para*-nitrobenzyl alcohol (13 mg, 0.086 mmol) was added and the reaction mixture was stirred for further 5 min. Finally, triethylamine (4.35 mg, 0.043 mmol) was added and the reaction mixture was stirred under an argon atmosphere overnight. The solvent was removed under reduced pressure and the product was dried in vacuo overnight. Purification was performed via preparative HPLC (ACN/H_2O (1% formic acid)) to obtain pure prodruct **24**.

Yield: 10mg (35%)

Characterization:

^{1}H NMR (500 MHz, MeOD): δ = 8.29 (d, *J* = 8.8 Hz, 2H), 8.12 (d, *J* = 1.6 Hz, 1H), 8.04 (s, 1H), 7.76 – 7.68 (m, 3H), 7.46 (dd, *J* = 9.0, 4.8 Hz, 1H), 7.34 (d, *J* = 1.7 Hz, 1H), 7.25 (t, *J* = 8.6 Hz, 1H), 6.30 (q, *J* = 6.6 Hz, 1H), 5.39 (s, 2H), 4.35 – 4.27 (m, 1H), 3.17 (d, *J* = 12.2 Hz, 2H), 2.50 (s, 5H), 2.18 (d, *J* = 24.3 Hz, 4H), 1.89 (d, *J* = 6.7 Hz, 3H)

ESI-MS in MeOH: m/z(positive) 643 (**24** – H^+)

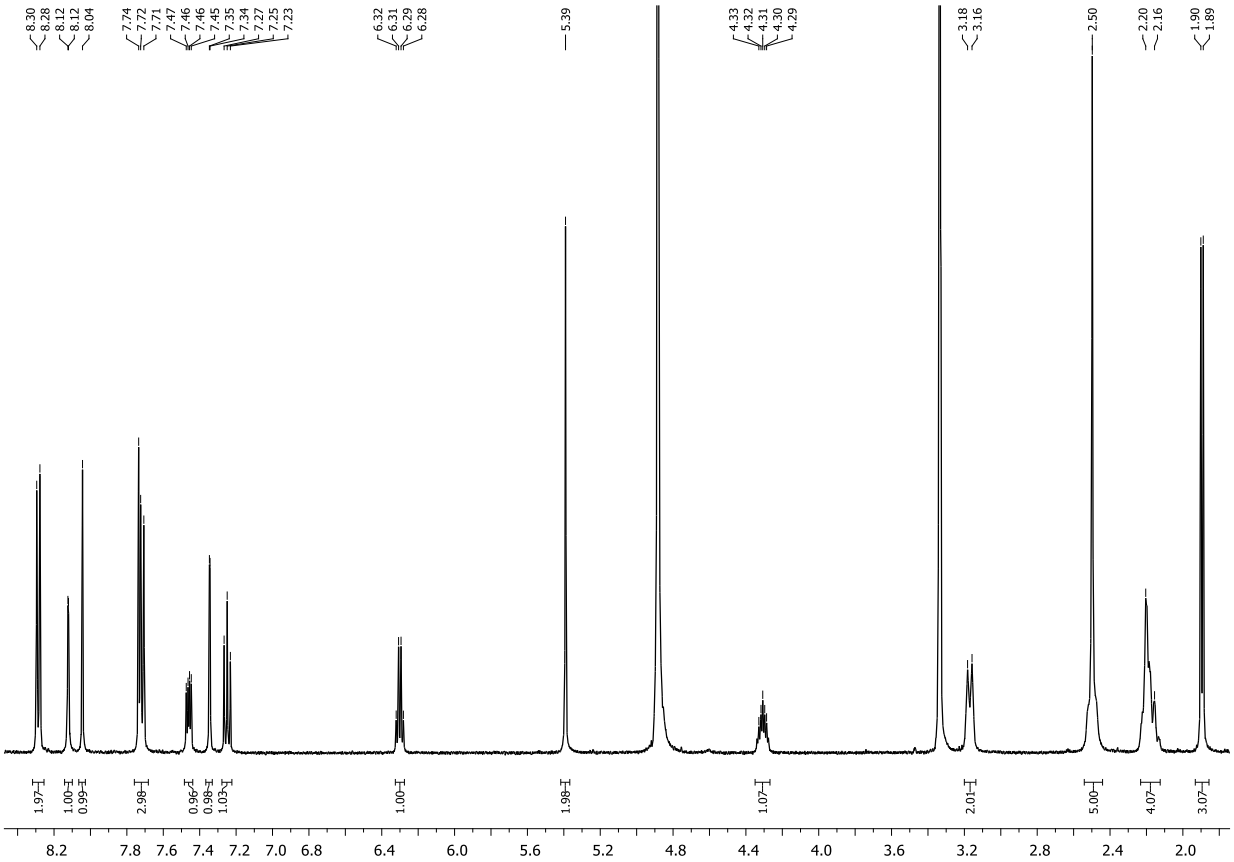
8.30
8.28
8.12
8.12
8.04
7.74
7.72
7.71
7.47
7.46
7.46
7.45
7.35
7.34
7.27
7.25
7.23
6.32
6.31
6.29
6.28
5.39
4.33
4.32
4.31
4.30
4.29
3.18
3.16
2.50
2.20
2.16
1.90
1.89
1.97
1.00
0.99
2.98
0.96
0.98
1.03
1.00
1.98
1.07
2.01
5.00
4.07
3.07
8.2
7.8
7.6
7.4
7.2
7.0
6.8
6.4
6.0
5.6
5.2
4.8
4.4
4.0
3.6
3.2
2.8
2.4
2.0

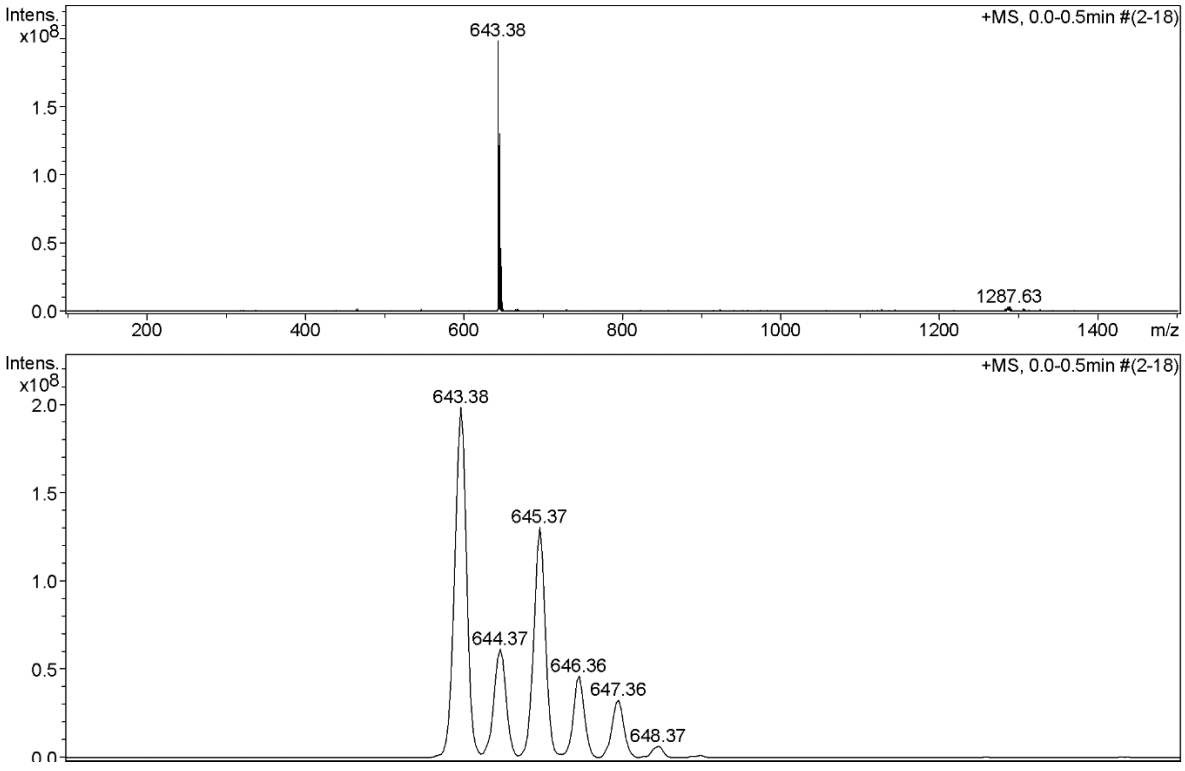
Intens.
x10^8
+MS, 0.0-0.5min #(2-18)
643.38
1287.63
1.5
1.0
0.5
0.0
200
400
600
800
1000
1200
1400
m/z
Intens.
x10^8
+MS, 0.0-0.5min #(2-18)
643.38
645.37
644.37
646.36
647.36
648.37
2.0
1.5
1.0
0.5
0.0

c. Cleavage tests

Enzymatic reduction of nitrobenzyl-crizotinib

E. coli nitroreductase (NTR) and NADH were purchased from SigmaAldrich Inc. All measurements were performed on a HPLC system with acetonitrile / H_2O (1% formic acid) as eluent on an Acquity UPLC® BEH C18 1.7 µm column. Release of free crizotinib shall be tested after reduction of the nitro group by the nitroreductase of *Escherichia coli* in presence of NADH. By this, a 10 µM phosphate buffer solution at pH 7 was prepared as well as a stock solutions of the prodrug (1 mM) in DMSO and NADH (1 mM) in buffer. The enzyme was prepared as 2 µg/mL solution in buffer. To prepare the samples for cleavage tests, 30 µL of sample stock solution was added to 150 µL of NADH stock solution and diluted with 320 µL of buffer solution. Finally, 1 mL of the enzyme solution was added, one equivalent of 250 µL was removed and injected into the HPLC. The sample was incubated at 37 °C and equivalents were taken every thirty minutes.

Enzymatic cleavage of the cathepsin K prodrug

A buffer solution was produced containing 100 mM sodium acetate at pH 5.5, 2.5 mM EDTA and 2.5 mM dithiothreitol. A substrate stock solution was prepared with 10 mM substrate in DMSO. The enzyme (0.023 mg/mL) was used in its prefabricated state in 50 mM sodium acetate, pH 5.5, containing 50 mM sodium chloride, 0.5 mM EDTA and 5mM DTT. Investigations were performed on a Tecan Infinite® 200 PRO microplate reader using Packard Optiplate-96 96 Flat Bottom white Polystyren inlets. To investigate the background emission of the prodrug, the measurement was additionally performed at reaction conditions in absence of cathepsin K. By this, 7.5 µL of the prodrug stock solution was diluted to 30 µL with DMSO and 720 µL buffer was added. The cleavage test was performed equally to the control by addition of 11 µL of the cathepsin K stock. Measuring intervals were set to two minutes for the first hour and 5min until the end of measurement. The excitation wavelength of the fluorophore was used as described in literature at 395 nm and the emission intensity was measured at 495 nm.

ABBREVIATION LIST

4-DMAP	4-dimethyl aminopyridine
ADEPT	antibody-directed enzyme prodrug therapy
ALK	anablastic lymphoma kinase
ALL	acute lymphoblastic leukemia
ADC	antibody-drug conjugate
CD30	cluster of differentiation 30
CDA	cytidine deaminase
CNS	central nervous system
CES1	carboxylesterase 1
CES2	carboxylesterase 2
c-met	hepatocyte growth factor receptor (HGFR)
DCC	dicyclohexyl carbodiimide
DCM	dichloromethane
DiBOC	di-tert-butyldicarbonat
DIC	diisopropyl carbodiimide
DIPEA	diisopropylethylamine
DMF	dimethylformamide
DMSO	dimethylsulfoxide
DHFR	dihydrofolate reductase
DNA	deoxyribonucleic acid
dThdPase	thymidine phosphorylase
DTT	dithiothreitol
E. coli	Escherichia coli
ECM	extracellular matrix
EDC	1-Ethyl-3-(3-dimethylaminopropyl)carbodiimide
EDTA	ethylenediaminetetraacetic acid
EEDQ	ethoxycarbonyl-2-ethoxy-1,2-dihydroquinoline
EGFR	epidermal growth factor receptor
FDA	US Food and Drug Administration
GKM	gatekeeper mutation
HL	Hodgkin lymphoma
HPLC	high pressure liquid chromatography
HOBt	hydroxyl benzotriazole
MMAE	monomethyl auristatin E
MMPs	metallomatrix proteinases

NADH	nicotinamide adenine dinucleotide
NCI	National Cancer Institute
NCCSC	National Cancer Chemotherapy Service Center
NMR	Nuclear Magnetic Resonance
NSCLC	non-small cell lung cancer
ONC	oncogene
PABC	*para*-aminobenzyloxycarbonyl
PABOH	*para*-aminobenzyl alcohol
PNP	*para*-nitrophenyl chloroformate
ROS	reactive oxygen species
ROS1	proto-oncogene tyrosine-protein kinase
RTF1	reduced folate transporter 1
TBTU	O-(Benzotriazol-1-yl)-N,N,N‘,N’-tetramethyluronium tetrafluoroborat
TEA	triethylamine
THF	tetrahydrofuran
TKI	tyrosine kinase inhibitor
TNF	tumor necrosis factor
TPG	tumor promotor gene
TSG	tumor suppressor gene

REFERENCES

1. Ferlay J, Steliarova-Foucher E, Lortet-Tieulent J, Rosso S, Coebergh JW, Comber H, Forman D, Bray F. Cancer incidence and mortality patterns in Europe: Estimates for 40 countries in 2012. *Eur J Cancer*. **49**(6), 1374-1403 (2013)
2. Statistics Austria: "Krebsinzidenz (Neuerkankungen pro Jahr) nach Lokalisationen und Geschlecht, Österreich seit 1983" (05.01.2014)
3. Evan GI, Vousden KH. Proliferation, cell cycle and apoptosis in cancer. *Nature* **411**, 342-348 (2011)
4. La Vecchia C, Negri E, Franceschi S, Gentile A. Family History and the Risk of Stomach and Colorectal Cancer. *Cancer* **70** (1), 50-55 (1992)
5. Feinberg AP, Tycko B. The history of cancer epigenetics. *Nature Rev. Cancer* **4**, 143-153 (2004)
6. Seaberg RM, Van Der Kooy D. Stem and progenitor cells: The premature desertion of rigorous definitions. *Trends in Neurosciences* **26** (3), 125–131 (2003)
7. Hanahan D, Weinberg R. A. Hallmarks of Cancer: The next generation. *Cell* **144**, 646-674 (2011)
8. Feinberg AP, Ohlsson R, Henikoff S. The epigenetic progenitor origin of human cancer. *Nature Rev. Gen*. **7**, 21-33 (2006)
9. Papac, R. J. Origins of cancer therapy. *Yale J. Biol. Med*. **74**, 391–398 (2001).
10. Farber S, Diamond LK, Mercer RD, Sylvester RF, Wolff JA. Temporary remissions in acute leukemia in children produced by folic antagonist, 4- aminopteroylglutamic acid (aminopterin). *N. Engl. J. Med*. 238, 787–793 (1948).
11. Li, M. C., Hertz, R. & Bergenstal, D. M. Therapy of choriocarcinoma and related trophoblastic tumors with folic acid and purine antagonists. *N. Engl. J. Med.* **259**, 66–74 (1958).
12. Jaffe N, Frei E. 3rd, Traggis D, Bishop Y. Adjuvant methotrexate and citrovorum-factor treatment of osteogenic sarcoma. *N. Engl. J. Med.* **291**, 994–997 (1974).
13. Jolivet J, Cowan KH, Curt GA, Clendeninn NJ, Chabner BA. The pharmacology and clinical use of methotrexate. *N. Engl. J. Med*. **309**, 1094–1104 (1983)
14. Skipper, H. E., Thomson, J. R., Elion, G. B. & Hitchings, G. H.Observations on the anticancer activity of 6-mercaptopurine. *Cancer Res*. **14**, 294–298 (1954).
15. Moertel CG, et al. Levamisole and fluorouracil for adjuvant therapy of resected colon carcinoma. *N. Engl. J. Med*. **322**, 352–358 (1990).
16. Frei E. 3rd, et al. The effectiveness of combinations of antileukemic agents in inducing and maintaining remission in children with acute leukemia. *Blood* **26**, 642–656 (1965).
17. Ganansia-Leymarie V, Bischoff P, Bergerat JP, et al. Signal transduction pathways of taxanes-induced apoptosis. *Curr Med Chem Anti-Canc Agents*. **3**, 291–306 (2003)
18. Venditto VJ, Simanek EE. Cancer Therapies Utilizing the Camptothecins: A Review of the in Vivo Literature. *Mol. Pharm. Rev.* **7**(2), 307–349 (2010)
19. Thorna CF, Oshiroa C, Marshe S, Hernandez-Boussardb T, McLeodd H, Kleina TE, Altmana RB. Doxorubicin pathways: pharmacodynamics and adverse effects. *Pharmacogenet. Genomics*. **21**(7), 440–446 (2011)
20. Rosenberg B, Camp LV, Krigas T. Inhibition of cell division in Escherichia coli by electrolysis products from a platinum electrode. *Nature* **205**, 698-699 (1965)
21. Kelland L. The resurgence of platinum-based cancer chemotherapy. *Nat. Rev. Cancer*. **7**, 573-584 (2007)
22. Sawyers S. Targeted cancer Therapy. *Nature* **432**, 294-297 (2004)
23. Li T, Perez-Soler R. Skin toxicities associated with epidermal growth factor receptor inhibitors. *Targ Oncol* **4**, 107–119 (2009)
24. Kratz F, Müller IA, Ryppa C, Warnecke A. Prodrug Strategies in Anticancer Chemotherapy. *ChemMedChem* **3**, 20–53 (2008)

25. Tranoy-Opalinski I, Fernandes A, Thomas M, Gesson JP, Papot S. Design of Self-Immolative Linkers for Tumour-Activated Prodrug Therapy. *Anti-Cancer Agents Med Chem*. **8**(5), 618-637 (2008)
26. Maskell L, Blanche EA, Colucci MA, Whatmore JL, Moody CJ. Synthesis and evaluation of prodrugs for anti-angiogenic pyrrolylmethylidenyl oxindoles. *Bioorg. Med. Chem. Lett*. 17(6), 1575-1578 (2007)
27. Shabat D, Lode HN, Pertl U, Reisfeld, RA, Rader C, Lerner RA, Barbas III, CF. In vivo activity in a catalytic antibody-prodrug system: Antibody catalyzed etoposide prodrug activation for selective chemotherapy. *Proc. Natl. Acad. Sci.* **98**, 7528-7533 (2001)
28. Warneke A. Site-specific prodrug activation and the concept of self-immolation. *In: Drug Delivery in Oncology*. P. 558 (2012), ISBN: 978-3-527-32823-9
29. Carl PL, Chakravarty PK, Katzenellenbogen JA. A novel connector linkage applicable in prodrug design. *J. Med. Chem.* **24**, 479-480 (1981)
30. Perry-Feigenbaum R, Baran PS, Shabat D. The pyridinone-methide elimination. *Org. Biomol. Chem.* **7**, 4825-4828 (2009)
31. Brown JM, Wilson WR. Exploiting tumor hypoxia in cancer treatment. *Nat. Rev. Canc*. **4**, 437-447 (2004)
32. Denny WA, Wilson WR, Hay MP. Recent developments in the design of bioreductive drugs. *Br. J. Canc*. **74**, 32-38 (1996)
33. Object: NCT01746979, Website: http://www.clinicaltrials.gov, Link: (https://clinicaltrials.gov/ct2/show/NCT01746979?term=NCT01746979&rank=1)
34. Vafa O, Wade M, Kern S, et al. c-Myc can induce DNA damage, increase reactive oxygen species, and mitigate p53 function: a mechanism for oncogene-induced genetic instability. *Mol Cell*. **9**,1031–1044 (2002)
35. Afanasev I. Reactive oxygen species signaling in cancer: comparison with aging. *Aging Dis.* **2**, 219–230 (2011)
36. Sahin E, Colla S, Liesa M, et al. Telomere dysfunction induces metabolic and mitochondrial compromise. *Nature*. **470**, 359–65 (2011)
37. Kratz F, Warnecke A, Scheuermann K, Stockmar C, Schwab J, Lazar P, Drueckes P, Esser N, Drevs J, Rognan D, Bissantz C, Hinderling C, Folkers G, Fichtner I, Unger C. Probing the Cysteine-34 Position of Endogenous Serum Albumin with Thiol-Binding Doxorubicin Derivatives. Improved Efficacy of an Acid-Sensitive Doxorubicin Derivative with Specific Albumin-Binding Properties Compared to that of the Parent Compound. *J. Med. Chem.* **45**, 5523-5533 (2002)
38. Traverso N, Ricciarelli R, Nitti M, Marengo B, Furfaro AL, Pronzato MA, Marinari UM, Domenicotti C. Role of Glutathione in Cancer Progression and Chemoresistance. *Oxid. Med. Cell. Long.* **2013**, Article ID 972913 (2013)
39. Xu Y, Chen J, Li Y, Peng S, Gu X, Sun M, Gao K, Fang J. Synthesis and biological studies of the thiols triggered anticancer prodrug for a more effective cancer therapy. *Org. Biomol. Chem.* **13**, 2634-2639 (2015)
40. Sankar R, Kumbhare RS, Dharmaraja AT, Chakrapani H. A phenacrylate scaffold for tunable thiol activation and release. *Chem. Commun*. **50**, 15323-15326 (2014)
41. Miwa M, et al. Design of a novel oral fluoropyrimidine carbamate, capecitabine, which generates 5-fluorouracil selectively in tumours by enzymes concentrated in human liver and cancer tissue. *Eur. J. Cancer* **34**, 1274–1281 (1998).
42. Quinney SK, et al. Hydrolysis of capecitabine to 5′-deoxy-5-fluorocytidine by human carboxylesterases and inhibition by loperamide. *J. Pharmacol. Exp. Ther.* **313**, 1011–1016 (2005).
43. Pro B, Advani R, Brice P, Bartlett NL, Rosenblatt JD, Illidge T, Matous J, Ramchandren R, Fanale M, Connors JM, Yang Y, Sievers EL, Kennedy DA, Shustov A. Brentuximab vedotin (SGN-35) in patients with relapsed or refractory systemic anaplastic large-cell lymphoma: results of a phase II study. *J Clin Oncol.* **30**(18), 2190-2196 (2012)
44. Quesada V, et al. The Degradome database: mammalian proteases and diseases of proteolysis. *Nucleic Acids Res.* **37**, D239–D243 (2009)
45. Mason SD, Joyce JA. Proteolytic networks in cancer. *Trends Cell Biol*. **21**, 4 (2011)
46. Mohamed MM, Sloane BF. Cysteine cathepsins: multifunctional enzymes in cancer. *Nature Rev Canc*. **6**, 764-775 (2006)

47. Cavallo-Medved D, Sloane BF. Cell-surface cathepsin B: understanding its functional significance. *Curr. Top. Dev. Biol*. **54**, 313–341 (2003)
48. Reddy VY, Zhang QY, Weiss SJ. Pericellular mobilization of the tissue-destructive cysteineproteinases, cathepsins B, L, and S, by human monocyte-derived macrophages. *Proc. Natl Acad. Sci*. *USA* **92**, 3849–3853 (1995)
49. Reinheckel T, Deussing J, Roth W, Peters C. Towards specific functions of lysosomal cysteine peptidases: phenotypes of mice deficient for cathepsin B or cathepsin L. *Biol. Chem*. **382**, 735–741 (2001).
50. Halangk W, Lerch MM, Brandt-Nedelev B, Roth W, Ruthenbuerger M, Reinheckel T, Domschke W, Lippert H, Peters C, Deussing J. Role of cathepsin B In intracellular trypsinogen activation and the onset of acute pancreatitis. *J Clin Invest*. **106**, 773-781 (2000)
51. Motyckova G, Fisher DE. Pycnodysostosis: role and regulation of cathepsin K in osteoclast function and human disease. *Curr. Mol. Med.* **2**, 407–421 (2002)
52. Felbor U, Kessler B, Mothes W, Goebel HH, Ploegh HL, Bronson RT, Olsen BR. Neuronal loss and brain atrophy in mice lacking cathepsins B and L. *Proc. Natl. Acad. Sci.* **99**, 7883–7888 (2002)
53. Gondi CS, Rao JS. Cathepsin B as a cancer target. *Expert Opin Ther Targets.* **17**(3), 281–291 (2013)
54. Choe Y, Leonetti F, Greenbaum DC, Lecaille F, Bogyo M, Brömme D, Ellman JA, Craik CS. Substrate Profiling of Cysteine Proteases Using a Combinatorial Peptide Library Identifies Functionally Unique Specificities. *J. Biol. Chem.* **281**(18), 12824–12832 (2006)
55. Vasiljeva O, Reinheckel T, Peters C, Turk D, Turk V, Turk B. Emerging Roles of Cysteine Cathepsins in Disease and their Potential as Drug Targets. *Curr. Pharm.* **13**, 385-401 (2007)
56. Nägler DK, Storer AC, Portaro FCV, Carmona E, Juliano L, Menard R. Major Increase in Endopeptidase Activity of Human Cathepsin B upon Removal of Occluding Loop Contacts. *Biochemistry* **36**, 12608-12615 (1997)
57. Musil D, Zu D, Turk D, Engh RA, Mayr I, Huber R, et al. The refined 2.15 A X-ray crystal structure of human liver cathepsin B: the structural basis for its specificity. *EMBO J.* **10**, 2321-30 (1991)
58. Guncar G, Podobnik M, Pungercar J, Strukelj B, Turk V, Turk D. Crystal structure of porcine cathepsin H determined at 2.1 A resolution: location of the mini-chain C-terminal carboxyl group defines cathepsin H aminopeptidase function. *Structure*. **6**, 51-61 (1998).
59. Turk D, Janji V, Stern I, Podobnik M, Lamba D, Dahl SW, et al. Structure of human dipeptidyl peptidase I (cathepsin C): exclusion domain added to an endopeptidase framework creates the machine for activation of granular serine proteases. *EMBO J*. **20**, 6570-82 (2001)
60. Joyce JA, Hanahan D. Multiple roles for cysteine cathepsins in cancer. *Cell Cycle*. **3**(12), 1516-1519 (2004)
61. Watzke A, Kosec G, Kindermann M, Jeske V, Nestler HP, Turk V, Turk B, Wendt KU. Selective Activity-Based Probes for Cysteine Cathepsins. *Angew. Chem. Int. Ed.* **47**, 406-409 (2008)
62. Verdoes M, Bender KO, Segal E, van der Linden WA, Syed S, Withana NP, Sanman LE, Bogyo M. Improved Quenched Fluorescent Probe for Imaging of Cysteine Cathepsin Activity. *J. Am. Chem. Soc.* **135**, 14726−14730 (2013)
63. Watzke A, Kosec G, Kindermann M, Jeske V, Nestler HP, Turk V, Turk B, Wendt KU. Selective Activity-Based Probes for Cysteine Cathepsins. *Angew. Chem*. **47**, 406 –409 (2008)
64. Kazandjian D, Blumenthal G, Chen HY, He K, Patel M, Justice R, Keegan P, Pazdur R. Approval Summary: Crizotinib for the Treatment of Metastatic Non-Small Cell Lung Cancer With Anaplastic Lymphoma Kinase Rearrangements. *The Oncologist*. **19**, e5–e11 (2014)
65. Shaw AT, Jänne PA, et al. Crizotinib versus Chemotherapy in Advanced ALK-Positive Lung Cancer. *N Engl J Med.* **368**(25), 2385-2394
66. Kobayashi, N. E. U. Patent 1,972,636, 2007 (p. 67)
67. Alouane A, Labruere R, Le Saux T, Aujard I, Dubruille S, Schmidt F, Jullien L. Light Activation for the Versatile and Accurate Kinetic Analysis of Disassembly of Self-Immolative Spacers. *Chem. Eur. J.* **19**, 11717 – 11724 (2013)
68. Knolker HJ, Braxmeier T, Schlechtingen G. A Novel Method for the Synthesis of Isocyanates Under Mild Conditions. *Angew. Chem. Int. Ed. Engl.* **34**(22), 2497-2500

69. Pasquato L, Modena G, Cotarca L, Delogu P, Mantovani S. Conversion of Bis(trichloromethyl) Carbonate to Phosgene and Reactivity of Triphosgene, Diphosgene, and Phosgene with Methanol. J. Org. Chem. **65**, 8224-8228 (2000)
70. Chowdhury MA, Moya IA, Bhilocha S, McMillan CC, Vigliarolo BG, Zehbe I, Phenix CP. Prodrug-Inspired Probes Selective to Cathepsin B over Other Cysteine Cathepsins. *J. Med. Chem.* **57**, 6092-6104 (2014)
71. J.D.Cheng et al. Promotion of tumor growth by murine fibroblast activation protein, a serine protease, in an animal model. *Cancer Res.* **62**, 4767-4772 (2002)
72. Crystal AS, Shaw AT, Sequist LV, Friboulet L, Niederst MJ, Lockerman EL, Frias RL, Gainor JF, Amzallag A, Greninger P. Patient-derived models of acquired resistance can identify effective drug combinations for cancer. *Science* **346**, 1480-1486 (2014)
73. Crystal AS, Shaw AT, Sequist LV, Friboulet L, Niederst MJ, Lockerman EL, Frias RL, Gainor JF, Amzallag A, Greninger P, Lee D, Kalsy A, Gomez-Caraballo M, Elamine L, Emily Howe E, Hur W, Lifshits E, Robinson HE, Katayama R, Faber AC, Awad MM, Ramaswamy S, Mino-Kenudson M, Iafrate AJ, Benes CH, Engelman JA. Patient-derived models of acquired resistance can identify effective drug combinations for cancer. *Cancer Therapy*. **346** (6216), 1480-1486
74. Bang YJ. The potential for crizotinib in non-small cell lung cancer: a perspective review. *Ther. Adv. Med. Oncol*. **3**(6), 279-291 (2011)
75. Cui JJ, Tran-Dube M, Shen H, Nambu M, Kung PP, Pairish M, Jia L, Meng J, Funk L, Botrous I, Mctigue M, Grodsky N, Ryan K, Padrique E, Alton G, Timofeevski S, Yamazaki S, Li Q, Zou H, Christensen J, Mroczkowski B, Bender S, Kania RS, Edwards MP. Structure based drug design of crizotinib (PF-02341066), a potent and selective dual inhibitor of mesenchymal-epithelial transition factor (c-MET) kinase and anaplastic lymphoma kinase (ALK). *J.Med.Chem* **54,** 6342- 6363 (2011)
76. Cui JJ, Tran-Dube M, Shen H, Nambu M, Kung PP, Pairish M.Structure based drug design of crizotinib (PF-02341066), a potent andselective dual inhibitor of mesenchymal-epithelial transition factor (c-MET) kinase and anaplastic lymphoma kinase (ALK). *J. Med. Chem.* **54**, 6342-63 (2011)
77. Duyster J, Bai RY, Morris SW. Translocations involving anaplastic lymphoma kinase (ALK). *Oncogene* **20**, 5623-5637 (2001)
78. Wu P, Nielsen TE, Clausen MH. FDA-approved small-molecule kinase inhibitors. *Trends Pharmacol Sci.* **36**(7), 422-438 (2015)
79. Hay MP, Sykes BM, Denny WA, O'Connor CJ. Substituent effects on the kinetics of reductively-initiated fragmentation of nitrobenzyl carbamates designed as triggers for bioreductive prodrugs. *J. Chem. Soc., Perkin Trans.* **1**, 2759–2770 (1999)
80. Abel, U. WO 2012/164085 A1, 2012 (p. 184)
81. Chaturvedi D. Perspectives on the synthesis of organic carbamates. *Tetrahedron* **68**, 15-45 (2012)

Ich habe mich bemüht, sämtliche Inhaber der Bildrechte ausfindig zu machen und ihre Zustimmung zur Verwendung der Bilder in dieser Arbeit eingeholt. Sollte dennoch eine Urheberrechtsverletzung bekannt werden, ersuche ich um Meldung bei mir.

CURRICULUM VITAE

BJÖRN BIELEC, BSC.

Date and Place of Birth: 01.12.1987, Viersen

Citizenship: German

E-mail: bjoern.bielec@univie.ac.at

Education

since 01/2014	Master thesis at the Insitute of Cancer Research
	Supervisor: Prof. Dr. Bernhard Keppler/ Dr. Christian Kowol
	Title of the thesis: Development of novel anti-cancer prodrug strategies
03/2012	Master study of Biochemistry at the University of Vienna
11/2011	Bachelor thesis *„Synthesis of novel protecting groups for amino acids based on 2-acyldimedone“* at the Insitut für Analytik, University of Vienna;
	Supervisor: Prof. Dr. Wolfgang Lindner
10/2007	Study of Chemistry, University of Vienna
7/2007	High school degree, Bischöfliche Marienschule, Mönchengladbach, Germany

Language Skills

German (mother tongue)

English